A THIRD ORDER NUMERICAL METHOD FOR 3D DOUBLY PERIODIC ELECTROMAGNETIC SCATTERING PROBLEMS

by

Michael J. Nicholas

Department of Mathematics
Duke University

Date: _____

Approved:

_____
J. Thomas Beale, Advisor

_____
Stephanos Venakides

_____
Mike Reed

_____
John Trangenstein

Dissertation submitted in partial fulfillment of the
requirements for the degree of Doctor of Philosophy
in the Department of Mathematics
in the Graduate School of
Duke University

2007

ABSTRACT

(Mathematics)

A THIRD ORDER NUMERICAL METHOD FOR 3D DOUBLY PERIODIC ELECTROMAGNETIC SCATTERING PROBLEMS

by

Michael J. Nicholas

Department of Mathematics
Duke University

Date: _____

Approved:

_____
J. Thomas Beale, Advisor

_____
Stephanos Venakides

_____
Mike Reed

_____
John Trangenstein

An abstract of a dissertation submitted in partial fulfillment of the requirements for the degree of Doctor of Philosophy in the Department of Mathematics in the Graduate School of Duke University

2007

Abstract

We here developed a third-order accurate numerical method for scattering of 3D electromagnetic waves by doubly periodic structures. The method is an intuitively simple numerical scheme based on a boundary integral formulation. It involves smoothing the singular Green's functions in the integrands and finding correction terms to the resulting smooth integrals. The analytical method is based on the singular integral methods of J. Thomas Beale, while the scattering problem is motivated by the 2D work of Stephanos Venakides, Mansoor Haider, and Stephen Shipman. The 3D problem was done with boundary element methods by Andrew Barnes. We present a method that is both more straightforward and more accurate.

In solving these problems, we have used the Müller integral equation formulation of Maxwell's equations, since it is a Fredholm integral equation of the second kind and is well-posed. Müller derived his equations for the case of a compact scatterer. We outline the derivation and adapt it to a periodic scatterer. The periodic Green's functions found in the integral equation contain singularities which make it difficult to evaluate them numerically with accuracy. These functions are also very time consuming to evaluate numerically. We use Ewald splitting to represent these functions in a way that can be computed rapidly.

We present a method of smoothing the singularity of the Green's function while maintaining its periodicity. We do local analysis of the singularity in order to identify and eliminate the largest sources of error introduced by this smoothing. We prove that with our derived correction terms, we can replace the singular integrals

with smooth integrals and only introduce a error that is third order in the grid spacing size. The derivation of the correction terms involves transforming to principal directions using concepts from differential geometry. The correction terms are necessarily invariant under this transformation and depend on geometric properties of the scatterer such as the mean curvature and the differential of the Gauss map.

Able to evaluate the integrals to a higher order, we implement a GMRES algorithm to approximate solutions of the integral equation. From these solutions, Müller's equations allow us to compute the scattered fields and transmission coefficients. We have also developed acceleration techniques that allow for more efficient computation.

We provide results for various scatterers, including a test case for which exact solutions are known. The implemented method does indeed converge with third order accuracy. We present results for which the method successfully resolves Wood's anomaly resonances in transmission.

Acknowledgements

I am very grateful to my advisor, Professor J. Thomas Beale, for his instruction, advice, and friendship. He helped me find direction three years ago when I was wandering mathematically, and he has been an ideal mentor since then. He has been willing, patient, and kind.

The Duke math faculty and staff have been wonderful and have helped make my experience here a great period of personal and professional development. I am especially grateful to Professors Stephanos Venakides, Tom Witelski, Stephen Shipman, Harold Layton, Anita Layton, Mike Reed, John Trangenstein, Mark Huber, and Paul Aspinwall for their instruction and guidance.

My friends in the department have been a great strength to me and have made life here more enjoyable. My office mates have been especially good friends. Thanks to Melanie Bain, Mike Gratton, Thomas Laurent, and Nick Robbins for being accepting, helpful, and fun office mates.

I have been privileged to teach classes to wonderful and bright Duke undergraduate students. Whenever my research has been a source of frustration, my teaching has been a buoy to me. Thanks to all my students for being cheerful and eager and to Jim Tomberg and Lewis Blake for giving good teaching advice.

It has been a blessing to have great ecclesiastical leaders in Durham and would like to thank Bishops Roger Miller, Jay Condie, and David Meyer for their encouragement and for giving me opportunities to serve.

The friendships I've had in Durham and at Duke have bred a love for these places

in my heart. I feel grateful for 6 years worth of positive experiences and relationships. Thanks to all here who have known and cared about me.

I offer great thanks and love to my family. My parents have encouraged and supported me in my studies at Duke as in every other part of my life. If there is anything good about me, I owe it first to them. Jenny, Dave, and Tom are my greatest friends, and I am thankful to know that geography cannot separate us.

Peter Michael is the newest joy in my life. He fills me with wonder and hope, and he provides me with motivation. Even before he came, he and his siblings were my reason to do hard things like boundary integral equations.

I cannot express enough thanks to Amanda. She has given me encouragement, energy, and ability when I have needed it most. She is loving, forgiving, and genuine. She is mine, and I am hers, and so it will be forever. Amanda, thank you; I love you.

Contents

Abstract **iv**

Acknowledgements **vi**

List of Tables **xiii**

List of Figures **xiv**

1 Introduction **1**

2 Electromagnetic Scattering **7**

2.1 Maxwell's Equations 7

2.2 Scattering 9

2.3 3D Doubly Periodic Scatterers 10

2.4 The Scattering Problem 11

2.5 The Incident Wave 12

2.6 Pseudoperiodicity of the Fields 14

2.7 Transmission 15

2.8 Transmission Resonances 16

3 The Green's Functions **18**

3.1 A Periodic Green's Function Condition 18

3.2 Derivation of the Periodic Green's Function 19

3.3 The Green's Function 22

3.4 Properties of the Green's Function 22

3.5 Derivatives of the Green's Function 23

4 The Integral Equations **25**

4.1 Derivation of the Integral Equations 26

4.1.1 Interior Representation Theorem 27

4.1.2 Exterior Representation Theorem 27

4.1.3 Surface Currents and Charges 32

4.1.4 Jump Conditions 33

4.1.5 The Field Equations 35

4.2 The Müller Integral Equations 41

4.3 Operator Notation 42

4.4 Singularities in the Integral Equations 43

5 Ewald Splitting **45**

5.1 G1 51

5.2 Properties of G1 and G2 53

5.2.1 G1 Properties 53

5.2.2 G2 Properties 54

5.3 Choosing the Splitting Parameter 55

6 Corrections **56**

6.1 Smoothing 57

6.2 The Single Layer Potential 60

6.3 The Double Layer Potential 70

6.4 The Singular Müller Integrals 75

6.4.1 The First Singular Integral 75

6.4.2 The Second Singular Integral 76

6.5 Discretization Error 79
6.6 The Corrected Müller Integral Equations 80

7 Implementation **81**

7.1 Inputs and Outputs 81
7.1.1 Inputs 81
7.1.2 Outputs 84
7.2 Overview of the Method 84
7.2.1 Preprocessing 85
7.2.2 The Main Computations 85
7.2.3 Postprocessing 86
7.3 Numerical Issues 86
7.3.1 Special Functions 86
7.3.2 The Green's Functions 87
7.3.3 Double Infinite Sums 88
7.3.4 Evaluating the Smoothed Green's Functions 89
7.3.5 The Correction Terms 92
7.3.6 The λ Singularity 94
7.3.7 Size 96
7.4 Acceleration Techniques 97
7.4.1 Fast Fourier Transforms 97
7.4.2 Green's Function Precomputing and Storage 100
7.4.3 Symmetry 102
7.4.4 Interpolation 103

7.4.5 GMRES 104

8 Results **106**

8.1 Richardson Extrapolation 106

8.2 A Green's Function Test 107

8.3 Integrals on Curved Surfaces 110

8.4 A Flat Slab Scattering Problem 111

8.4.1 Derivation of the Flat Slab Test Case 112

8.4.2 Results in the Flat Slab Test Case 115

8.5 Smooth Dimpled Scatterer 115

8.6 Non-Smooth Dimpled Scatterer 119

8.7 Corrugated Roof Surface 120

8.8 Discussion of Results 127

9 Conclusion **130**

A Derivatives of the Green's Functions **132**

A.1 Fourier Form 132

A.2 Ewald Form G1 133

A.3 Ewald Form G2 135

B The Poisson Summation Formula **137**

C The Exponential Integral Function **142**

C.1 Singularities 143

C.2 Decay 144

D An Alternate Derivation for a Correction Term **146**

Bibliography **155**

Biography **160**

List of Tables

8.1 Table of Results for Single and Double Layer Potentials on a Smooth Dimpled Surface 112

List of Figures

6.1 G, G_δ comparison 59

8.1 One periodic block of the flat slab scatterer 108

8.2 One periodic block of the smooth, dimpled scatterer 111

8.3 The flat slab scattering problem 113

8.4 The flat slab test case. On the left are the numerical approximations with corrections. On the right, the corrections have been omitted. N=32. $\epsilon = 5$. $\delta = h$. 116

8.5 The flat slab test case for N=16. $\epsilon = 5$. $\delta = h$. 116

8.6 The flat slab test case with $\epsilon = 15$. $N = 32$. $\delta = h$. 117

8.7 The flat slab test case with $\epsilon = 15 + 0.5i$. $N = 32$. $\delta = h$. 117

8.8 Transmission coefficients for the smooth dimpled scatterer. $\epsilon = 15$. $N = 32$. $\delta = h$. 118

8.9 Numbers of GMRES iterations for the smooth dimpled scatterer. $\epsilon = 15$. $N = 32$. $\delta = h$. 119

8.10 One periodic block of the non-smooth dimpled scatterer 120

8.11 Transmission coefficients for the non-smooth dimpled scatterer. $\epsilon = 15$. $N = 32$. $\delta = h$. 121

8.12 One periodic block of the corrugated roof scatterer 122

8.13 Transmission coefficients for the corrugated roof scatterer. $\epsilon = 15$. $N = 32$. $\delta = h$. 123

8.14 Closer look at the $\omega = 0.37$ resonance for the corrugated roof scatterer. $N = 32$. $\epsilon = 15$. $C = 0.25.\delta = h$ 124

8.15 The $\omega = 0.37$ resonance for three values of the coefficient C on the corrugated roof scatterer. $N = 32$. $\epsilon = 15$. $\delta = h$ 125

8.16 Richardson ratios (8.1) for the transmission coefficients on the corrugated roof scatterer for $N = 16$, $N = 24$, and $N = 32$. $\epsilon_{int} = 15$. $\delta = h$. 126

8.17 One periodic block of the wavy roof scatterer 127

8.18 Transmission coefficients for the wavy roof scatterer with $L = \pi$. $N = 32$. $\epsilon = 15$. $C = 0.25 . \delta = h$ 128

Chapter 1

Introduction

We here present an accurate numerical method for scattering of 3D electromagnetic waves by doubly periodic structures. The method is an intuitively simple numerical scheme based on a boundary integral formulation. This scheme involves smoothing the singular Green's functions in the integrands and finding correction terms to the resulting smooth integrals. The analytical method is based on the singular integral methods of J. Thomas Beale [6] [8] [7], while the scattering problem is motivated by the work of Stephanos Venakides, Mansoor Haider, Stephen Shipman, and Andrew Barnes [42] [21] [34] [33] [35] [5].

Periodic scattering problems are of interest to electrical engineers and physicists who apply them to photonic crystal lattices [14] [30] [18] [22] [37]. The propagation of waves through such lattices depends sensitively on the crystals' geometry, their material properties, and on the nature of the incident waves. The recent numerical and experimental discoveries of resonances in transmission have generated interest in periodic electromagnetic scattering problems [15] [47] [19]. They are of interest to

those who would hope to use them in the design of electrical and optical devices.

Much numerical work investigating these problems and resonances has been done in the 2D case [42] [21] [34] [33], but little work has been done in the 3D problem. There is numerical evidence of Fano resonances in the 3D case [5], but it appears to be difficult to resolve them with first order methods. Besides savings in time, a higher order method is desirable in electromagnetic scattering in order to more fully resolve these resonances.

We outline the mathematics and physics of the scattering problem in Chapter 2. Maxwell's equations govern the behavior of electromagnetic waves. In scattering problems, it is common to represent solutions of Maxwell's equations as boundary integrals over the surface of the scatterer [28] [43]. In 3D problems, singularities in the integrals can cause low accuracy in basic numerical schemes, and the Green's functions found in the integrands are very time consuming to evaluate numerically. In periodic problems, these issues are more complicated, since the singularities are less straightforward and the Green's functions converge more slowly. We derive and examine these Green's functions in Chapter 3.

Methods that deal with these problems are usually rather involved and use complicated boundary elements [5] [30] [14] [46]. Using a representation of the Green's functions developed by P.P. Ewald known as Ewald splitting [17] in connection with local analysis of the singularity, we deal with these issues in an effective and straightforward way. Following the 2D work of Venakides and Shipman [42], we derive the Ewald splitting method for a 3D problem in Chapter 5. Other methods of dealing with the periodic Green's function include summation by parts [9], lattice sums [45],

and various other transformation methods [23] [25] [36].

In solving these problems, we have used the Müller integral equation formulation [27], since it is a Fredholm integral equation of the second kind and is well posed. Müller derived his equations for the case of a compact scatterer. We outline the derivation and adapt it to a periodic scatterer in Chapter 4. The singularities in question occur in the periodic Helmholtz Green's function (3.10) and its derivatives:

$$G(x,y,z) = \frac{1}{8\pi^2} \sum_{n,m} \frac{e^{-\sqrt{-\lambda_{mn}}|z|}}{\sqrt{-\lambda_{mn}}} e^{im(x)+in(y)}$$

where the sum over n and m is a doubly infinite sum.

Several difficulties arise from the properties of this sum. At $z = z'$ the sum diverges, and for small values of $|z - z'|$, it converges very slowly. Furthermore, it is not clear how to regularize the singularity, since multiplying by customary smoothing functions will destroy the function's periodicity. We use the Ewald representation of the Green's function in order to deal with the singularity and to speed up convergence. This Ewald method splits the sum into a local sum and a smooth sum. The singularity in the function is entirely contained in the local sum. The two Ewald sums converge more quickly than the Fourier representation above, and, with this technique, it is possible to regularize the Green's function in a natural way while maintaining periodicity, which we outline in Chapter 6.

The Müller formulation involves singular integrals of surface currents that include single layer potentials, double layer potentials, and one more complicated integral involving tangential derivatives of the Green's functions. For each of these, we replace the Green's functions in question with their regularized, but still periodic, counter-

parts. A smoothing parameter δ controls the radius of the smoothing, and we set it on the order of the grid spacing h. The smoothing has a local effect like replacing a $1/r$ singularity with the smooth function $\frac{\mathrm{erf}(r/\delta)}{r}$. In Chapter 6, we do local analysis of the singularity in order to identify the largest sources of error introduced by this smoothing. From this analysis, we derive correction terms for each integral that remove the largest part of this smoothing error. We prove that with the correction terms, the smoothing error in the integrals is $O(\delta^3)$. Estimates exist [7] that show the discretization error in numerically evaluating these integrals is also small [7]. The correction involves various Taylor expansions, and the method thus requires a surface in C^3.

The correction terms for the smoothed integrals are derived through analysis near the singularity. The derivation involves transforming to principal directions using concepts from differential geometry. The correction terms are necessarily invariant under this transformation and depend on geometric properties of the scatterer such as the mean curvature and the differential of the Gauss map.

With the ability to evaluate the integrals to a higher order, we implement a GMRES algorithm to approximate solutions of the integral equation. We outline the implementation in Chapter 7. From these solutions, we can compute the scattered fields and transmission coefficients. We implement the method to perform the integration for any C^3 surface periodic in x and y with a finite thickness in z given by $z = f(x, y)$.

The scattering problem is exactly solvable for a flat slab scatterer. This provides a test case for our method. The derivation of the test case and numerical results

are given in Chapter 8. Agreement in the test case is excellent. Chapter 8 includes results on various curved scatterers as well. In all cases, third order convergence is observed. In general, as frequencies increase, the error also increases. In previous work, grids had to be refined for even small increases in the frequency in order to obtain reliable results [5]. Our method significantly extends the range of coefficients obtainable without refining a grid.

In addition to the Ewald splitting, we employ other time saving techniques for implementing the method. These are outlined in Chapter 7. The most significant of these is the evaluation of one of the Ewald summations using fast Fourier transforms. To reduce the number of evaluations of expensive exponential integrals, we use FFTs to precompute and store sums. This technique actually leads to savings in both the smooth and the local parts of the Ewald sum.

In Chapter 8 we present results in which certain resonances known as Wood's anomalies are resolved very nicely. Wood's anomalies are present at certain frequencies at which singularities in the Green's functions exist and have been observed experimentally [44] [47] [19]. We present results of resonant behavior consistent with predicted results for Wood's anomalies. Our Wood's anomaly resonances are unique from previously known anomalies in that they occur near singularities of the interior Green's function instead of the exterior Green's function.

The scattering problem presented in this thesis is motivated by the 2D problems of Venakides and Shipman [21]. We follow their approach in defining the problem and in using Ewald summation to evaluate the Green's functions. The problem was previously solved in 3D by Barnes [5], who used a boundary element method

to approximate solutions with $O(h)$ accuracy. Our method is more intuitive and more accurate. The increased accuracy appears to be beneficial in terms of resolving resonant peaks in transmission. Barnes was able to implement his method for a more general class of scatterers than we here implement, but our method is adaptable to more general geometries.

Chapter 2

Electromagnetic Scattering

The scattering of electromagnetic radiation by various media is an active field of both theoretical and experimental study. In a scattering experiment, an object called the scatterer is introduced to a region in which traveling electromagnetic waves are present. The scatterer has different electromagnetic properties than the medium through which the waves were initially traveling. The goal of the problem is to determine the effect of the scatterer - to find the resulting electric and magnetic fields in all of $\mathbb{R}^3$.

2.1 Maxwell's Equations

Maxwell's equations describe the behavior of electromagnetic waves. These are linear partial differential equations in the vector valued electric field **E** and magnetic field **H**. In the absence of any electric or magnetic sources, these equations are

$$\begin{aligned}
\nabla \times \mathbf{H} &= \epsilon\mu \frac{\partial \mathbf{E}}{\partial t} \\
\nabla \times \mathbf{E} &= -\frac{\partial \mathbf{H}}{\partial t} \\
\nabla \cdot \mathbf{E} &= 0 \\
\nabla \cdot \mathbf{H} &= 0
\end{aligned} \tag{2.1}$$

where ϵ and μ are properties of the medium in which the waves are traveling, known respectively as electric permittivity and magnetic permeability. We will work only with materials for which ϵ and μ are constants - electromagnetically homogeneous materials. Travelling waves can be characterized by their frequency ω. We will assume t dependence in the fields of the form $e^{-i\omega t}$. Then (2.1) become the time-independent Maxwell's equations:

$$\begin{aligned}
\nabla \times \mathbf{H} &= -i\omega\epsilon\mu \mathbf{E} \\
\nabla \times \mathbf{E} &= i\omega \mathbf{H} \\
\nabla \cdot \mathbf{E} &= 0 \\
\nabla \cdot \mathbf{H} &= 0
\end{aligned} \tag{2.2}$$

where $\mathbf{E}$ and $\mathbf{H}$ are now functions of $\mathbf{x}$ only. Taking the curl of the first two of these equations gives:

$$\nabla \times (\nabla \times \mathbf{H}) = -i\omega\epsilon\mu \, (\nabla \times \mathbf{E}) = \omega^2 \epsilon\mu \mathbf{H}$$

$$\nabla \times (\nabla \times \mathbf{E}) = i\omega \, (\nabla \times \mathbf{H}) = \omega^2 \epsilon\mu \mathbf{E}$$

Remembering that $\mathbf{E}$ and $\mathbf{H}$ are divergence free (2.1), the vector calculus identity

$$\nabla \times (\nabla \times \mathbf{A}) = \nabla \, (\nabla \cdot \mathbf{A}) - \nabla \cdot \nabla \mathbf{A}$$

allows us to see that our fields each satisfy the Helmholtz equation:

$$\begin{aligned} \Delta \mathbf{E} + \omega^2 \epsilon \mu \mathbf{E} &= 0 \\ \Delta \mathbf{H} + \omega^2 \epsilon \mu \mathbf{H} &= 0 \end{aligned} \tag{2.3}$$

Finally, we let $k^2 = \omega^2 \epsilon \mu$, so the equations that we will solve in our scattering experiments are

$$\begin{aligned} \Delta \mathbf{E} + k^2 \mathbf{E} &= 0 \\ \Delta \mathbf{H} + k^2 \mathbf{H} &= 0 \end{aligned}$$

2.2 Scattering

In a scattering experiment, we start with incident fields $\mathbf{E}_{inc}$ and $\mathbf{H}_{inc}$ that are smooth and that satisfy (2.3) in all of $\mathbb{R}^3$. We introduce a scatterer - a domain $\Omega \subset \mathbb{R}^3$. The objective of the experiment is to determine the resulting total electric and magnetic fields in both Ω and in $\Omega^C = \mathbb{R}^3 \setminus \Omega$. The fields in Ω are called the interior fields and are denoted here as $\mathbf{E}_{int}$ and $\mathbf{H}_{int}$. The fields in Ω^C are the exterior fields $\mathbf{E}_{ext}$ and $\mathbf{H}_{ext}$. Finally, in Ω^C the differences between the exterior and incident fields are called the scattered fields $\mathbf{E}_{scatt} = \mathbf{E}_{ext} - \mathbf{E}_{inc}$ and $\mathbf{H}_{scatt} = \mathbf{H}_{ext} - \mathbf{H}_{inc}$.

For our methods, the surface of the scatterer $\partial\Omega$ must be in C^3. This will be important in certain Taylor series taken on the surface in Chapter 6. The constants ϵ and μ of the scatterer are different than those of its exterior. In Ω we will call these ϵ_{int} and μ_{int}. In Ω^C they will be ϵ_{ext} and μ_{ext}. Although each of these four constants can take any value in $\mathbb{C}$, we will always take $\epsilon_{ext} = 1$ and $\mu_{ext} = \mu_{int} = 1$. Such an assumption is consistent with natural materials and with current scattering experiments [42] [21] [34]. The permittivity of the scatterer ϵ_{int} is also known as

its dielectric contrast. Materials for which ϵ_{int} is real-valued are known as lossless materials, and materials for which ϵ_{int} has an imaginary part are called lossy.

2.3 3D Doubly Periodic Scatterers

We will work in $\mathbb{R}^3$ and will use scatterers Ω that are periodic in the x and y directions and of finite thickness in the z direction. Specifically, we will work with scatterers that are 2π periodic in both the x and y directions, although generalization to any period is not difficult. We have done numerical simulations only for scatterers where $\partial\Omega$ can be represented as a function of x and y - surfaces where $z = f(x, y)$ for some f sufficiently smooth. We specify two such functions $F_1(x, y)$ and $F_2(x, y)$ that represent the front and the back of the scatterer. These functions must be 2π periodic in both x and y and cannot intersect.

The method developed in this thesis, however, is fully adaptable to any Ω such that $\partial\Omega$ is in C^3. Extension of our results to a more general surface can be done through establishing coordinate patches to cover the surface as in [7].

Our methods allow us to do all of our calculations on just one period in both x and y of the scatterer. From this point on, we will let Ω and $\partial\Omega$ refer to just one periodic block of the scatterer.

Periodic scatterers are of interest as they simulate the surfaces of diffraction gratings or the structure of photonic crystals. Using a periodic scatterer introduces many difficulties that are absent with a compact scatterer. The most significant difficulty is in the fact that the periodic Green's functions involved do not have a simple, closed form like the free-space Green's functions.

2.4 The Scattering Problem

Our problem then is to solve (2.3) in the presence of the scatterer. For this problem to be fully specified, we need boundary conditions on $\partial\Omega$ and radiation conditions that the fields satisfy at $\pm\infty$. The boundary conditions at an electromagnetic interface are tangential continuity:

$$\begin{aligned} \mathbf{n} \times \mathbf{E}_{ext} &= \mathbf{n} \times \mathbf{E}_{int} \\ \mathbf{n} \times \mathbf{H}_{ext} &= \mathbf{n} \times \mathbf{H}_{int} \end{aligned} \tag{2.4}$$

Generally, the Silver-Müller [27] radiation conditions are used in electromagnetic scattering problems. These ensure that the scattered waves propagate and decay properly. For periodic problems, however, a modified set of radiation conditions is necessary [33]. These conditions still ensure that the fields propagate or decay at $\pm\infty$ but also require them to maintain pseudoperiodicity (see Section 2.6). We require that the scattered fields have the form

$$\begin{aligned} \mathbf{E} &= \sum_{m,n} \mathbf{E}^{\pm}_{mn} e^{-\sqrt{-\lambda_{mn}}|z|} e^{i(m+\alpha)x + i(n+\beta)y} \\ \mathbf{H} &= \sum_{m,n} \mathbf{H}^{\pm}_{mn} e^{-\sqrt{-\lambda_{mn}}|z|} e^{i(m+\alpha)x + i(n+\beta)y} \end{aligned} \tag{2.5}$$

as $z \to \pm\infty$. Here $\lambda_{mn} = k^2 - (m+\alpha)^2 - (n+\beta)^2$, and $\mathbf{E}^{\pm}_{mn}$ and $\mathbf{H}^{\pm}_{mn}$ are constant vectors as $z \to \pm\infty$. Since our fields are periodic, they can be written as Fourier series. These radiation conditions specify large z behavior of the modes in such series. The negative sign in the exponentials ensures that the modes decay whenever $\mathrm{Re}\left(\sqrt{-\lambda_{mn}}\right)$ is nonzero. If, however, $\mathrm{Re}\left(\sqrt{-\lambda_{mn}}\right) = 0$, we must choose the

negative square root instead of the principal square root so that the waves propagate in the correct direction (from negative to positive z). That is, we must choose $\text{Im}\left(\sqrt{-\lambda_{mn}}\right) < 0$. We adopt the same sign conventions for the modes of the Green's function that will be introduced in Chapter 3.

2.5 The Incident Wave

We will always take the incident wave to be a plane wave propagating from the negative z to positive z direction. The direction of the incident wave is given by the unit vector $\vec{\gamma} = (\gamma_1, \gamma_2, \gamma_3)$. In spherical coordinates with azimuthal angle θ and polar angle from the z-axis ϕ, $\vec{\gamma}$ is

$$\begin{pmatrix} \gamma_1 \\ \gamma_2 \\ \gamma_3 \end{pmatrix} = \begin{pmatrix} \cos\theta \sin\phi \\ \sin\theta \sin\phi \\ \cos\phi \end{pmatrix}$$

For a plane wave, the electric and magnetic fields are contained in planes perpendicular to the direction of propagation $\vec{\gamma}$. The directions of polarization

$$\vec{u_\theta} = \frac{\frac{d\vec{\gamma}}{d\theta}}{\left|\frac{d\vec{\gamma}}{d\theta}\right|} = \begin{pmatrix} -\sin\theta \\ \cos\theta \\ 0 \end{pmatrix} \quad \text{and} \quad \vec{u_\phi} = \frac{\frac{d\vec{\gamma}}{d\phi}}{\left|\frac{d\vec{\gamma}}{d\phi}\right|} = \begin{pmatrix} \cos\theta\cos\phi \\ \sin\theta\cos\phi \\ -\sin\phi \end{pmatrix}$$

define these planes. The electric and magnetic fields must be linear combinations of these two vectors. We call a field θ-polarized or ϕ-polarized if it is in the $\vec{u_\theta}$ or $\vec{u_\phi}$ direction, respectively. For a plane wave,

$$\mathbf{E}_{inc}(x, y, z) = e^{ik(\gamma_1 x + \gamma_2 y + \gamma_3 z)} \left[a\vec{u_\theta} + b\vec{u_\phi}\right] = e^{ik\vec{\gamma}\cdot\mathbf{x}} \left[a\vec{u_\theta} + b\vec{u_\phi}\right]$$

for constants a and b. It is easy to check that this equation satisfies the Helmholtz equation (2.3) and that the field is divergence free. Keeping in mind that for an

incident wave $\epsilon_{ext} = \mu_{ext} = 1$, we can see from Maxwell's equations (2.2) that the corresponding magnetic field is

$$\mathbf{H}_{inc}(x, y, z) = e^{ik\vec{\gamma}\cdot\mathbf{x}}\left[b\vec{u_\theta} - a\vec{u_\phi}\right]$$

Since the incident field propagates from negative z to positive z and since the time dependent part of the waves is $e^{-i\omega t}$, we must have

$$0 \leq \phi < \frac{\pi}{2} \quad \text{and} \quad \gamma_3 > 0$$

Often, we are interested in normally incident plane waves. In this special case, ϕ and θ are both zero, and the direction vector is

$$\vec{\gamma} = \begin{pmatrix} 0 \\ 0 \\ 1 \end{pmatrix}$$

The directions of polarization are just the unit vectors in the x and y directions

$$\vec{u_\phi} = \begin{pmatrix} 1 \\ 0 \\ 0 \end{pmatrix} \quad \text{and} \quad \vec{u_\theta} = \begin{pmatrix} 0 \\ 1 \\ 0 \end{pmatrix}$$

Thus, a normally incident ϕ-polarized electric field looks like

$$\mathbf{E} = e^{ik\vec{\gamma}\cdot\mathbf{x}}\vec{u_\phi} = \begin{pmatrix} e^{ikz} \\ 0 \\ 0 \end{pmatrix} \tag{2.6}$$

and has a corresponding magnetic field

$$\mathbf{H} = e^{ik\vec{\gamma}\cdot\mathbf{x}}\vec{u_\theta} = \begin{pmatrix} 0 \\ e^{ikz} \\ 0 \end{pmatrix} \tag{2.7}$$

2.6 Pseudoperiodicity of the Fields

Our incident fields are not quite periodic. Since $\epsilon_{ext} = \mu_{ext} = 1$, the products $k\gamma_1$ and $k\gamma_2$ are real valued and can be written as

$$k\gamma_1 = \hat{m} + \alpha \quad \text{and} \quad k\gamma_2 = \hat{n} + \beta$$

for some integers $\hat{m}$ and $\hat{n}$ and some constants $\alpha, \beta \in \left(-\frac{1}{2}, \frac{1}{2}\right]$. The constants α and β depend on k and on the angles of incidence ϕ and θ. Since $\vec{\gamma}$ is a unit vector, we can write γ_3 in terms of α and β

$$\begin{aligned}
\gamma_3 &= \sqrt{1 - \gamma_1^2 - \gamma_2^2} \\
&= \sqrt{1 - \left(\frac{\hat{m} + \alpha}{k}\right)^2 - \left(\frac{\hat{n} + \beta}{k}\right)^2} \\
&= \frac{\sqrt{k^2 - (\hat{m} + \alpha)^2 - (\hat{n} + \beta)^2}}{k}
\end{aligned}$$

Then our electric field becomes

$$\begin{aligned}
\mathbf{E}_{inc}(x, y, z) &= e^{ik(\gamma_1 x + \gamma_2 y + \gamma_3 z)} \left[a\vec{\theta} + b\vec{\phi}\right] \\
&= e^{i(\hat{m}+\alpha)x + i(\hat{n}+\beta)y + i\sqrt{k^2 - (\hat{m}+\alpha)^2 - (\hat{n}+\beta)}z} \left[a\vec{\theta} + b\vec{\phi}\right] \\
&= e^{i(\alpha x + \beta y)} e^{i\hat{m}x + i\hat{n}y + i\sqrt{k^2 - (\hat{m}+\alpha)^2 - (\hat{n}+\beta)^2}z} \left[a\vec{\theta} + b\vec{\phi}\right]
\end{aligned}$$

The function

$$e^{i(\alpha x + \beta y)}$$

is not necessarily 2π periodic in x and y. We will call it a phasor function. The incident electric field can now be written as a product of a phasor function with a

doubly periodic function:

$$\mathbf{E}_{inc}(x,y,z) = e^{i(\alpha x+\beta y)} e^{i\hat{m}x+i\hat{n}y+i\sqrt{k^2-(\hat{m}+\alpha)^2-(\hat{n}+\beta)}z} \left[a\vec{\theta}+b\vec{\phi}\right]$$

Since the incident fields are doubly 2π periodic up to a phasor function, we call them pseudoperiodic. The pseudoperiodicity will be accounted for in our Green's functions and is enough for us to be able to limit all calculations to one periodic block of the scatterer.

For normally incident fields, the constants α and β are both zero, and the fields are periodic and not merely pseudoperiodic.

2.7 Transmission

A quantity of interest in scattering problems is the transmission coefficient T. This is a relative measure of energy that compares the energy in the incident fields to that in the total external fields far from the scatterer. The Poynting vector

$$\mathbf{S} = \bar{\mathbf{E}} \times \mathbf{H}$$

is a measurement of an electromagnetic field's energy flux [20]. Here $\bar{\mathbf{E}}$ is the complex conjugate of $\mathbf{E}$. For any surface F far from the scatterer Ω and normal to the incident fields, we define the incident and transmitted energy flows by

$$U_{inc} = \int_F \mathrm{Re}\left(\mathbf{S}_{inc}(\mathbf{x}) \cdot \mathbf{n}(\mathbf{x})\right) dS(\mathbf{x})$$

$$U_{tran} = \int_F \mathrm{Re}\left(\mathbf{S}_{ext}(\mathbf{x}) \cdot \mathbf{n}(\mathbf{x})\right) dS(\mathbf{x})$$

where $\mathbf{n}$ is an outward unit normal to F. These flows are measures of the energy passing through the surface F. Then the transmission coefficient is defined as

$$T = \sqrt{\frac{U_{tran}}{U_{inc}}} \tag{2.8}$$

We take the surface F to be far enough from Ω that the decaying modes of the field are negligible, and only the propagating modes contribute to the calculation.

The scattering problems of this thesis will have normally incident fields. We will deal with the case where the incident wave is a uniform plane wave traveling in the z direction. With such a wave, the form of the transmission coefficient is more simple. The incident electric and magnetic fields are as in (2.6) and (2.7). Then

$$\mathbf{S}_{inc} = \begin{bmatrix} 0 \\ 0 \\ 1 \end{bmatrix} \quad \text{and} \quad U_{inc} = 4\pi^2$$

2.8 Transmission Resonances

Of particular interest in scattering problems are frequencies near which the transision coefficient changes dramatically. A sudden, sharp rise or fall in transmission is a behavior known to occur near resonant frequencies — frequencies where the linear system of integral equations is singular. Resonant behavior corresponds to real frequencies close to an imaginary frequency for which there is a zero eigenvalue in the linear system [33]. Resonant phenomena of materials are of interest scientifically as there is potential to exploit them in optical devices. Various resonances have been observed in photonic crystals both theoretically and experimentally [14] [18] [15] [22] [37]. Our periodic scatterers model such crystals.

The Wood's anomaly is a specific type of resonance that has been observed in photonic crystal scattering experiments. These resonances can have various effects on the transmission, but they always result from waves that travel in a direction nearly parallel to the scatterer. The constants λ_{mn} in the radiation conditions are a measure of this. When λ_{mn} is close to zero, the m, n mode is almost orthogonal to the incident wave. Numerically, this situation corresponds to a singularity in λ_{mn} in the Green's function (see Section 3.4).

Wood's anomalies have been observed and discussed in [44], [47], and [19].

Chapter 3

The Green's Functions

A Green's function for the free space Helmholtz equation must satisfy

$$\Delta G(\mathbf{r}) + k^2 G(\mathbf{r}) = -\delta(\mathbf{r})$$

It can be shown that

$$G(\mathbf{r}) = \frac{e^{ik\mathbf{r}}}{4\pi\mathbf{r}} \tag{3.1}$$

satisfies this equation. It is an outgoing solution since the t dependence of the fields is $e^{-i\omega t}$.

3.1 A Periodic Green's Function Condition

A periodic Green's function must satisfy

$$\Delta G(x,y,z) + k^2 G(x,y,z) = -\delta(z) \sum_{\mu,\nu} \delta(x + 2\pi\mu)\,\delta(y + 2\pi\nu) \tag{3.2}$$

where the sums over μ and ν are from $-\infty$ to ∞. The values of x and y may fall within one period ($0 \leq x, y < 2\pi$), and the summation of delta functions represent periodic

reflections of this period. They ensure the inclusion of each period's contribution to a solution. Of course, our problem is not strictly periodic but is pseudoperiodic (see Section 2.6). The condition that we need to satisfy is actually

$$\Delta G(x,y,z) + k^2 G(x,y,z) = -\delta(z)\, e^{i(\alpha x+\beta y)} \sum_{\mu,\nu} \delta(x+2\pi\mu)\,\delta(y+2\pi\nu) \tag{3.3}$$

where α and β are as defined in Section 2.6. We will seek a Green's function that, like the incident fields, is pseudoperiodic:

$$G(x,y,z) = e^{i(\alpha x+\beta y)} G_{per}(x,y,z)$$

for a doubly periodic function G_{per}.

3.2 Derivation of the Periodic Green's Function

To find a Green's function that satisfies (3.3), we first see that since G_{per} is periodic in x and y, it can be written as a Fourier series:

$$\begin{aligned} G(x,y,z) &= e^{i(\alpha x+\beta y)} G_{per}(x,y,z) \\ &= e^{i(\alpha x+\beta y)} \sum_{m,n} \tilde{G}_{mn}(z)\, e^{i(mx+ny)} \\ &= \sum_{m,n} \tilde{G}_{mn}(z)\, e^{i[(m+\alpha)x+(n+\beta)y]} \end{aligned} \tag{3.4}$$

for some coefficient functions $\tilde{G}_{mn}(z)$. Again, the sums over m and n are both from $-\infty$ to ∞. For the remainder, we will use μ and ν as indexes to represent the physical periodic reflections as in (3.2), and we will use m and n as indexes

representing Fourier modes. The right hand side of (3.2) can be written in another form using the Poisson summation formula (see Appendix B):

$$-\delta(z)\sum_{\mu,\nu}\delta(x+2\pi\mu)\,\delta(y+2\pi\nu)=\frac{-\delta(z)}{4\pi^2}\sum_{m,n}e^{i(mx+ny)} \tag{3.5}$$

The derivatives of G are

$$G_{xx}(x,y,z)=\sum_{m,n}-(m+\alpha)^2\,\tilde{G}_{mn}(z)\,e^{i[(m+\alpha)x+(n+\beta)y]}$$

$$G_{yy}(x,y,z)=\sum_{m,n}-(n+\beta)^2\,\tilde{G}_{mn}(z)\,e^{i[(m+\alpha)x+(n+\beta)y]}$$

$$G_{zz}(x,y,z)=\sum_{m,n}D_{zz}\tilde{G}_{mn}(z)\,e^{i[(m+\alpha)x+(n+\beta)y]}$$

The condition that the Green's function must satisfy (3.3) becomes

$$\begin{aligned}\Delta G(x,y,z)+k^2G(x,y,z)&=\sum_{m,n}-\left[(m+\alpha)^2+(n+\beta)^2-k^2\right]\tilde{G}_{mn}e^{i[(m+\alpha)x+(n+\beta)y]}\\&\quad+\sum_{m,n}D_{zz}\tilde{G}_{mn}e^{i[(m+\alpha)x+(n+\beta)y]}\\&=-\delta(z)\sum_{m,n}e^{i[(m+\alpha)x+(n+\beta)y]}\end{aligned}$$

So, matching coefficients, we need

$$D_{zz}\tilde{G}_{mn}(z)-\left[(m+\alpha)^2+(n+\beta)^2-k^2\right]\tilde{G}_{mn}(z)=\frac{-\delta(z)}{4\pi^2} \tag{3.6}$$

Without the delta function on the right hand side, this equation would have a general solution consisting of the sum of a positive and a negative exponential function. Of course these are smooth and cannot satisfy (3.6). The function

$$\tilde{G}_{mn}(z)=C_{mn}e^{-\sqrt{(m+\alpha)^2+(n+\beta)^2-k^2}|z|} \tag{3.7}$$

for constants C_{mn} has a discontinuity in its derivative at $z = 0$ and therefore may be made to satisfy our equation. A solution without the negative in the exponential could also satisfy (3.6), but we need the negative sign to ensure that each mode of the Fourier series (3.4) satisfies the radiation conditions (2.5). We must now choose the C_{mn}'s so that the delta function condition of (3.6) is satisfied. We integrate:

$$\int_{-\epsilon}^{\epsilon} \left[D_{zz}\tilde{G}_{mn}(z) - \left[(m+\alpha)^2 + (n+\beta)^2 - k^2 \right] \tilde{G}_{mn}(z) \right] dz = \int_{-\epsilon}^{\epsilon} \frac{-\delta(z)}{4\pi^2} dz = -\frac{1}{4\pi^2}$$

Then

$$D_z\tilde{G}_{mn}(z)\Big|_{-\epsilon}^{\epsilon} - \int_{-\epsilon}^{\epsilon} \left[(m+\alpha)^2 + (n+\beta)^2 - k^2 \right] \tilde{G}_{mn}(z)\, dz = -\frac{1}{4\pi^2} \tag{3.8}$$

Knowing from (3.7) that the $\tilde{G}_{mn}(z)$ are continuous, we see that the integral in (3.8) tends to 0 as $\epsilon \to 0$. In this limit (3.8) becomes

$$\left[D_z\tilde{G}_{mn}(0) \right]_-^+ = -\frac{1}{4\pi^2}$$

From (3.7),

$$D_z\tilde{G}_{mn}(z) = -C_{mn}\,\mathrm{sgn}(z) \sqrt{(m+\alpha)^2 + (n+\beta)^2 - k^2}\, e^{-\sqrt{(m+\alpha)^2+(n+\beta)^2-k^2}|z|}$$

So

$$\left[D_z\tilde{G}_{mn}(0) \right]_-^+ = -2C_{mn}\sqrt{(m+\alpha)^2 + (n+\beta)^2 - k^2}$$

$$= -\frac{1}{4\pi^2}$$

And

$$C_{mn} = \frac{1}{8\pi^2\sqrt{(m+\alpha)^2 + (n+\beta)^2 - k^2}}$$

Thus the following Fourier series is a Green's function for the periodic Helmholtz equation:

$$G(x,y,z) = \frac{1}{8\pi^2} \sum_{m,n} \frac{e^{-\sqrt{(m+\alpha)^2+(n+\beta)^2-k^2}|z|}}{\sqrt{(m+\alpha)^2+(n+\beta)^2-k^2}} e^{i[(m+\alpha)x+(n+\beta)y]} \tag{3.9}$$

3.3 The Green's Function

We will let $P_{mn} = e^{i[(m+\alpha)x+(n+\beta)y]}$ and $\lambda_{mn} = k^2 - (m+\alpha)^2 - (n+\beta)^2$. Then

$$G(x,y,z) = \frac{1}{8\pi^2} \sum_{m,n} \frac{e^{-\sqrt{-\lambda_{mn}}|z|}}{\sqrt{-\lambda_{mn}}} P_{mn} \tag{3.10}$$

We will need all first and second derivatives of this function. A list of these derivatives can be found in Appendix A.

3.4 Properties of the Green's Function

Although it is not clear from its appearance, this periodic Green's function has the same $1/4\pi\mathbf{r}$ singularity as the free space Green's function (3.1). It is clear that this series diverges at $z = 0$. The singularity in this function will be explored more in Chapters 5 and 6.

The constant $\lambda_{mn} = \omega^2\epsilon\mu - (m+\alpha)^2 - (n+\beta)^2$ is important and determines the nature of each Fourier mode in the Green's function. The physical constant ϵ can have a positive imaginary part, so, in general, $k^2 = \omega^2\epsilon\mu$ is a complex number with positive imaginary part. For z away from 0, each mode of the Green's function (3.10) is analytic in λ_{mn} for all λ_{mn} in the upper half complex plane except for

$\lambda_{mn} = 0$. Since λ_{mn} never has a negative imaginary part, we can take the customary branch cut for the square root function - the negative real axis. The negative sign in the exponential in (3.10) ensures that the modes decay whenever $\mathrm{Re}\left(\sqrt{-\lambda_{mn}}\right)$ is nonzero. If, however, $\mathrm{Re}\left(\sqrt{-\lambda_{mn}}\right) = 0$, we must choose the negative square root instead of the principal square root so that the waves propagate in the correct direction (so that they satisfy the radiation conditions (2.5)). That is, we must choose $\mathrm{Im}\left(\sqrt{-\lambda_{mn}}\right) < 0$.

Much of the physical interest in scattering deals with lossless media (see Section 2.2) where the λ_{mn} are real-valued. In this case, there are a finite number of modes (including $m = n = 0$) for which $\sqrt{-\lambda_{mn}}$ is purely imaginary. These modes are known as oscillating or propagating modes [42]. They occur for the finite number of integers m and n such that

$$m^2 + n^2 < k^2$$

The infinite number of other modes all decay as $z \to \pm\infty$ and are known as decaying modes. It is possible that $\lambda_{mn} = 0$ for one mode, in which case there is a λ singularity in the Green's function (3.10). At this singularity, the Green's function must take on another form with a linear term. In scattering problems at frequencies where λ_{mn} is close to zero for an m and n, these singularities give rise to transmission resonances known as Wood's anomalies (see Sections 2.8 and 7.3.6)

3.5 Derivatives of the Green's Function

We have derived the Green's function as a function of $\mathbf{x} = (x, y, z)$. In Chapter 5, we also treat the Green's function in this way. In practice, however, the Green's

function is always evaluated at $\mathbf{x}' - \mathbf{x}$. When derivatives of the Green's function are necessary, it is the function $G(\mathbf{x}' - \mathbf{x})$ that we must differentiate with respect to $\mathbf{x}$. Thus $D_x G = D_x(G(\mathbf{x}' - \mathbf{x}))$. We state this here to avoid any ambiguity in the notation.

Chapter 4

The Integral Equations

The scattering problem defined by the Helmholtz equations (2.3), the boundary conditions of tangential continuity (2.4), the radiation conditions (2.5), and the scatterer can be rewritten as a system of integral equations on the boundary $\partial\Omega$ known as the Müller integral equations. There are three main advantages to working with these integral equations instead of the differential equations: (1) the theoretical properties of the integral equation are desirable, (2) we do not need artificial boundary conditions to truncate the problem and are able instead to use the very natural radiation conditions, and (3) by working only on the boundary, we reduce the dimension of the problem from three dimensional space to a two dimensional surface. In addition, by working with integrals we can avoid the numerical issues of stability that arise in finite difference methods. The cost of this is numerical - in the end, we have a dense linear system to solve instead of a sparse system, and the memory costs are very high. See [28] and [43] for more details.

The Müller integral equations are a set of electromagnetic integral equations

which are Fredholm of the 2nd kind (they can be represented as a compact perturbation of the identity matrix). Their resulting well-posedness makes them a good choice of equations to work with, since we know that solutions exist and can be approximated numerically. Müller derives these equations in [27] for a compact scatterer with the free-space Green's function (3.1). Since the singularities in the free-space and the periodic Green's functions are of the same nature (see Section 5.2.1), most of this derivation holds for our periodic scatterer. Following [5], we will present a derivation of the equations for a periodic scatterer here but will only include one proof where the details differ from Müller's derivation. For the other proofs, the details are the same, and we will refer the reader to Müller's work [27].

4.1 Derivation of the Integral Equations

We begin with two representation theorems. These were originally derived for a free-space Green's function and a compact scatterer in [39], and the proofs can be found there and in [27]. Each includes surface integrals involving the periodic Green's function (3.10) evaluated at $(\mathbf{x}' - \mathbf{x})$ for an $\mathbf{x}'$ not on the surface $\partial\Omega$. Thus, there are no singularities in these integrals.

Throughout this section, we let Ω be one periodic block of our scatterer. We will assume that $\partial\Omega$ is in C^2, and we will assume $\mathbf{E}$ and $\mathbf{H}$ are in C^1. Whenever $\mathbf{E}$ or $\mathbf{H}$ appears without an argument in a surface integral, it will go unstated that the field is evaluated at $(\mathbf{x})$. Whenever G appears without an argument, it will go unstated that G is evaluated at $(\mathbf{x}' - \mathbf{x})$.

4.1.1 Interior Representation Theorem

Theorem: 4.1.1. *Suppose* $\mathbf{E}$ *and* $\mathbf{H}$ *are pseudoperiodic solutions of Maxwell's equations (2.1) in the interior of our scatterer* Ω*. Then for* $\mathbf{x}'$ *in the interior of* Ω

$$\mathbf{E}(\mathbf{x}') = \int_{\partial\Omega} \left[-i\omega\mu\,(\mathbf{n}\times\mathbf{H})\,G - (\mathbf{n}\times\mathbf{E})\times\nabla G - (\mathbf{n}\cdot\mathbf{E})\,\nabla G\right] dS(\mathbf{x})$$

$$\mathbf{H}(\mathbf{x}') = \int_{\partial\Omega} \left[i\omega\epsilon\,(\mathbf{n}\times\mathbf{E})\,G - (\mathbf{n}\times\mathbf{H})\times\nabla G - (\mathbf{n}\cdot\mathbf{H})\,\nabla G\right] dS(\mathbf{x})$$

Here $\mathbf{n}$ *is the outward unit normal vector at* $\mathbf{x}$*. For* $\mathbf{x}'$ *in the exterior of* Ω*, both integrals above are* 0*.*

This theorem, as stated, has been proved in [39] and [27] for the non-periodic scattering problem. The adaptation of the proof to one periodic block of our scatterer is straightforward, since the singularities in the Green's function are the same. The pseudoperiodicity of the fields is an issue. The fields $\mathbf{E}$ and $\mathbf{H}$ are products of a phasor $e^{i\alpha x+i\beta y}$ with a periodic function. The Green's function is a product of a phasor $e^{i\alpha(x'-x)+i\beta(y'-y)}$ with a periodic function. In the integrands of the interior representation theorem, the x and y dependence in the phasors is canceled. The integrands are therefore truly periodic, and the theorem can be adapted without difficultly.

4.1.2 Exterior Representation Theorem

We will now state and prove an exterior analogue to the interior representation theorem. The proof of this theorem for a periodic problem is different from that for the non-periodic scatterer, and it merits inclusion.

Theorem: 4.1.2. *Suppose* $\mathbf{E}$ *and* $\mathbf{H}$ *are pseudoperiodic solutions of Maxwell's equations (2.1) in the exterior of our scatterer* Ω*. Suppose also that the radiation conditions (2.5) hold. Then for* $\mathbf{x}'$ *in the exterior of* Ω

$$\mathbf{E}(\mathbf{x}') = \int_{\partial\Omega} \left[i\omega\mu (\mathbf{n} \times \mathbf{H}) G + (\mathbf{n} \times \mathbf{E}) \times \nabla G + (\mathbf{n} \cdot \mathbf{E}) \nabla G \right] dS(\mathbf{x})$$

$$\mathbf{H}(\mathbf{x}') = \int_{\partial\Omega} \left[-i\omega\epsilon (\mathbf{n} \times \mathbf{E}) G + (\mathbf{n} \times \mathbf{H}) \times \nabla G + (\mathbf{n} \cdot \mathbf{H}) \nabla G \right] dS(\mathbf{x})$$

For $\mathbf{x}'$ *in the interior of* Ω*, both integrals above equal* 0*.*

Proof. We let $\mathbf{x}' = (x', y', z')$. Let S be the square cylinder given by one periodic block of space, $S = \{\mathbf{x} : 0 \leq x, y \leq 2\pi\}$. Choose M large enough that the planes $\pm z = M$ are to the exterior of Ω and $|z'| < M$. Let Ω_M be the set of points in the exterior of Ω such that $|z| \leq M$. This region is bounded by $\partial\Omega$, $|z| = M$, and ∂S. Now, apply the Interior Representation Theorem 4.1.1 to the region Ω_M. We have, if $\mathbf{x}'$ is in the exterior of Ω,

$$\begin{aligned} \mathbf{E}(\mathbf{x}') &= \int_{\partial\Omega_M} \left[-i\omega\mu (\tilde{\mathbf{n}} \times \mathbf{H}) G - (\tilde{\mathbf{n}} \times \mathbf{E}) \times \nabla G - (\tilde{\mathbf{n}} \cdot \mathbf{E}) \nabla G \right] dS(\mathbf{x}) \\ \mathbf{H}(\mathbf{x}') &= \int_{\partial\Omega_M} \left[i\omega\epsilon (\tilde{\mathbf{n}} \times \mathbf{E}) G - (\tilde{\mathbf{n}} \times \mathbf{H}) \times \nabla G - (\tilde{\mathbf{n}} \cdot \mathbf{H}) \nabla G \right] dS(\mathbf{x}) \end{aligned} \tag{4.1}$$

The fields $\mathbf{E}$ and $\mathbf{H}$ here are evaluated at $\mathbf{x}$, and the Green's functions are evaluated at $(\mathbf{x}' - \mathbf{x})$. The vector $\tilde{\mathbf{n}}$ is the outward unit normal to $\partial\Omega_M$. If $\mathbf{x}'$ is in the interior of Ω, by Theorem 4.1.1 both integrals in (4.1) are zero, as desired. We will break the integrals (4.1) into three boundary integrals. We will proceed here only with the $\mathbf{E}$

integral. The proof for the $\mathbf{H}$ integral is identical.

$$\begin{aligned}\mathbf{E}(\mathbf{x}') = &\int_{\partial\Omega} \left[i\omega\mu\,(\mathbf{n}\times\mathbf{H})\,G + (\mathbf{n}\times\mathbf{E})\times\nabla G + (\mathbf{n}\cdot\mathbf{E})\,\nabla G\right] dS(\mathbf{x}) \\ &+ \int_{\partial S\cap\partial\Omega_M} \left[-i\omega\mu\,(\tilde{\mathbf{n}}\times\mathbf{H})\,G - (\tilde{\mathbf{n}}\times\mathbf{E})\times\nabla G - (\tilde{\mathbf{n}}\cdot\mathbf{E})\,\nabla G\right] dS(\mathbf{x}) \\ &+ \int_{|z|=M} \left[-i\omega\mu\,(\tilde{\mathbf{n}}\times\mathbf{H})\,G - (\tilde{\mathbf{n}}\times\mathbf{E})\times\nabla G - (\tilde{\mathbf{n}}\cdot\mathbf{E})\,\nabla G\right] dS(\mathbf{x})\end{aligned} \tag{4.2}$$

We use $\mathbf{n}$ to denote the outward unit normal on $\partial\Omega$, which is opposite in direction to the outward normal $\tilde{\mathbf{n}}$ of $\partial\Omega_M$. This accounts for the change in sign in the $\partial\Omega$ integral above.

We will show that the second of these integrals (4.2) is zero and that the third approaches zero as $M\to\infty$. The pseudoperiodic part of $\mathbf{E}$ is $e^{i\alpha x+i\beta y}$, while that of the Green's function (or its derivatives) is $e^{i\alpha(x'-x)+i\beta(y'-y)}$. In a product of $\mathbf{E}$ with G (or a derivative of G), the x and y dependence of these phasors will cancel out. The integrand is therefore periodic. On opposide sides of ∂S, the $\partial S\cap\partial\Omega_M$ integrals cancel due to this periodicity and the fact that the normal vectors on opposite sides of ∂S point in opposite directions. The second integral of (4.2) is therefore zero.

We will show that the integral over $z=M$ of (4.2) approaches 0 as $M\to\infty$. The $z=-M$ integral can be shown to approach 0 using the same reasoning. The integral is

$$\int_{z=M} \left[-i\omega\mu\,(\tilde{\mathbf{n}}\times\mathbf{H})\,G - (\tilde{\mathbf{n}}\times\mathbf{E})\times\nabla G - (\tilde{\mathbf{n}}\cdot\mathbf{E})\,\nabla G\right] dS(\mathbf{x})$$

In the integrand, we substitute $i\omega\mu\,(\tilde{\mathbf{n}}\times\mathbf{H}) = \tilde{\mathbf{n}}\times(\nabla\times\mathbf{E})$ from Maxwell's equations

(2.2).

$$\int_{z=M} \left[-\tilde{\mathbf{n}} \times (\nabla \times \mathbf{E})\, G - (\tilde{\mathbf{n}} \times \mathbf{E}) \times \nabla G - (\tilde{\mathbf{n}} \cdot \mathbf{E})\, \nabla G\right] dS\,(\mathbf{x})$$

Here $\tilde{\mathbf{n}} = (0, 0, 1)$, and we expand the integrand:

$$\begin{bmatrix} GE_{1,z} - E_1 G_z - GE_{3,x} - E_3 G_x \\ GE_{2,z} - E_2 G_z - GE_{3,y} - E_3 G_y \\ E_1 G_x + E_2 G_y - E_3 G_z \end{bmatrix}$$

where E_1, E_2, and E_3 denote the x, y, and z components of $\mathbf{E}$, respectively. We will first deal with the term $(GE_{1,z} - E_1 G_z)$. As $M \to \infty$, we can represent the fields by the radiation conditions (2.5). With (3.10) for G, we can write

$$\begin{aligned} &\int_{z=M} \left(G\,(\mathbf{x}' - \mathbf{x})\, E_{1,z}\,(\mathbf{x}) - E_1\,(\mathbf{x})\, G_z\,(\mathbf{x}' - \mathbf{x})\right) dS\,(\mathbf{x}) = \\ &\frac{1}{8\pi^2} \int_0^{2\pi} \int_0^{2\pi} \left(\sum_{m,n} e^{i(m+\alpha)(x'-x) + i(n+\beta)(y'-y)} \frac{e^{-\sqrt{-\lambda_{mn}}|z'-M|}}{\sqrt{-\lambda_{mn}}} \right) \\ &\qquad \times \left(\sum_{m',n'} E^{+}_{1,m'n'} e^{i(m'+\alpha)x + i(n'+\beta)y} \sqrt{-\lambda_{m'n'}}\, e^{-\sqrt{-\lambda_{m'n'}} M} \right) dxdy \qquad (4.3) \\ &-\frac{1}{8\pi^2} \int_0^{2\pi} \int_0^{2\pi} \left(\sum_{m,n} e^{i(m+\alpha)(x'-x) + i(n+\beta)(y'-y)} e^{-\sqrt{-\lambda_{mn}}|z'-M|} \right) \\ &\qquad \times \left(\sum_{m',n'} E^{+}_{1,m'n'} e^{i(m'+\alpha)x + i(n'+\beta)y} e^{-\sqrt{-\lambda_{m'n'}} M} \right) dxdy \end{aligned}$$

Each term in either integrand of (4.3) is of the form

$$\int_0^{2\pi} \int_0^{2\pi} C e^{i(m+\alpha)(x'-x) + i(n+\beta)(y'-y)} e^{i(m'+\alpha)x + i(n'+\beta)y} dxdy$$

for some constant C. Rearranging and cancelling α and β, we see that most of these

terms are 0:

$$\int_0^{2\pi}\int_0^{2\pi} Ce^{i(m+\alpha)x'+i(n+\beta)y'}e^{i(m'-m)x+i(n'-n)y}dxdy =$$

$$4\pi^2 Ce^{i(m+\alpha)x'+i(n+\beta)y'}\delta_{m-m'}\delta_{n-n'}$$

The non-zero terms of the integrands in (4.3) are those for which $m' = m$ and $n' = n$, and (4.3) reduces to

$$\begin{aligned}
&\int_{z=M} \left(G\left(\mathbf{x}'-\mathbf{x}\right)E_{1,z}\left(\mathbf{x}\right) - E_1\left(\mathbf{x}\right)G_z\left(\mathbf{x}'-\mathbf{x}\right)\right)dS\left(\mathbf{x}\right) = \\
&\frac{1}{8\pi^2}\int_0^{2\pi}\int_0^{2\pi}\left(\sum_{m,n}\frac{e^{-\sqrt{-\lambda_{mn}}|z'-M|}}{\sqrt{-\lambda_{mn}}}E^+_{1,mn}\sqrt{-\lambda_{mn}}e^{-\sqrt{-\lambda_{mn}}M}\right)dxdy \qquad (4.4)\\
&-\frac{1}{8\pi^2}\int_0^{2\pi}\int_0^{2\pi}\left(\sum_{m,n}e^{-\sqrt{-\lambda_{mn}}|z'-M|}E^+_{1,mn}e^{-\sqrt{-\lambda_{mn}}M}\right)dxdy
\end{aligned}$$

which clearly sums to 0.

The terms $GE_{2,z} - E_2G_z$, $-GE_{3,x} - E_3G_x$, and $-GE_{3,y} - E_3G_y$ can all be shown in the same way to integrate to 0 as $M \to \infty$. There is a sign change from the derivative of the Green's function that makes this possible. We are left with the term $E_1G_x + E_2G_y - E_3G_z$, which we first integrate by parts:

$$\int_{z=M} E_1G_x + E_2G_y - E_3G_z dxdy = \int_{z=M} -E_{1,x}G - E_{2,y}G + E_3G_z dxdy \qquad (4.5)$$

The boundary from the integration by parts is zero due to the periodicity of the integrand. Now, since $\mathbf{E}$ is divergence free, $-E_{1,x}G - E_{2,y}G = -E_{3,z}G$, and (4.5) becomes

$$\int_{z=M} E_3G_z - E_{3,z}G dxdy$$

This integral can be shown to approach 0 in the same way that the integral (4.3) does.

The other surface integrals have been shown to be zero as $M \to \infty$, and we are left with our result for $\mathbf{E}$

$$\mathbf{E}(\mathbf{x}') = \int_{\partial\Omega} \left[i\omega\mu (\mathbf{n} \times \mathbf{H}) G + (\mathbf{n} \times \mathbf{E}) \times \nabla G + (\mathbf{n} \cdot \mathbf{E}) \nabla G \right] dS(\mathbf{x})$$

As stated, the proof for $\mathbf{H}$ follows the same steps. □

4.1.3 Surface Currents and Charges

We do not work directly with $\mathbf{E}$ and $\mathbf{H}$ on the surface $\partial\Omega$. The integral equations are instead in terms of tangential components of the fields known as surface currents $\mathbf{j}$ and $\mathbf{j}'$:

$$\begin{aligned} \mathbf{j} &= -\mathbf{n} \times \mathbf{H} \\ \mathbf{j}' &= \mathbf{n} \times \mathbf{E} \end{aligned} \tag{4.6}$$

These surface currents are also known as the traces of the fields on $\partial\Omega$. We also define the surface charges ρ and ρ'

$$i\omega\rho = \nabla_s \cdot \mathbf{j}$$

$$i\omega\rho' = \nabla_s \cdot \mathbf{j}'$$

Here $\nabla_s \cdot$ is the surface divergence as defined in [27, page 157].

We will restate Propositions 4.1.1 and 4.1.2 in terms of $\mathbf{j}$ and $\mathbf{j}'$. To do this, we need the relations

$$\mathbf{n} \cdot \mathbf{E} = -\rho/\epsilon$$

$$\mathbf{n} \cdot \mathbf{H} = -\rho'/\epsilon$$

which are proved in [27, page 159].

The integrals of the interior representation theorem become:

$$\begin{aligned}\mathbf{E}(\mathbf{x}') &= \int_{\partial\Omega}\left[i\omega\mu\mathbf{j}(\mathbf{x})\,G - \mathbf{j}'(\mathbf{x})\times\nabla G + \frac{\rho(\mathbf{x})}{\epsilon}\nabla G\right]dS(\mathbf{x})\\ \mathbf{H}(\mathbf{x}') &= \int_{\partial\Omega}\left[i\omega\epsilon\mathbf{j}'(\mathbf{x})\,G + \mathbf{j}(\mathbf{x})\times\nabla G + \frac{\rho'(\mathbf{x})}{\mu}\nabla G\right]dS(\mathbf{x})\end{aligned} \tag{4.7}$$

and the integrals of the exterior representation theorem are

$$\begin{aligned}\mathbf{E}(\mathbf{x}') &= \int_{\partial\Omega}\left[-i\omega\mu\mathbf{j}(\mathbf{x})\,G + \mathbf{j}'(\mathbf{x})\times\nabla G - \frac{\rho(\mathbf{x})}{\epsilon}\nabla G\right]dS(\mathbf{x})\\ \mathbf{H}(\mathbf{x}') &= \int_{\partial\Omega}\left[-i\omega\epsilon\mathbf{j}'(\mathbf{x})\,G - \mathbf{j}(\mathbf{x})\times\nabla G - \frac{\rho'(\mathbf{x})}{\mu}\nabla G\right]dS(\mathbf{x})\end{aligned} \tag{4.8}$$

4.1.4 Jump Conditions

We will eventually have surface integrals where $\mathbf{x}'$ is actually on the surface $\partial\Omega$. We start here by looking at the limits of various integrals as $\mathbf{x}'$ approaches $\partial\Omega$ from the interior and exterior along a normal direction. The results of this section depend heavily on the singularity of the Green's function. Since the singularities in the periodic problem are the same as those in the non-periodic problem, we will not include the proofs here and will instead refer the reader to the proofs in [27].

Proposition: 4.1.3. *For a tangential surface vector* $\mathbf{j}$ *continuous on* $\partial\Omega$*, the integral*

$$\int_{\partial\Omega}\mathbf{j}(\mathbf{x})\,G(\mathbf{x}'-\mathbf{x})\,dS(\mathbf{x})$$

is continuous for all $\mathbf{x}'$*.*

For proof of this proposition, see [27, page 202].

We will adopt the notation of [27] and define

$$\int_{int\to\partial\Omega} G(\mathbf{x}'-\mathbf{x})\,dS(\mathbf{x}) = \lim_{\mathbf{y}\to\mathbf{x}'}\int_{\partial\Omega} G(\mathbf{y}-\mathbf{x})\,dS(\mathbf{x})$$

where the limit on the right hand side is taken as $\mathbf{y}\to\mathbf{x}'$ for $\mathbf{y}$ in the interior of Ω along a direction normal to $\partial\Omega$ at $\mathbf{x}'\in\partial\Omega$. We define $\int_{ext\to\partial\Omega}$ similarly for $\mathbf{y}$ along an exterior normal.

Proposition: 4.1.4. *For our surface charges ρ as defined, and for all $\mathbf{x}'\in\partial\Omega$, the integral*

$$\int_{\partial\Omega} \mathbf{n}(\mathbf{x}')\times\rho(\mathbf{x})\,\nabla G(\mathbf{x}'-\mathbf{x})\,dS(\mathbf{x}) \tag{4.9}$$

is well-defined as a principal value integral, and

$$\mathbf{n}(\mathbf{x}')\times\int_{int\to\partial\Omega}\rho(\mathbf{x})\,\nabla G(\mathbf{x}'-\mathbf{x})\,dS(\mathbf{x}) = \mathbf{n}(\mathbf{x}')\times\int_{ext\to\partial\Omega}\rho(\mathbf{x})\,\nabla G(\mathbf{x}'-\mathbf{x})\,dS(\mathbf{x}) \tag{4.10}$$

For proof of this proposition, see [27, page 205]. We will use the integral (4.9) to denote either of the limits of (4.10).

Proposition: 4.1.5. *For $\mathbf{x}'\in\partial\Omega$ and $\mathbf{j}$ a continuous surface vector field on $\partial\Omega$, the integral*

$$\int_{\partial\Omega}\mathbf{n}(\mathbf{x}')\times[\mathbf{j}(\mathbf{x})\times\nabla G]\,dS(\mathbf{x})$$

is absolutely integrable, and

$$\mathbf{n}(\mathbf{x}')\times\int_{int\to\partial\Omega}\mathbf{j}(\mathbf{x})\times\nabla G dS(\mathbf{x}) = -\frac{1}{2}\mathbf{j}(\mathbf{x}')+\int_{\partial\Omega}\mathbf{n}(\mathbf{x}')\times[\mathbf{j}(\mathbf{x})\times\nabla G]\,dS(\mathbf{x})$$

$$\mathbf{n}(\mathbf{x}')\times\int_{ext\to\partial\Omega}\mathbf{j}(\mathbf{x})\times\nabla G dS(\mathbf{x}) = +\frac{1}{2}\mathbf{j}(\mathbf{x}')+\int_{\partial\Omega}\mathbf{n}(\mathbf{x}')\times[\mathbf{j}(\mathbf{x})\times\nabla G]\,dS(\mathbf{x})$$

The proof of this proposition can be found in [27, page 205].

4.1.5 The Field Equations

We will apply the results of Section 4.1.4 to the interior and exterior representation theorems for the interior fields $\mathbf{E}_{int}$ and $\mathbf{H}_{int}$, the exterior scattered fields $\mathbf{E}_{scatt}$ and $\mathbf{H}_{scatt}$, and the incident fields $\mathbf{E}_{inc}$ and $\mathbf{H}_{inc}$.

Interior Fields

Let $\mathbf{y}$ lie in the interior of Ω, and let $\mathbf{x}' \in \partial\Omega$. We take the cross product of $\mathbf{n}(\mathbf{x}')$ with each side of the equations of the interior representation theorem (4.7). We then take the limit as $\mathbf{y} \to \mathbf{x}'$ along the interior normal. Then, using all of the propositions of Section 4.1.4 and combining the $\mathbf{j}(\mathbf{x}')$ terms, we have

$$\begin{aligned}
\frac{1}{2}\mathbf{j}'_{int}(\mathbf{x}') &= \int_{\partial\Omega} i\omega\mu_{int}\left[\mathbf{n}(\mathbf{x}') \times \mathbf{j}_{int}(\mathbf{x})\right] G^{int} dS(\mathbf{x}) \\
&\quad - \int_{\partial\Omega} \mathbf{n}(\mathbf{x}') \times \left[\mathbf{j}'_{int}(\mathbf{x}) \times \nabla G^{int}\right] dS(\mathbf{x}) \\
&\quad + \frac{1}{\epsilon_{int}} \int_{\partial\Omega} \mathbf{n}(\mathbf{x}') \times \rho_{int}(\mathbf{x}) \nabla G^{int} dS(\mathbf{x}) \\
-\frac{1}{2}\mathbf{j}_{int}(\mathbf{x}') &= \int_{\partial\Omega} i\omega\epsilon_{int}\left[\mathbf{n}(\mathbf{x}') \times \mathbf{j}'_{int}(\mathbf{x})\right] G^{int} dS(\mathbf{x}) \\
&\quad + \int_{\partial\Omega} \mathbf{n}(\mathbf{x}') \times \left[\mathbf{j}_{int}(\mathbf{x}) \times \nabla G^{int}\right] dS(\mathbf{x}) \\
&\quad + \frac{1}{\mu_{int}} \int_{\partial\Omega} \mathbf{n}(\mathbf{x}') \times \rho'_{int}(\mathbf{x}) \nabla G^{int} dS(\mathbf{x})
\end{aligned} \tag{4.11}$$

Exterior Scattered Fields

Let $\mathbf{y}$ lie in the exterior of Ω, and let $\mathbf{x}' \in \partial\Omega$. We take the cross product of $\mathbf{n}(\mathbf{x}')$ with each side of the equations of the exterior representation theorem (4.8) for the scattered fields. We then take the limit as $\mathbf{y} \to \mathbf{x}'$ along the exterior normal. Then, the propositions of Section 4.1.4 give us

$$\begin{aligned}
\frac{1}{2}\mathbf{j}'_{scatt}(\mathbf{x}') &= -\int_{\partial\Omega} i\omega\mu_{ext}\left[\mathbf{n}(\mathbf{x}') \times \mathbf{j}_{scatt}(\mathbf{x})\right] G^{ext} dS(\mathbf{x}) \\
&\quad + \int_{\partial\Omega} \mathbf{n}(\mathbf{x}') \times \left[\mathbf{j}'_{scatt}(\mathbf{x}) \times \nabla G^{ext}\right] dS(\mathbf{x}) \\
&\quad - \frac{1}{\epsilon_{ext}} \int_{\partial\Omega} \mathbf{n}(\mathbf{x}') \times \rho_{scatt}(\mathbf{x}) \nabla G^{ext} dS(\mathbf{x}) \\
-\frac{1}{2}\mathbf{j}_{scatt}(\mathbf{x}') &= -\int_{\partial\Omega} i\omega\epsilon_{ext}\left[\mathbf{n}(\mathbf{x}') \times \mathbf{j}'_{scatt}(\mathbf{x})\right] G^{ext} dS(\mathbf{x}) \\
&\quad - \int_{\partial\Omega} \mathbf{n}(\mathbf{x}') \times \left[\mathbf{j}_{scatt}(\mathbf{x}) \times \nabla G^{ext}\right] dS(\mathbf{x}) \\
&\quad - \frac{1}{\mu_{ext}} \int_{\partial\Omega} \mathbf{n}(\mathbf{x}') \times \rho'_{scatt}(\mathbf{x}) \nabla G^{ext} dS(\mathbf{x})
\end{aligned} \tag{4.12}$$

Incident Fields

The incident fields are, by definition, the fields that would exist in the absence of the scatterer. In other words, they are the fields that would exist if $\epsilon = \epsilon_{ext}$ and $\mu = \mu_{ext}$ everywhere. The internal representation formulas (4.7) are valid for the incident fields with these constants and with the Green's function G^{ext}. We do not use the external representation theorem for the incident fields because this theorem depends on the radiation conditions, and the incident fields do not have to satisfy these conditions.

Let $\mathbf{y}$ lie in the interior of Ω, and let $\mathbf{x}' \in \partial\Omega$. Apply the interior representation theorem (4.7) to the incident fields (but with the exterior constants and Green's function). We take the cross product of $\mathbf{n}(\mathbf{x}')$ with each side of the resulting equations. We then take the limit as $\mathbf{y} \to \mathbf{x}'$ along the interior normal. Then, the propositions of Section 4.1.4 give us

$$\begin{aligned}
\frac{1}{2}\mathbf{j}'_{inc}(\mathbf{x}') &= \int_{\partial\Omega} i\omega\mu_{ext}\left[\mathbf{n}(\mathbf{x}') \times \mathbf{j}_{inc}(\mathbf{x})\right] G^{ext} dS(\mathbf{x}) \\
&\quad - \int_{\partial\Omega} \mathbf{n}(\mathbf{x}') \times \left[\mathbf{j}'_{inc}(\mathbf{x}) \times \nabla G^{ext}\right] dS(\mathbf{x}) \\
&\quad + \frac{1}{\epsilon_{ext}} \int_{\partial\Omega} \mathbf{n}(\mathbf{x}') \times \rho_{inc}(\mathbf{x}) \nabla G^{ext} dS(\mathbf{x}) \\
-\frac{1}{2}\mathbf{j}_{inc}(\mathbf{x}') &= \int_{\partial\Omega} i\omega\epsilon_{ext}\left[\mathbf{n}(\mathbf{x}') \times \mathbf{j}'_{inc}(\mathbf{x})\right] G^{ext} dS(\mathbf{x}) \\
&\quad + \int_{\partial\Omega} \mathbf{n}(\mathbf{x}') \times \left[\mathbf{j}_{inc}(\mathbf{x}) \times \nabla G^{ext}\right] dS(\mathbf{x}) \\
&\quad + \frac{1}{\mu_{ext}} \int_{\partial\Omega} \mathbf{n}(\mathbf{x}') \times \rho'_{inc}(\mathbf{x}) \nabla G^{ext} dS(\mathbf{x})
\end{aligned} \tag{4.13}$$

Matching Conditions

We apply the boundary conditions of tangential continuity at $\partial\Omega$:

$$\mathbf{j}_{scatt} + \mathbf{j}_{inc} = \mathbf{j}_{int}$$

$$\mathbf{j}'_{scatt} + \mathbf{j}'_{inc} = \mathbf{j}'_{int}$$

We substitute $\mathbf{j}_{scatt} = \mathbf{j}_{int} - \mathbf{j}_{inc}$ on both sides of (4.12):

$$\begin{aligned}
\frac{\epsilon_{ext}}{2}\mathbf{j}'_{int}(\mathbf{x}') - \frac{\epsilon_{ext}}{2}\mathbf{j}'_{inc}(\mathbf{x}') = &-\epsilon_{ext}\int_{\partial\Omega} i\omega\mu_{ext}\left[\mathbf{n}(\mathbf{x}')\times\mathbf{j}_{int}(\mathbf{x})\right]G^{ext}dS(\mathbf{x}) \\
&+\epsilon_{ext}\int_{\partial\Omega}\mathbf{n}(\mathbf{x}')\times\left[\mathbf{j}'_{int}(\mathbf{x})\times\nabla G^{ext}\right]dS(\mathbf{x}) \\
&-\int_{\partial\Omega}\mathbf{n}(\mathbf{x}')\times\rho_{int}(\mathbf{x})\nabla G^{ext}dS(\mathbf{x}) \\
&+\epsilon_{ext}\int_{\partial\Omega} i\omega\mu_{ext}\left[\mathbf{n}(\mathbf{x}')\times\mathbf{j}_{inc}(\mathbf{x})\right]G^{ext}dS(\mathbf{x}) \\
&-\epsilon_{ext}\int_{\partial\Omega}\mathbf{n}(\mathbf{x}')\times\left[\mathbf{j}'_{inc}(\mathbf{x})\times\nabla G^{ext}\right]dS(\mathbf{x}) \\
&+\int_{\partial\Omega}\mathbf{n}(\mathbf{x}')\times\rho_{inc}(\mathbf{x})\nabla G^{ext}dS(\mathbf{x}) \\
\frac{\mu_{ext}}{2}\mathbf{j}_{int}(\mathbf{x}') - \frac{\mu_{ext}}{2}\mathbf{j}_{inc}(\mathbf{x}') = &\,\mu_{ext}\int_{\partial\Omega} i\omega\epsilon_{ext}\left[\mathbf{n}(\mathbf{x}')\times\mathbf{j}'_{int}(\mathbf{x})\right]G^{ext}dS(\mathbf{x}) \\
&+\mu_{ext}\int_{\partial\Omega}\mathbf{n}(\mathbf{x}')\times\left[\mathbf{j}_{int}(\mathbf{x})\times\nabla G^{ext}\right]dS(\mathbf{x}) \\
&+\int_{\partial\Omega}\mathbf{n}(\mathbf{x}')\times\rho'_{int}(\mathbf{x})\nabla G^{ext}dS(\mathbf{x}) \\
&-\mu_{ext}\int_{\partial\Omega} i\omega\epsilon_{ext}\left[\mathbf{n}(\mathbf{x}')\times\mathbf{j}'_{inc}(\mathbf{x})\right]G^{ext}dS(\mathbf{x}) \\
&-\mu_{ext}\int_{\partial\Omega}\mathbf{n}(\mathbf{x}')\times\left[\mathbf{j}_{inc}(\mathbf{x})\times\nabla G^{ext}\right]dS(\mathbf{x}) \\
&-\int_{\partial\Omega}\mathbf{n}(\mathbf{x}')\times\rho'_{inc}(\mathbf{x})\nabla G^{ext}dS(\mathbf{x})
\end{aligned}$$

To this we add the interior equations (4.11)

$$
\begin{aligned}
&\frac{\epsilon_{ext}+\epsilon_{int}}{2}\mathbf{j'}_{int}\left(\mathbf{x'}\right)-\frac{\epsilon_{ext}}{2}\mathbf{j'}_{inc}\left(\mathbf{x'}\right)= \\
&-\int_{\partial\Omega} i\omega\left[\mathbf{n}\left(\mathbf{x'}\right)\times\mathbf{j}_{int}\left(\mathbf{x}\right)\right]\left(\epsilon_{ext}\mu_{ext}G^{ext}-\epsilon_{int}\mu_{int}G^{int}\right)dS\left(\mathbf{x}\right) \\
&+\int_{\partial\Omega}\mathbf{n}\left(\mathbf{x'}\right)\times\left[\mathbf{j'}_{int}\left(\mathbf{x}\right)\times\nabla\left(\epsilon_{ext}G^{ext}-\epsilon_{int}G^{int}\right)\right]dS\left(\mathbf{x}\right) \\
&-\int_{\partial\Omega}\mathbf{n}\left(\mathbf{x'}\right)\times\rho_{int}\left(\mathbf{x}\right)\nabla\left(G^{ext}-G^{int}\right)dS\left(\mathbf{x}\right) \\
&+\epsilon_{ext}\int_{\partial\Omega} i\omega\mu_{ext}\left[\mathbf{n}\left(\mathbf{x'}\right)\times\mathbf{j}_{inc}\left(\mathbf{x}\right)\right]G^{ext}dS\left(\mathbf{x}\right) \\
&-\epsilon_{ext}\int_{\partial\Omega}\mathbf{n}\left(\mathbf{x'}\right)\times\left[\mathbf{j'}_{inc}\left(\mathbf{x}\right)\times\nabla G^{ext}\right]dS\left(\mathbf{x}\right) \\
&+\int_{\partial\Omega}\mathbf{n}\left(\mathbf{x'}\right)\times\rho_{inc}\left(\mathbf{x}\right)\nabla G^{ext}dS\left(\mathbf{x}\right) \\
&\frac{\mu_{ext}+\mu_{int}}{2}\mathbf{j}_{int}\left(\mathbf{x'}\right)-\frac{\mu_{ext}}{2}\mathbf{j}_{inc}\left(\mathbf{x'}\right)= \\
&\int_{\partial\Omega} i\omega\left[\mathbf{n}\left(\mathbf{x'}\right)\times\mathbf{j'}_{int}\left(\mathbf{x}\right)\right]\left(\epsilon_{ext}\mu_{ext}G^{ext}-\epsilon_{int}\mu_{int}G^{int}\right)dS\left(\mathbf{x}\right) \\
&+\int_{\partial\Omega}\mathbf{n}\left(\mathbf{x'}\right)\times\left[\mathbf{j}_{int}\left(\mathbf{x}\right)\times\nabla\left(\mu_{ext}G^{ext}-\mu_{int}G^{int}\right)\right]dS\left(\mathbf{x}\right) \\
&+\int_{\partial\Omega}\mathbf{n}\left(\mathbf{x'}\right)\times\rho'_{int}\left(\mathbf{x}\right)\nabla\left(G^{ext}-G^{int}\right)dS\left(\mathbf{x}\right) \\
&-\mu_{ext}\int_{\partial\Omega} i\omega\epsilon_{ext}\left[\mathbf{n}\left(\mathbf{x'}\right)\times\mathbf{j'}_{inc}\left(\mathbf{x}\right)\right]G^{ext}dS\left(\mathbf{x}\right) \\
&-\mu_{int}\int_{\partial\Omega}\mathbf{n}\left(\mathbf{x'}\right)\times\left[\mathbf{j}_{inc}\left(\mathbf{x}\right)\times\nabla G^{ext}\right]dS\left(\mathbf{x}\right) \\
&-\int_{\partial\Omega}\mathbf{n}\left(\mathbf{x'}\right)\times\rho'_{inc}\left(\mathbf{x}\right)\nabla G^{ext}dS\left(\mathbf{x}\right)
\end{aligned}
\tag{4.14}
$$

Now we can recognize that the integrals over $\mathbf{j}_{inc}$ in (4.14) are the same as the integrals in the incident equations (4.13). We can substitute the left hand side of (4.13) for these integrals. We get

$$\begin{aligned}
&\frac{\epsilon_{ext}+\epsilon_{int}}{2}\mathbf{j'}_{int}\left(\mathbf{x'}\right)-\epsilon_{ext}\mathbf{j'}_{inc}\left(\mathbf{x'}\right)= \\
&-\int_{\partial\Omega} i\omega\left[\mathbf{n}\left(\mathbf{x'}\right)\times\mathbf{j}_{int}\left(\mathbf{x}\right)\right]\left(\epsilon_{ext}\mu_{ext}G^{ext}-\epsilon_{int}\mu_{int}G^{int}\right)dS\left(\mathbf{x}\right) \\
&+\int_{\partial\Omega}\mathbf{n}\left(\mathbf{x'}\right)\times\left[\mathbf{j'}_{int}\left(\mathbf{x}\right)\times\nabla\left(\epsilon_{ext}G^{ext}-\epsilon_{int}G^{int}\right)\right]dS\left(\mathbf{x}\right) \\
&-\frac{1}{\epsilon_{ext}}\int_{\partial\Omega}\mathbf{n}\left(\mathbf{x'}\right)\times\rho_{int}\left(\mathbf{x}\right)\nabla\left(G^{ext}-G^{int}\right)dS\left(\mathbf{x}\right) \\
&\frac{\mu_{ext}+\mu_{int}}{2}\mathbf{j}_{int}\left(\mathbf{x'}\right)-\mu_{ext}\mathbf{j}_{inc}\left(\mathbf{x'}\right)= \\
&\int_{\partial\Omega} i\omega\left[\mathbf{n}\left(\mathbf{x'}\right)\times\mathbf{j'}_{int}\left(\mathbf{x}\right)\right]\left(\epsilon_{ext}\mu_{ext}G^{ext}-\epsilon_{int}\mu_{int}G^{int}\right)dS\left(\mathbf{x}\right) \\
&+\int_{\partial\Omega}\mathbf{n}\left(\mathbf{x'}\right)\times\left[\mathbf{j}_{int}\left(\mathbf{x}\right)\times\nabla\left(\mu_{ext}G^{ext}-\mu_{int}G^{int}\right)\right]dS\left(\mathbf{x}\right) \\
&+\frac{1}{\mu_{ext}}\int_{\partial\Omega}\mathbf{n}\left(\mathbf{x'}\right)\times\rho'_{int}\left(\mathbf{x}\right)\nabla\left(G^{ext}-G^{int}\right)dS\left(\mathbf{x}\right)
\end{aligned} \tag{4.15}$$

These are the Müller equations, but we will make one more change. Two of the integrals involve the surface divergence of a surface current. In order to make these integrals more manageable numerically, we replace them as in the following proposition, which is proved in [27, page 300]:

Proposition: 4.1.6. *With all quantities as previously defined*

$$\int_{\partial\Omega}\mathbf{n}\left(\mathbf{x'}\right)\times\rho\left(\mathbf{x}\right)\nabla\left(G^{ext}-G^{int}\right)dS\left(\mathbf{x}\right)=$$

$$\int_{\partial\Omega}\mathbf{n}\left(\mathbf{x'}\right)\times\left[\left(\mathbf{j}\left(\mathbf{x}\right)\cdot\nabla\right)\nabla\left(G^{ext}-G^{int}\right)\right]dS\left(\mathbf{x}\right)$$

4.2 The Müller Integral Equations

We rearrange a few of the constants in (4.15) and make the substitutions of Proposition 4.1.6 to obtain the equations in their final form [27, page 319]:

$$\begin{aligned}
\mathbf{j}_{inc}(\mathbf{x}') &= \frac{\mu_{int}+\mu_{ext}}{2\mu_{ext}}\mathbf{j}_{int}(\mathbf{x}') \\
&\quad - \frac{1}{\mu_{ext}}\int_{\partial\Omega}\mathbf{n}(\mathbf{x}')\times\left[\mathbf{j}_{int}(\mathbf{x})\times\nabla\left(\mu_{ext}G^{ext}-\mu_{int}G^{int}\right)\right]dS(\mathbf{x}) \\
&\quad - \frac{i}{\mu_{ext}\omega}\int_{\partial\Omega}\left[\mathbf{n}(\mathbf{x}')\times\mathbf{j}'_{int}(\mathbf{x})\right]\left(k^2_{ext}G^{ext}-k^2_{int}G^{int}\right)dS(\mathbf{x}) \\
&\quad - \frac{i}{\mu_{ext}\omega}\int_{\partial\Omega}\mathbf{n}(\mathbf{x}')\times\left[\left(\mathbf{j}'_{int}(\mathbf{x})\cdot\nabla\right)\nabla\left(G^{ext}-G^{int}\right)\right]dS(\mathbf{x}) \\
\mathbf{j}'_{inc}(\mathbf{x}') &= \frac{\epsilon_{int}+\epsilon_{ext}}{2\epsilon_{ext}}\mathbf{j}'_{int}(\mathbf{x}') \\
&\quad - \frac{1}{\epsilon_{ext}}\int_{\partial\Omega}\mathbf{n}(\mathbf{x}')\times\left[\mathbf{j}'_{int}(\mathbf{x})\times\nabla\left(\epsilon_{ext}G^{ext}-\epsilon_{int}G^{int}\right)\right]dS(\mathbf{x}) \\
&\quad - \frac{i}{\epsilon_{ext}\omega}\int_{\partial\Omega}\left[\mathbf{n}(\mathbf{x}')\times\mathbf{j}_{int}(\mathbf{x})\right]\left(k^2_{ext}G^{ext}-k^2_{int}G^{int}\right)dS(\mathbf{x}) \\
&\quad - \frac{i}{\epsilon_{ext}\omega}\int_{\partial\Omega}\mathbf{n}(\mathbf{x}')\times\left[\left(\mathbf{j}_{int}(\mathbf{x})\cdot\nabla\right)\nabla\left(G^{ext}-G^{int}\right)\right]dS(\mathbf{x})
\end{aligned} \tag{4.16}$$

The Müller equations are a coupled system of integral equations. The incident currents $\mathbf{j}_{inc}$ and $\mathbf{j}'_{inc}$ are known. This system of integral equations can be solved for the interior surface currents $\mathbf{j}_{int}$ and $\mathbf{j}'_{int}$.

Once we have the interior surface currents, we can use the interior and exterior representation theorems to find the scattered and the interior electric and magnetic

fields:

$$\mathbf{E}_{int}(\mathbf{x}') =$$

$$\int_{\partial\Omega}\left[i\omega\mu_{int}\mathbf{j}_{int}(\mathbf{x})G^{int}-\mathbf{j}'_{int}(\mathbf{x})\times\nabla G^{int}+\frac{1}{\epsilon_{int}}(\mathbf{j}(\mathbf{x})\cdot\nabla)\nabla G^{int}\right]dS(\mathbf{x})$$

$$\mathbf{H}_{int}(\mathbf{x}') =$$

$$\int_{\partial\Omega}\left[i\omega\epsilon_{int}\mathbf{j}'_{int}(\mathbf{x})G^{int}+\mathbf{j}_{int}(\mathbf{x})\times\nabla G^{int}+\frac{1}{\mu_{int}}(\mathbf{j}'(\mathbf{x})\cdot\nabla)\nabla G^{int}\right]dS(\mathbf{x})$$

$$\mathbf{E}_{scatt}(\mathbf{x}') =$$

$$-\int_{\partial\Omega}\left[i\omega\mu_{ext}\mathbf{j}_{int}(\mathbf{x})G^{ext}-\mathbf{j}'_{int}(\mathbf{x})\times\nabla G^{int}+\frac{1}{\epsilon_{ext}}(\mathbf{j}(\mathbf{x})\cdot\nabla)\nabla G^{ext}\right]dS(\mathbf{x})$$

$$\mathbf{H}_{scatt}(\mathbf{x}') =$$

$$-\int_{\partial\Omega}\left[i\omega\epsilon_{ext}\mathbf{j}'_{int}(\mathbf{x})G^{ext}+\mathbf{j}_{int}(\mathbf{x})\times\nabla G^{ext}+\frac{1}{\mu_{ext}}(\mathbf{j}'(\mathbf{x})\cdot\nabla)\nabla G^{ext}\right]dS(\mathbf{x}) \tag{4.17}$$

4.3 Operator Notation

We would like to have a concise representation of the integral equations. We follow Barnes [5] and introduce the integral operators

$$(L_\epsilon\mathbf{j})(\mathbf{r}') = \int_{\partial\Omega}\mathbf{n}(\mathbf{r}')\times\left[\mathbf{j}(\mathbf{x})\times\nabla\left(\epsilon_{ext}G^{ext}-\epsilon_{int}G^{int}\right)\right]dS(\mathbf{x})$$

$$(L_\mu\mathbf{j})(\mathbf{r}') = \int_{\partial\Omega}\mathbf{n}(\mathbf{r}')\times\left[\mathbf{j}(\mathbf{x})\times\nabla\left(\mu_{ext}G^{ext}-\mu_{int}G^{int}\right)\right]dS(\mathbf{x})$$

$$(M\mathbf{j})(\mathbf{r}') = \frac{i}{\omega}\int_{\partial\Omega}\left[\mathbf{n}(\mathbf{r}')\times\mathbf{j}(\mathbf{x})\right]\left(k_{ext}^2G^{ext}-k_{int}^2G^{int}\right)dS(\mathbf{x})$$

$$(N\mathbf{j})(\mathbf{r}') = \frac{i}{\omega}\int_{\partial\Omega}\mathbf{n}(\mathbf{r}')\times\left[(\mathbf{j}(\mathbf{x})\cdot\nabla)\nabla\left(G^{ext}-G^{int}\right)\right]dS(\mathbf{x})$$

The the integral equations (4.16) become

$$\mathbf{j}_{inc}(\mathbf{x}') =$$

$$\frac{\mu_{ext}+\mu_{int}}{2\mu_{ext}}\mathbf{j}_{int}(\mathbf{x}') - \frac{1}{\mu_{ext}}(L_{\mu}\mathbf{j}_{int})(\mathbf{x}') - \frac{1}{\mu_{ext}}(M\mathbf{j}_{int})(\mathbf{x}') - \frac{1}{\mu_{ext}}(N\mathbf{j}_{int})(\mathbf{x}')$$

$$\mathbf{j'}_{inc}(\mathbf{x}') =$$

$$\frac{\epsilon_{ext}+\epsilon_{int}}{2\mu_{ext}}\mathbf{j'}_{int}(\mathbf{x}') - \frac{1}{\epsilon_{ext}}(L_{\epsilon}\mathbf{j}_{int})(\mathbf{x}') + \frac{1}{\epsilon_{ext}}(M\mathbf{j}_{int})(\mathbf{x}') + \frac{1}{\epsilon_{ext}}(N\mathbf{j}_{int})(\mathbf{x}')$$

or

$$\begin{pmatrix}\mathbf{j}_{inc}\\ \mathbf{j'}_{inc}\end{pmatrix} = (I+P)\begin{pmatrix}\mathbf{j}_{int}\\ \mathbf{j'}_{int}\end{pmatrix} \tag{4.18}$$

with

$$I = \begin{pmatrix}\frac{\mu_{ext}+\mu_{int}}{2\mu_{ext}} & 0\\ 0 & \frac{\epsilon_{ext}+\epsilon_{int}}{2\epsilon_{ext}}\end{pmatrix}$$

and

$$P = \begin{pmatrix}-\frac{L_{\mu}}{\mu_{ext}} & -\frac{M+N}{\mu_{ext}}\\ \frac{M+N}{\epsilon_{ext}} & -\frac{L_{\epsilon}}{\epsilon_{ext}}\end{pmatrix}$$

We will abbreviate this even further:

$$\mathbf{J_{inc}} = A\mathbf{J_{int}} \tag{4.19}$$

4.4 Singularities in the Integral Equations

Since the Green's functions have singularities at $\mathbf{x}=\mathbf{0}$, the Müller equations include some convergent improper integrals. The integrals:

$$\int_{\partial\Omega}\left[\mathbf{n}(\mathbf{x}')\times\mathbf{j}(\mathbf{x})\right]\left(k_{ext}^2G^{ext}-k_{int}^2G^{int}\right)dS(\mathbf{x}) \tag{4.20}$$

and

$$\int_{\partial\Omega} \mathbf{n}(\mathbf{x}') \times \left[\mathbf{j}(\mathbf{x}) \times \nabla\left(\epsilon_{ext} G^{ext} - \epsilon_{int} G^{int}\right)\right] dS(\mathbf{x}) \tag{4.21}$$

are both singular integrals. The first of these, (4.20), is a single layer potential. The second, (4.21), contains something like a double layer potential as well as another type of singular integral. These will be investigated more in Chapter 6. The other integrals that appear in the Müller equations are not singular as the singularities are subtracted out in $G_{ext} - G_{int}$.

Chapter 5

Ewald Splitting

The numerical solution of the Müller equations (4.16) will require many evaluations of the Green's function and its derivatives. The Green's function as a Fourier series (3.10)

$$G(x,y,z) = \frac{1}{8\pi^2} \sum_{m,n} \frac{e^{-\sqrt{-\lambda_{mn}}|z|}}{\sqrt{-\lambda_{mn}}} P_{mn}$$

presents two numerical difficulties. First, this function converges very slowly when z is close to 0. Since it is a double infinite sum, including many terms slows down numerical integration to the point of impracticability. Second, the singularity in the Green's function is difficult to analyze and to work with. We will deal with the first problem in this chapter and with the second in Chapter 6.

To accelerate convergence of certain Green's functions, P.P. Ewald devised a way to represent them differently [17]. His new representation splits the function into two parts which each can converge more quickly than the Fourier series (3.10). His technique is known as Ewald splitting or Ewald summation, and it can be applied to our periodic Helmholtz Green's function. Our $3D$ treatment of Ewald's technique

will follow that outlined in $2D$ in [21] and [29]. It is based on a connection between the Green's function and a solution to a type of heat equation

Proposition: 5.0.1. *Let $u(z,t)$ be a bounded (in z) solution to the the partial differential equation $u_t = u_{zz} + au$ for some constant a with $u(z,0) = \delta(z)$. Then*

$$u(z,t) = \frac{1}{\sqrt{4\pi t}} e^{-\frac{z^2}{4t} + at}$$

Proof. Let $v(z,t)$ be such that $v_t - v_{xx} = 0$ with $v(z,0) = \delta(z)$. This is just a heat equation, and we know the solution is the heat kernel:

$$v(z,t) = \frac{1}{\sqrt{4\pi t}} e^{-\frac{z^2}{4t}} \tag{5.1}$$

Now let $u(z,t) = e^{at} v(z,t)$. Then

$$u_t(z,t) = a e^{at} v(z,t) + e^{at} v_t(z,t)$$

$$u_{zz} = e^{at} v_{zz}(z,t)$$

Then

$$u_t(z,t) - u_{zz}(z,t) = e^{at}\left(a v(z,t) + v_t(z,t) - v_{zz}(z,t)\right) = a e^{at} v(z,t) = a u(z,t)$$

Thus $u_t = u_{zz} + au$,

$$u(z,0) = v(z,0) = \delta(z)$$

and

$$u(z,t) = e^{at} v(z,t) = \frac{1}{\sqrt{4\pi t}} e^{-\frac{z^2}{4t} + at}$$

□

With this solution to a heat equation, we can rewrite the periodic Green's function.

Proposition: 5.0.2. *For λ on the negative real axis,*

$$\frac{1}{2}\frac{e^{-\sqrt{-\lambda}|z|}}{\sqrt{-\lambda}} = \int_0^\infty \frac{1}{\sqrt{4\pi t}} e^{\lambda t - \frac{z^2}{4t}}\, dt$$

Proof. Let $u_t(z,t) = u_{zz}(z,t) + \lambda u(z,t)$ with $u(z,t)$ a bounded function of z and $u(z,0) = \delta(z)$. Then, as in Proposition 5.0.1,

$$u(z,t) = \frac{1}{\sqrt{4\pi t}} e^{-\frac{z^2}{4t} + \lambda t}$$

Now let $U(z)$ be the distribution defined as

$$U(z) = \int_0^\infty u(z,t)\, dt$$

for a test function ϕ. Then

$$\begin{aligned}
(U_{zz}(z) + \lambda U(z), \phi(z)) &= \left(\int_0^\infty u_{zz}(z,t) + \lambda u(z,t)\, dt, \phi(z) \right) \\
&= \left(\int_0^\infty u_t(z,t)\, dt, \phi(z) \right) \\
&= \left(\lim_{b\to\infty} [u(z,b) - u(z,0)], \phi(z) \right) \\
&= (-\delta(z), \phi(z)) \\
&= -\phi(0)
\end{aligned}$$

where the limit of $u(z,b)$ is zero since λ lies on the negative real axis. We saw in the derivation of the periodic Green's function (3.6) that

$$G(z) = \frac{1}{2}\frac{e^{-\sqrt{-\lambda}|z|}}{\sqrt{-\lambda}}$$

for λ on the negative real axis is the unique solution that decays at ∞ of the differential equation

$$D_{zz}G(z) + \lambda G(z) = -\delta(z)$$

Since $U(z)$ satisfies this same equation and since $U(z) \to 0$ as $z \to \infty$, $U(z)$ and $G(z)$ must be the same by uniqueness. □

We would like to use Proposition 5.0.2 to get a new representation for the periodic Green's function:

$$G(x,y,z) = \frac{1}{8\pi^2}\sum_{m,n}\frac{e^{-\sqrt{-\lambda_{mn}}|z|}}{\sqrt{-\lambda_{mn}}}P_{mn} = \frac{1}{4\pi^2}\sum_{m,n}P_{mn}\int_0^\infty \frac{1}{\sqrt{4\pi t}}e^{\lambda_{mn}t-\frac{z^2}{4t}}dt \qquad (5.2)$$

where, again,

$$P_{mn} = e^{i(m+\alpha)x+i(n+\beta)y} \quad \text{and} \quad \lambda_{mn} = (m+\alpha)^2 + (n+\beta)^2 - k^2$$

Unfortunately, we cannot quite do this. Equation (5.2) would be true if λ_{mn} were always on the negative real axis. The sums in (5.2), however, necessarily include λ's that have positive real part. The constant λ_{00}, for example, will always have a positive real part, and there may be - depending on k - other modes with this characteristic. It is easy to see that the integrals on the right hand side of (5.2) will not even converge for λ_{mn} with positive real part.

We have seen in Chapter 3 that the Fourier series representation of the Green's function (the left hand side of (5.2)) is analytic for λ_{mn} in the upper half plane excluding $\lambda_{mn} = 0$. We need to preserve this analyticity property of the Green's function.

Now, Proposition 5.0.2 is true on for λ on the negative real line, and for such λ, we can write:

$$\frac{1}{2}\frac{e^{-\sqrt{-\lambda}|z|}}{\sqrt{-\lambda}} = \int_0^{E^2} \frac{1}{\sqrt{4\pi t}} e^{\lambda t - \frac{z^2}{4t}} dt + \int_{E^2}^{\infty} \frac{1}{\sqrt{4\pi t}} e^{\lambda t - \frac{z^2}{4t}} dt$$

Breaking the integral up in this way is Ewald's splitting. It will eventually allow us to take G and to split it into two pieces $G1$ and $G2$. The constant E can be arbitrarily chosen to be any positive real number and is called the Ewald parameter or the splitting parameter. The first of the two integrals on the right hand side of this equation is an analytic function of λ for any λ in the upper half complex plane. The second is not. We will rewrite this integral in another form by first expanding the $\frac{z^2}{4t}$ term as a Taylor series:

$$\int_{E^2}^{\infty} \frac{1}{\sqrt{4\pi t}} e^{\lambda t - \frac{z^2}{4t}} dt = \int_{E^2}^{\infty} \frac{1}{\sqrt{4\pi t}} e^{\lambda t} \sum_{\ell=0}^{\infty} \frac{(-z)^{2\ell}}{4^\ell t^\ell} dt$$

$$= \frac{1}{2\sqrt{\pi}} \sum_{\ell=0}^{\infty} \frac{(-z)^{2\ell}}{4^\ell \ell!} \int_{E^2}^{\infty} \frac{e^{\lambda t}}{t^{\ell+1/2}} dt$$

By making the substitution $w = t/E^2$ in the integral above and remembering that we are dealing with λ on the negative real axis, we see that

$$\int_{E^2}^{\infty} \frac{1}{\sqrt{4\pi t}} e^{\lambda t - \frac{z^2}{4t}} dt = \frac{1}{2\sqrt{\pi}} \sum_{\ell=0}^{\infty} \frac{(-z)^{2\ell}}{4^\ell \ell! E^{2\ell-1}} \operatorname{ExpInt}_{\ell+1/2}\left(-\lambda E^2\right)$$

See Appendix C for a discussion of the exponential integral function of order n ExpInt_n. We now have, for λ on the negative real axis,

$$\begin{aligned}\frac{1}{2}\frac{e^{-\sqrt{-\lambda}|z|}}{\sqrt{-\lambda}} &= \int_0^{E^2} \frac{1}{\sqrt{4\pi t}} e^{\lambda t - \frac{z^2}{4t}} dt \\ &\quad + \frac{1}{2\sqrt{\pi}} \sum_{\ell=0}^{\infty} \frac{(-z)^{2\ell}}{4^\ell \ell! E^{2\ell-1}} \mathrm{ExpInt}_{\ell+1/2}\left(-\lambda E^2\right)\end{aligned} \tag{5.3}$$

This equality is true for all λ on the negative real axis. The left hand side of (5.3), however, is analytic for all λ in the upper half complex plane. Furthermore, exponential integral functions are analytic on the upper half complex plane and the sum in ℓ converges rapidly, and so the right hand side of (5.3) is as well. Since this equation holds on the negative real axis and since both sides of it are analytic in λ in the upper half complex plane, we can extend the equality to all λ in the upper half complex plane. We are finally able to write the Green's function in a new form that is valid for all the possible λ_{mn} modes:

$$G(x,y,z) = G1(x,y,z) + G2(x,y,z)$$

with

$$G1(x,y,z) = \frac{1}{4\pi^2} \sum_{m,n} P_{mn} \int_0^{E^2} \frac{1}{\sqrt{4\pi t}} e^{\lambda_{mn} t - \frac{z^2}{4t}} dt$$

$$G2(x,y,z) = \frac{1}{8\pi^{5/2}} \sum_{m,n} P_{mn} \sum_{\ell=0}^{\infty} \frac{(-z)^{2\ell}}{4^\ell \ell! E^{2\ell-1}} \mathrm{ExpInt}_{\ell+1/2}\left(-\lambda_{mn} E^2\right)$$

Again, the positive real number E is called the Ewald parameter. The singularity is now contained entirely in $G1$ in the t integral at the 0 endpoint of integration. The function $G2$ is smooth. We will see in section 5.2.2 that the $G2$ can converge

quickly if E is chosen large enough. We aim to rewrite the function $G1$ in a form that can also converge quickly.

5.1 G1

We would like to rewrite $G1$ into a form that converges quickly. We start by rearranging some terms:

$$\begin{aligned} G1\left(x,y,z\right) &= \frac{1}{4\pi^2}\sum_{m,n} P_{mn}\int_0^{E^2}\frac{1}{\sqrt{4\pi t}}e^{\lambda_{mn}t-\frac{z^2}{4t}}dt \\ &= \frac{1}{4\pi^2}\sum_{m,n}\int_0^{E^2}\frac{1}{\sqrt{4\pi t}}e^{k^2t-\frac{z^2}{4t}}e^{i(m+\alpha)x+i(n+\beta)y-(m+\alpha)^2t-(n+\beta)^2t}dt \qquad (5.4) \\ &= \frac{1}{4\pi^2}\int_0^{E^2}\frac{1}{\sqrt{4\pi t}}e^{k^2t-\frac{z^2}{4t}}\sum_{m,n}e^{i(m+\alpha)x+i(n+\beta)y-(m+\alpha)^2t-(n+\beta)^2t}dt \end{aligned}$$

The sum

$$\sum_{m,n} e^{i(m+\alpha)x+i(n+\beta)y-(m+\alpha)^2t-(n+\beta)^2t} = e^{i(\alpha x+\beta y)}\sum_{m,n} e^{imx+iny-(m+\alpha)^2t-(n+\beta)^2t} \qquad (5.5)$$

can be changed from a Fourier series to a physical summation over periodic reflections. One direct result of the Poisson summation formula (which we prove in Appendix B) is the identity:

$$e^{i(\alpha x+\beta y)}\sum_{m,n} e^{imx+iny-(x+\alpha)^2t-(y+\beta)^2t} = \frac{\pi}{t}\sum_{\mu,\nu} e^{-2\pi i(\alpha\mu+\beta\nu)}e^{-\frac{(x+2\pi\mu)^2+(y+2\pi\nu)^2}{4t}}$$

This identity states the equality between the fundamental solution of a periodic heat equation (on the right hand side) and its Fourier series (on the left) [40][38]. We use

it to write $G1$ as

$$G1\left(x,y,z\right)=\frac{1}{4\pi^2}\int_0^{E^2}\frac{1}{\sqrt{4\pi t}}e^{k^2t-\frac{z^2}{4t}}\left(\frac{\pi}{t}\sum_{\mu,\nu}e^{-2\pi i(\alpha\mu+\beta\nu)}e^{-\frac{(x+2\pi\mu)^2+(y+2\pi\nu)^2}{4t}}\right)dt$$

$$=\frac{1}{8\pi^{3/2}}\sum_{\mu,\nu}e^{-2\pi i(\alpha\mu+\beta\nu)}\int_0^{E^2}\frac{1}{t^{3/2}}e^{k^2t-\frac{(x+2\pi\mu)^2+(y+2\pi\nu)^2+z^2}{4t}}dt \tag{5.6}$$

$$=\frac{1}{8\pi^{3/2}}\sum_{\mu,\nu}e^{-2\pi i(\alpha\mu+\beta\nu)}\int_0^{E^2}\frac{1}{t^{3/2}}e^{k^2t-\frac{R_{\mu\nu}^2}{4t}}dt$$

for $R_{\mu\nu}^2=(x+2\pi\mu)^2+(y+2\pi\nu)^2+z^2$. This more physical representation of $G1$ is no longer a Fourier series, and we can see more clearly now how the Green's function is singular as $\mathbf{x}\to 0$. The t integral in the function is divergent when $R_{\mu\nu}=0$ because of the $t^{-3/2}$ in the integrand.

This form for $G1$, however, is not very practical numerically. We will expand the e^{k^2t} term in the integrand of (5.6) as a Taylor series. Then

$$G1\left(x,y,z\right)=\frac{1}{8\pi^{3/2}}\sum_{\mu,\nu}e^{-2\pi i(\alpha\mu+\beta\nu)}\sum_{\ell=0}^{\infty}\frac{k^{2\ell}}{\ell!}\int_0^{E^2}\frac{t^\ell}{t^{3/2}}e^{-\frac{R_{\mu\nu}^2}{4t}}dt$$

We can recognize the integral above as an exponential integral of order $\ell+1/2$ if we make the substitution $w=E^2/t$.

$$G1\left(x,y,z\right)=\frac{1}{8\pi^{3/2}}\sum_{\mu,\nu}e^{-2\pi i(\alpha\mu+\beta\nu)}\sum_{\ell=0}^{\infty}\frac{k^{2\ell}E^{2\ell-1}}{\ell!}\,\mathrm{ExpInt}_{\ell+1/2}\left(\frac{R_{\mu\nu}^2}{4E^2}\right) \tag{5.7}$$

In Appendix C, we discuss exponential integrals and their properties. Since computing with exponential integral functions is relatively fast, this is the form of $G1$ that

we will work with. We can now write G as a sum of $G1$ and $G2$:

$$\begin{aligned} G(x,y,z) &= \frac{1}{8\pi^2}\sum_{m,n}\frac{e^{-\sqrt{-\lambda_{mn}}|z|}}{\sqrt{-\lambda_{mn}}}P_{mn} \\ &= G1(x,y,z)+G2(x,y,z) \\ &= \frac{1}{8\pi^{3/2}}\sum_{\mu,\nu}e^{-2\pi i(\alpha\mu+\beta\nu)}\sum_{\ell=0}^{\infty}\frac{k^{2\ell}E^{2\ell-1}}{\ell!}\,\mathrm{ExpInt}_{\ell+1/2}\left(\frac{R_{\mu\nu}^2}{4E^2}\right) \\ &\quad+\frac{1}{8\pi^{5/2}}\sum_{m,n}P_{mn}\sum_{\ell=0}^{\infty}\frac{(-z)^{2\ell}}{4^\ell\ell!E^{2\ell-1}}\,\mathrm{ExpInt}_{\ell+1/2}\left(-\lambda_{mn}E^2\right) \end{aligned} \tag{5.8}$$

5.2 Properties of G1 and G2

5.2.1 G1 Properties

As hoped for, $G1$ involves quickly converging sums (relative to the sums in the Fourier form of the Green's function).

$$G1(x,y,z) = \frac{1}{8\pi^{3/2}}\sum_{\mu,\nu}e^{-2\pi i(\alpha\mu+\beta\nu)}\sum_{\ell=0}^{\infty}\frac{k^{2\ell}E^{2\ell-1}}{\ell!}\,\mathrm{ExpInt}_{\ell+1/2}\left(\frac{R_{\mu\nu}^2}{4E^2}\right)$$

The ℓ sum decays quickly due to the $\frac{1}{\ell!}$, and the μ and ν sums decay quickly as $R_{\mu\nu}^2$ grows (exponential integrals of any order decay exponentially as the argument increases - see Appendix C). The ℓ sum can converge much more slowly if the wave number $k=\omega\sqrt{\epsilon\mu}$ is large. This fact limits us to low frequency scattering problems. Finally, the Ewald parameter E must be small to ensure quick convergence (see 5.3).

All of the singularity of the Green's function is contained in $G1$. It occurs only in the exponential integral of order $\frac{1}{2}$. The derivatives of $G1$ include exponential integrals of order $-\frac{1}{2}$, and these too are singular as $R_{\mu\nu}\to 0$ (Appendix A lists the

needed derivatives of G). Using (C.3) and (C.4), we can see the exact nature of these singularities

$$\text{ExpInt}_{\frac{1}{2}}\left(\frac{R_{\mu\nu}^2}{4E^2}\right) \to \frac{2E\sqrt{\pi}}{R_{\mu\nu}} \quad \text{as} \quad R_{\mu\nu} \to 0$$

$$\text{ExpInt}_{-\frac{1}{2}}\left(\frac{R_{\mu\nu}^2}{4E^2}\right) \to \frac{8E^3\sqrt{\pi}}{R_{\mu\nu}^3} \quad \text{as} \quad R_{\mu\nu} \to 0$$

Note that as $\mathbf{x} \to 0$, $R_{\mu\nu} \to 0$ only for $\mu = \nu = 0$. We can then see that the singularity in $G1$ is the same in size as the singularity in the free space Green's function (3.1):

$$G1\left(x,y,z\right) \to \left(\frac{1}{8\pi^{3/2}}\right)\left(E^{-1}\right)\left(\frac{2E\sqrt{\pi}}{R_{00}}\right) = \frac{1}{4\pi\left|x\right|} \quad \text{as} \quad \left|x\right| \to 0$$

This fact was essential in deriving the Müller integral equations.

5.2.2 G2 Properties

$$G2\left(x,y,z\right) = \frac{1}{8\pi^{5/2}}\sum_{m,n} P_{mn} \sum_{\ell=0}^{\infty} \frac{\left(-z\right)^{2\ell}}{4^{\ell}\ell!E^{2\ell-1}} \text{ExpInt}_{\ell+1/2}\left(-\lambda_{mn}E^2\right)$$

It was mentioned that the sums in $G2$ can converge quickly, and we can now see that. The ℓ sum converges quickly due to the $\frac{1}{\ell!}$, and the m and n sums converge quickly as the argument of the exponential integrals gets large. The sum over ℓ is actually an alternating sum, and estimates of convergence are easily found. However, if either z or k is large, convergence can be slow. Again, we see that we are limited to low frequency problems. For $G2$, the Ewald parameter E must be sufficiently large in order to achieve quick convergence of the sums (see 5.3).

Some effort has been made to write $G2$ in such a way that it can be analytic for all λ_{mn} in the upper half complex plane. We still, however, need to be careful that the Green's function satisfies the radiation conditions (2.5) for these λ_{mn}. For (5.8) to hold, we must remember from Chapter 3 that when $\mathrm{Re}\left(\sqrt{-\lambda_{mn}}\right) = 0$, we choose the negative square root in the Fourier representation of the Green's function. This ensures that modes propagate in the correct direction. In our $G2$ expression, it is equivalent to choosing the negative square root when evaluating $G2$'s exponential integral functions (see (C.2)).

5.3 Choosing the Splitting Parameter

As has been shown, there is a trade off in the selection of the splitting parameter E. If E is large, $G2$ converges quickly, but $G1$ converges slowly. If E is small, the opposite occurs. It seems possible that some estimates could help in selecting this parameter well, but we have also found it easy to experimentally determine a choice for E. We will discuss this issue further in Chapter 7. More information can be found in [12] and [11].

Chapter 6

Corrections

Two types of integrals that appear in the integral equation (4.16) are singular integrals. These are difficult to evaluate numerically. The singularities introduce errors in Gaussian quadrature methods that are on the order of the step size. The other integrals in Müller's equations are smooth and pose no numerical problems. Our method for dealing with the singular integrals involves smoothing the integrand and then adding a correction term to the resulting integral. These types of methods were first developed by Beale in [6] for problems in periodic water waves. They have been furthered in [8] [7].

In this thesis, we are limited to C^3 surfaces. This condition allows us to take the Taylor expansions of functions on the surface that we need for our method. For numerical ease, we are also here limited to surfaces that are graphs - surfaces where z is a function of x and y. The method, however, is fully adaptable to a general C^3 surface, and we will do the smoothing and correction analysis in this chapter for a general C^3 surface $\partial\Omega$.

6.1 Smoothing

Many singular integral methods involve the smoothing of a singular kernel through multiplication by a smoothing function [6] [8] [7]. For the free space Helmholtz Green's function (3.1) $\Phi(r)$, for example, multiplication by $\operatorname{erf}\left(-\frac{r^2}{\delta^2}\right)$ for some smoothing parameter δ removes the singularity at $r = 0$. We thus replace the singular function with a smooth function:

$$\Phi(r) \to \Phi_\delta(r) = \Phi(r) \operatorname{erf}\left(-\frac{r^2}{\delta^2}\right)$$

This new function Φ_δ is smooth as $r \to 0$, and numerical integration of this function is accurate. Of course, one cannot just throw out a bad integrand, stick in a good one, and expect to get anything meaningful! Replacing Φ with Φ_δ in an integral introduces an error that we will call the smoothing error. Since the smoothing function quickly approaches 1 away from $r = 0$, $\Phi(r) \approx \Phi_\delta(r)$ for r away from zero. Thus, the smoothing error is centered around small r. If this error can be quantified, it can be used as a correction term to an integral over the smoothed function Φ_δ:

With the pseudoperiodic Green's function

$$G(x, y, z) = \frac{1}{8\pi^2} \sum_{m,n} \frac{e^{-\sqrt{(m+\alpha)^2+(n+\beta)^2-k^2}|z|}}{\sqrt{(m+\alpha)^2+(n+\beta)^2-k^2}} e^{i(m+\alpha)x+i(n+\beta)y},$$

it is not immediately clear how to create a smooth version G_δ. Multiplying by the same smoothing function $1 - e^{-\frac{r^2}{\delta^2}}$ may remove the singularity, but it also destroys periodicity. It is not clear how to pick a smoothing function for this G that is also periodic.

The Ewald formulation of the Green's function fortunately provides a clear way to achieve smoothing. The singularity in G is entirely contained in the $G1$ summation (5.7). It is easy to see the singularity in the exponential integral term as $R_{\mu\nu} \to 0$. It is in a different $G1$ representation (5.6), however, that we find an easy way to smooth the Green's function. Written in this way,

$$G1\left(x,y,z\right) = \frac{1}{8\pi^{3/2}} \sum_{\mu,\nu} e^{-2\pi i(\alpha\mu+\beta\nu)} \int_0^{E^2} \frac{e^{k^2 t - \frac{R_{\mu\nu}^2}{4t}}}{t^{3/2}} dt,$$

the singularity is located at the 0 endpoint of integration of the dt integral. If we just cut this singularity out by integrating from some small function of δ instead of from 0, we obtain a $G1_\delta$ that is smooth:

$$G1_\delta\left(x,y,z\right) = \frac{1}{8\pi^{3/2}} \sum_{\mu,\nu} e^{-2\pi i(\alpha\mu+\beta\nu)} \int_{\delta^2}^{E^2} \frac{e^{k^2 t - \frac{R_{\mu\nu}^2}{4t}}}{t^{3/2}} dt \tag{6.1}$$

This smoothed Green's function is not singular at $r = 0$, and it quickly approaches $G1$ as r increases (see Figure 6.1). It is also still periodic. Our strategy is therefore to replace G with G_δ in any of the singular integrals that appear in the Müller integral equations (introducing a smoothing error), to evaluate these integrals using a trapezoid method (accurately, since the integrands are now smooth), and to add correction terms to compensate for the smoothing error introduced. The error introduced through discretization of the smoothed integrals will be discussed at the end of this chapter (see Section 6.5).

We will apply this technique to both types of singular integral from (4.16). But first, we will first find correction terms for smoothed single and double layer potentials. These are related to the types of integrals in Müller's equations, and they

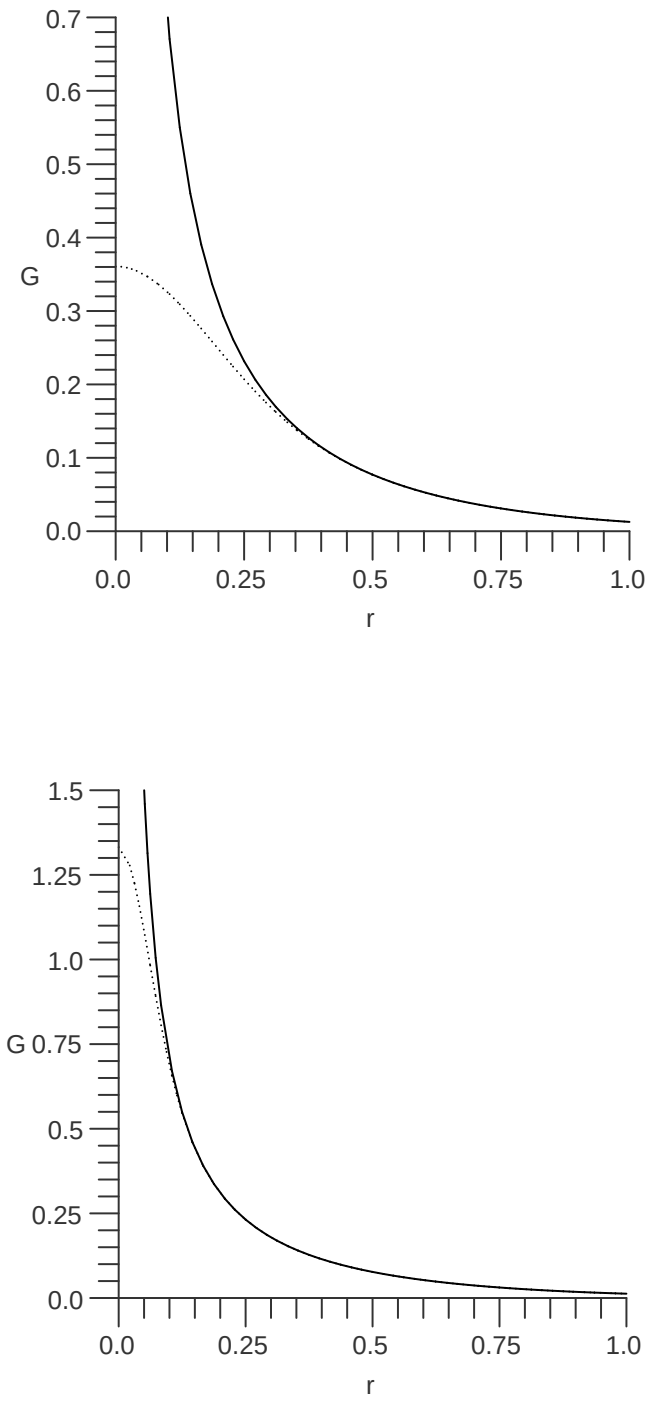

Figure 6.1: G and G_δ on the same axes. The upper plot is with $\delta = 0.01$. Below, $\delta = .001$. Both are for normally incident light. $E = 0.5$ and $k = 0.3$.

offer us a more general and clean look at this technique before we apply it to our scattering problem. In the proofs to follow, we will use the integrals

$$\begin{aligned}
\int_0^\infty s e^{-\frac{\delta^2 s^2}{4t}} ds &= \frac{2t}{\delta^2} \\
\int_0^\infty s^3 e^{-\frac{\delta^2 s^2}{4t}} ds &= \frac{8t^2}{\delta^4} \\
\int_0^\infty s^5 e^{-\frac{\delta^2 s^2}{4t}} ds &= \frac{64t^3}{\delta^6}
\end{aligned} \tag{6.2}$$

which can be shown through substitution and integration by parts methods.

The derivations of correction terms that follow involve some ideas from classical differential geometry. In particular, certain changes of variables are used to simplify various expressions. The corrections can be derived without such simplifications, and such a derivation is outlined in Appendix D.

Finally, for the duration of this chapter, we will shift the periodic block of $\partial\Omega$ so that the point $x = y = 0$ is centered in the block. One block will therefore be the portion of the scatterer that lies in the domain $-\pi \leq x, y \leq \pi$. This does not change any of the integrals, and it will simplify our calculations. In general, in the proofs to follow, we will change coordinates frequently to simplify the analysis. The correction terms, however, must be invariant quantities, and it does not matter what coordinate system we use.

6.2 The Single Layer Potential

The single layer potential with our periodic Helmholtz Green's function is:

$$\int_{\partial\Omega} G\left(\mathbf{x}' - \mathbf{x}\right) f\left(\mathbf{x}\right) dS\left(\mathbf{x}\right) \tag{6.3}$$

We are interested in investigating the error ϵ introduced by replacing the Green's function G with this regularized Green's function G_δ in a single layer potential when the reference variable $\mathbf{x}'$ is on the surface. We are able to identify and quantify the largest part of this error and use it as a correction to the smoothed integral. After correction, the error is small:

Proposition: 6.2.1. *For G, G_δ, and $\partial\Omega$ as defined and for $\mathbf{x}' \in \partial\Omega$,*

$$\int_{\partial\Omega} G\left(\mathbf{x}' - \mathbf{x}\right) f\left(\mathbf{x}\right) dS\left(\mathbf{x}\right) = \int_{\partial\Omega} G_\delta\left(\mathbf{x}' - \mathbf{x}\right) f\left(\mathbf{x}\right) dS\left(\mathbf{x}\right) + \frac{f\left(\mathbf{x}'\right)}{\pi^{1/2}}\delta + O\left(\delta^3\right)$$

Proof. The error is the difference between the two integrals:

$$\epsilon = \int_{\partial\Omega} \left[G\left(\mathbf{x}' - \mathbf{x}\right) - G_\delta\left(\mathbf{x}' - \mathbf{x}\right)\right] f\left(\mathbf{x}\right) dS\left(\mathbf{x}\right)$$

Without loss of generality, we take $\mathbf{x}' = \mathbf{0}$. The error becomes:

$$\epsilon = \frac{1}{8\pi^{3/2}} \int_{\partial\Omega} \left(\sum_{\mu,\nu} e^{-2\pi i(\alpha\mu + \beta\nu)} \int_0^{\delta^2} \frac{e^{k^2 t - \frac{(x-2\pi\mu)^2 + (y-2\pi\nu)^2 + z^2}{4t}}}{t^{3/2}} dt \right) f\left(\mathbf{x}\right) dS\left(\mathbf{x}\right) \tag{6.4}$$

The $\mu = \nu = 0$ term in the double sum will give the largest contribution to the error. We will show in Proposition 6.2.2 that the other terms are negligibly small.

Thus, writing these small terms as HOT, we have

$$\begin{aligned}\epsilon &= \frac{1}{8\pi^{3/2}} \int_{\partial\Omega} \left(\int_0^{\delta^2} \frac{e^{k^2 t - \frac{x^2+y^2+z^2}{4t}}}{t^{3/2}} dt \right) f(\mathbf{x})\, dS(\mathbf{x}) + HOT \\ &= \frac{1}{8\pi^{3/2}} \int_0^{\delta^2} \frac{e^{k^2 t}}{t^{3/2}} \left(\int_{\partial\Omega} e^{\frac{-r^2}{4t}} f(\mathbf{x})\, dS(\mathbf{x}) \right) dt + HOT\end{aligned} \tag{6.5}$$

where $r^2 = |x|^2$.

The error is highly concentrated around the singular point $r = |\mathbf{x}| = 0$. Away from this singularity, the error quickly decays, and the contribution to the error away from the singularity is negligible. We show in Proposition 6.2.2 that we can perform the surface integral only on a small set of $\partial\Omega$ including $r = 0$ and still find the largest part of the error. We let D be an open set in $\mathbb{R}^2$ with coordinates $\alpha = (\alpha_1, \alpha_2)$ such that α can be smoothly (at least C^3) mapped from D onto an open set in $\partial\Omega$. Then $\mathbf{x} \in \partial\Omega$ becomes $\mathbf{x}(\alpha)$. We choose this coordinate patch so that $\mathbf{x}(0) = \mathbf{0}$. The error can now be written as an integral in α over D:

$$\epsilon = \frac{1}{8\pi^{3/2}} \int_0^{\delta^2} \frac{e^{k^2 t}}{t^{3/2}} \left(\int_D e^{\frac{-r(\alpha)^2}{4t}} f(\alpha) \left| \frac{\partial \mathbf{x}}{\partial \alpha_1} \times \frac{\partial \mathbf{x}}{\partial \alpha_2} \right| d\alpha \right) dt + HOT$$

We will extend the $d\alpha$ integral from D to all of $\mathbb{R}^2$. This greatly simplifies the analysis that follows, and, since the error is concentrated around $r = 0$, we are only adding a negligibly small area to the integral.

$$\epsilon = \frac{1}{8\pi^{3/2}} \int_0^{\delta^2} \frac{e^{k^2 t}}{t^{3/2}} \left(\int_{\mathbb{R}^2} e^{\frac{-r(\alpha)^2}{4t}} f(\alpha) \left| \frac{\partial \mathbf{x}}{\partial \alpha_1} \times \frac{\partial \mathbf{x}}{\partial \alpha_2} \right| d\alpha \right) dt + HOT \tag{6.6}$$

In the following analysis, we will omit the HOT at the end of the error integral. This is done only for aesthetics, and it is to be understood that there are some very small corrections in the background.

We now do some geometry. As outlined in [2], we can choose (rotating and translating as necessary) coordinates α so that the Christoffel symbols are zero at $\mathbf{x}' = \mathbf{0}$. We then make a linear change of variables so that the tangential vectors $\mathbf{T_j} = \frac{\partial \mathbf{x}}{\partial \alpha_j}$ point in the directions of the principal curvatures of the surface and the metric tensor is the identity at $\mathbf{x}' = \mathbf{0}$. We call these vectors the principal directions. We then have at this point an orthonormal coordinate system $(\mathbf{T_1}, \mathbf{T_2}, \mathbf{n_0})$. We will refer to this system as the normal coordinate system. The error integral becomes:

$$\epsilon = \frac{1}{8\pi^{3/2}} \int_0^{\delta^2} \frac{e^{k^2 t}}{t^{3/2}} \left(\int_D e^{\frac{-r(\alpha)^2}{4t}} f(\alpha) |\mathbf{T_1} \times \mathbf{T_2}| d\alpha \right) dt$$

Following [2] and [7], we expand $\mathbf{x}(\alpha)$ in a Taylor series around $\alpha = 0$. What makes the normal coordinates so special is that there is no $\alpha_1 \alpha_2$ term among the second order terms:

$$\mathbf{x}(\alpha) = \mathbf{T_1}(0)\alpha_1 + \mathbf{T_2}(0)\alpha_2 + \frac{1}{2}\kappa_1 \mathbf{n_0} \alpha_1^2 + \frac{1}{2}\kappa_2 \mathbf{n_0} \alpha_2^2 + O\left(|\alpha|^3\right) \tag{6.7}$$

Where $\mathbf{n_0}$ is the unit normal at $\alpha = 0$ and where κ_1 and κ_2 are the principal curvatures at $\mathbf{x}' = \mathbf{0}$. The vectors $\mathbf{T_1}(0)$, $\mathbf{T_2}(0)$, and $\mathbf{n_0}$ form an orthonormal system at the origin. Then, using the facts $\mathbf{T_i}(0) \cdot \mathbf{T_j}(0) = \delta_{ij}$ and $\mathbf{T_j}(0) \cdot \mathbf{n_0} = 0$,

$$\begin{aligned} r^2 &= \mathbf{x}(\alpha) \cdot \mathbf{x}(\alpha) \\ &= \alpha_1^2 + \alpha_2^2 + \frac{1}{4}\kappa_1^2 \alpha_1^4 + \frac{1}{4}\kappa_1 \kappa_2 \alpha_1^2 \alpha_2^2 + \frac{1}{4}\kappa_2^2 \alpha_2^4 + O\left(\alpha_1 |\alpha|^3\right) + O\left(\alpha_2 |\alpha|^3\right) \qquad (6.8) \\ &= |\alpha|^2 + O\left(|\alpha|^4\right) \end{aligned}$$

In the last step (and in other places in this chapter), we make use of the inequalities $\alpha_j^2 \leq |\alpha|^2$. We now do a change of variables $\alpha \to \xi$ such that $|\xi|^2 = r^2$ and $\xi_i / |\xi| =$

$\alpha_i/|\alpha|$. This change seems to be small, but it is essential to our analysis. We make the change in order to simplify the δ dependence in the exponential term of our error integral. Without this change, there are quickly changing high order terms in the argument of the exponential. The substitution eliminates these terms from the exponential while allowing ξ to have the same direction as α. That this is necessary will become clear as we advance in this proof. Then from (6.8)

$$|\xi|^2 = |\alpha|^2 + O\left(|\alpha|^4\right)$$

and thus

$$|\xi| = |\alpha|\sqrt{1 + O\left(|\alpha|^2\right)} = |\alpha| + O\left(|\alpha|^3\right)$$

Since $O\left(|\alpha|^3\right) = O\left(|\xi|^3\right)$ we have

$$|\alpha| = |\xi| + O\left(|\xi|^3\right)$$

and then

$$\begin{aligned} \alpha_i &= \left(\xi_i/|\xi|\right)|\alpha| \\ &= \left(\xi_i/|\xi|\right)\left(|\xi| + O\left(|\xi|^3\right)\right) \\ &= \xi_i + O\left(|\xi|^3\right) \end{aligned} \tag{6.9}$$

Writing $f\left(\alpha\left(\xi\right)\right)$ as just $f\left(\xi\right)$, the error is now

$$\epsilon = \frac{1}{8\pi^{3/2}} \int_0^{\delta^2} \frac{e^{k^2 t}}{t^{3/2}} \left(\int_D e^{\frac{-|\xi|^2}{4t}} f\left(\xi\right) \det\left(\partial\alpha/\partial\xi\right) |\mathbf{T_1} \times \mathbf{T_2}| d\xi \right) dt \tag{6.10}$$

We expand $f\left(\alpha\right)$:

$$f\left(\alpha\right) = f\left(0\right) + f_j\left(0\right)\alpha_j + \frac{1}{2} f_{ij}\left(0\right)\alpha_i\alpha_j + O\left(|\alpha|^3\right)$$

Or, in ξ:

$$f(\xi) = f(0) + f_j(0)\xi_j + \frac{1}{2}f_{ij}(0)\xi_i\xi_j + O(|\xi|^3)$$

with the terms being summed over i and j. Using (6.9), we can compute derivatives of α with repsect to ξ:

$$(\partial\alpha_i/\partial\xi_j) = \delta_{ij} + O\left(|\xi|^2\right)$$

With this equation, we see that the determinant of the Jacobian is:

$$\begin{aligned}
\det\left(\partial\alpha/\partial\xi\right) &= \det\begin{bmatrix} \frac{\partial\alpha_1}{\partial\xi_1} & \frac{\partial\alpha_1}{\partial\xi_2} \\ \frac{\partial\alpha_2}{\partial\xi_1} & \frac{\partial\alpha_2}{\partial\xi_2} \end{bmatrix} \\
&= \det\begin{bmatrix} 1 + O\left(|\xi|^2\right) & O\left(|\xi|^2\right) \\ O\left(|\xi|^2\right) & 1 + O\left(|\xi|^2\right) \end{bmatrix} \\
&= 1 + O\left(|\xi|^2\right)
\end{aligned}$$

Remembering that

$$\mathbf{T_j}\left(\alpha\right) = \frac{\partial\mathbf{x}}{\partial\alpha_j} = \mathbf{T_j}(0) + \kappa_j\mathbf{n_0}\alpha_j + O\left(|\alpha|^2\right)$$

and that

$$\mathbf{T_1}(0) \times \mathbf{T_2}(0) = \mathbf{n_0}$$

$$\mathbf{T_2}(0) \times \mathbf{n_0} = \mathbf{T_1}(0)$$

$$\mathbf{n_0}(0) \times \mathbf{T_1}(0) = \mathbf{T_2}(0)$$

we obtain

$$
\begin{aligned}
|\mathbf{T_1} \times \mathbf{T_2}| &= \left|\left(\mathbf{T_1}(0) + \kappa_1 \mathbf{n_0} \alpha_1 + O\left(|\alpha|^2\right)\right) \times \left(\mathbf{T_2}(0) + \kappa_2 \mathbf{n_0} \alpha_2 + O\left(|\alpha|^2\right)\right)\right| \\
&= |\mathbf{n_0} - \kappa_1 \alpha_1 \mathbf{T_1}(0) - \kappa_2 \alpha_2 \mathbf{T_2}(0)| \\
&= \left[(\mathbf{n_0} - \kappa_1 \alpha_1 \mathbf{T_1}(0) - \kappa_2 \alpha_2 \mathbf{T_2}(0)) \cdot (\mathbf{n_0} - \kappa_1 \alpha_1 \mathbf{T_1}(0) - \kappa_2 \alpha_2 \mathbf{T_2}(0))\right]^{\frac{1}{2}} \\
&= \left[1 + \kappa_1^2 \alpha_1^2 + \kappa_2^2 \alpha_2^2 + O\left(|\alpha|^2\right)\right]^{\frac{1}{2}} \\
&= \left[1 + O(|\alpha|^2)\right]^{\frac{1}{2}} \\
&= 1 + O(|\alpha|^2) \\
&= 1 + O(|\xi|^2)
\end{aligned}
$$

To approximate the error, we substitute these expansions back into (6.10). The integrand of the $d\xi$ integral becomes:

$$
\begin{aligned}
& e^{\frac{-|\xi|^2}{4t}} (f(0) + f_j(0)\xi_j + \frac{1}{2} f_{ij}(0)\xi_i \xi_j + O(|\xi|^3))(1 + O(|\xi|^2)(1 + O(|\xi|^2)) \\
&= (f(0) + f_i(0)\xi_i + O\left(|\xi|^2\right)) e^{\frac{-|\xi|^2}{4t}} \\
&= (f(0) + f_i(0)\xi_i + R(\xi)) e^{\frac{-|\xi|^2}{4t}}
\end{aligned}
$$

Where the remainder function $R(\xi)$, from the Taylor series integral remainder theorem, has the form

$$R(\xi) = C_1 \xi_1^2 + C_2 \xi_2^2 + C_3 \xi_1 \xi_2$$

for constants C_1, C_2, and C_3.

Since the $f_i(0)\xi_i$ and $C_3 \xi_1 \xi_2$ terms are odd in ξ_i, they integrate to zero and contribute nothing to the error. To analyze the contribution of the remaining terms, we make the change of variables $\xi = \delta\zeta$. Then we can write the remainder term

$R(\xi) = \delta^2 (C_1\zeta_1^2 + C_2\zeta_2^2) = \delta^2 \tilde{R}(\zeta)$. With $d\xi = \delta^2 d\zeta$, the error is now seen to be:

$$\epsilon = \frac{1}{8\pi^{3/2}} \int_0^{\delta^2} \frac{e^{k^2 t}}{t^{3/2}} \left(\int_{\mathbb{R}^2} \left(\delta^2 f(0) + \delta^4 \tilde{R}(\zeta) \right) e^{\frac{-\delta^2 |\zeta|^2}{4t}} d\zeta \right) dt$$

$$= \frac{1}{8\pi^{3/2}} \int_0^{\delta^2} \frac{e^{k^2 t}}{t^{3/2}} \left(\int_{\mathbb{R}^2} \delta^2 f(0) e^{\frac{-\delta^2 |\zeta|^2}{4t}} d\zeta \right) dt + I_{\tilde{R}}$$

We will save our examination of the $\tilde{R}$ integral $I_{\tilde{R}}$ until later and will proceed with the other integral above. We write this $d\zeta$ integral in polar coordinates. We let $s = |\zeta|$ and use (6.2):

$$\epsilon = \frac{\delta^2 f(0)}{8\pi^{3/2}} \int_0^{\delta^2} \frac{e^{k^2 t}}{t^{3/2}} \left(\int_0^{\infty} \int_0^{2\pi} s e^{\frac{-\delta^2 s^2}{4t}} ds d\theta \right) dt + I_{\tilde{R}}$$

$$= \frac{\delta^2 f(0)}{4\pi^{1/2}} \int_0^{\delta^2} \frac{e^{k^2 t}}{t^{3/2}} \left(\int_0^{\infty} s e^{\frac{-\delta^2 s^2}{4t}} ds \right) dt + I_{\tilde{R}}$$

$$= \frac{f(0)}{2\pi^{1/2}} \int_0^{\delta^2} \frac{e^{k^2 t}}{t^{1/2}} dt + I_{\tilde{R}}$$

$$= \frac{f(0)}{2\pi^{1/2}} \int_0^{\delta^2} \frac{1 + k^2 t + \frac{k^4 t^2}{2} + \dots}{t^{1/2}} dt + I_{\tilde{R}}$$

$$= \frac{f(0)}{2\pi^{1/2}} \int_0^{\delta^2} \left(t^{-1/2} + k^2 t^{1/2} + \frac{1}{2} k^4 t^{3/2} + \dots \right) dt + I_{\tilde{R}}$$

$$= \frac{f(0)}{\pi^{1/2}} \delta + O(\delta^3) + I_{\tilde{R}}$$

The *HOT* terms that we have not been writing can now be safely absorbed into the $O(\delta^3)$.

Let us now examine the integral $I_{\tilde{R}}$. We extended in (6.6) the domain of what is now the $d\zeta$ integral from a bounded domain to all of $\mathbb{R}^2$. This indroduced a negligible error, and it has simplified calculations. Here, however, we need to remember that

the domain of integration was originally bounded. We can cut off the function $\tilde{R}(\zeta)$ to these original bounds and therefore have that $\tilde{R}(\zeta)$ is bounded:

$$I_{\tilde{R}} = \frac{1}{8\pi^{3/2}} \int_0^{\delta^2} \frac{e^{k^2 t}}{t^{3/2}} \left(\int_{\mathbb{R}^2} \left(\delta^4 \tilde{R}(\zeta) \right) e^{\frac{-\delta^2 |\zeta|^2}{4t}} d\zeta \right) dt$$

$$\leq \frac{C\delta^4}{8\pi^{3/2}} \int_0^{\delta^2} \frac{e^{k^2 t}}{t^{3/2}} \left(\int_{\mathbb{R}^2} e^{\frac{-\delta^2 |\zeta|^2}{4t}} d\zeta \right) dt$$

We follow the same steps that we used to find the order δ error term. Namely, we convert to polar coordinates and evaluate this integral. We discover that

$$I_{\tilde{R}} \leq C\delta^3$$

The error is thus

$$\epsilon = \frac{f(0)}{\pi^{1/2}} \delta + O\left(\delta^3\right)$$

□

We have omitted proof of the fact that the error is concentrated around the singular point $\mathbf{x} = \mathbf{0}$ so that only the coordinate patch containing the origin need be included and only the $\mu = \nu = 0$ term in our summation need be included. We now prove that fact:

Proposition: 6.2.2. *For the error integral of (6.4) with δ sufficiently small, we can perform the $\partial\Omega$ integral only over one coordinate patch of the surface containing $\mathbf{x} = \mathbf{0}$ without introducing significant error (error greater that $O(\delta^3)$). Furthermore, the error contribution from any but the $\mu = \nu = 0$ term of the summation is negligible.*

Proof. The error is

$$\epsilon = \frac{1}{8\pi^{3/2}} \int_{\partial\Omega} \left(\sum_{\mu,\nu} e^{-2\pi i(\alpha\mu+\beta\nu)} \int_0^{\delta^2} \frac{e^{k^2 t - \frac{R_{\mu\nu}^2}{4t}}}{t^{3/2}} dt \right) f(\mathbf{x})\, dS(\mathbf{x}) \tag{6.11}$$

for $R_{\mu\nu}^2 = (x+2\pi\mu)^2 + (y+2\pi\nu)^2 + z^2$. Then, since the function $f(\mathbf{x})$ is bounded on $\partial\Omega$ by the constant C,

$$\begin{aligned} |\epsilon| &\leq \frac{C}{8\pi^{3/2}} \int_{\partial\Omega} \left(\sum_{\mu,\nu} \int_0^{\delta^2} \left| \frac{e^{k^2 t - \frac{R_{\mu\nu}^2}{4t}}}{t^{3/2}} \right| dt \right) dS(\mathbf{x}) \\ &\leq \frac{C \left| e^{k^2\delta^2} \right|}{8\pi^{3/2}} \int_{\partial\Omega} \left(\sum_{\mu,\nu} \int_0^{\delta^2} \frac{e^{-\frac{R_{\mu\nu}^2}{4t}}}{t^{3/2}} dt \right) dS(\mathbf{x}) \\ &= \frac{C \left| e^{k^2\delta^2} \right|}{4\pi} \sum_{\mu,\nu} \int_{\partial\Omega} \frac{\operatorname{erfc}\left(\frac{R_{\mu\nu}}{2\delta}\right)}{R_{\mu\nu}} dS(\mathbf{x}) \end{aligned}$$

where we have integrated the dt integral exactly through the substitution $u = R/2t^{1/2}$. From [1], we have the inequality

$$\operatorname{erfc} x \leq \frac{e^{-x^2}}{x + \sqrt{x^2 + 4/\pi}}$$

The $\partial\Omega$ integral can thus be bounded

$$\int_{\partial\Omega} \frac{\operatorname{erfc}\left(\frac{r}{2\delta}\right)}{r} dS(\mathbf{x}) \leq \int_{\partial\Omega} \frac{2\delta e^{-\frac{r^2}{4\delta^2}}}{r^2 + r\sqrt{r^2 + 16\delta^2/\pi}} dS(\mathbf{x}) \leq \int_{\partial\Omega} \frac{\delta e^{-\frac{r^2}{4\delta^2}}}{r^2} dS(\mathbf{x})$$

We can center one patch of $\partial\Omega$ at $\mathbf{x} = \mathbf{0}$. From $\mathbf{0}$ this patch extends to some minimum distance r_0. Let $\partial\Omega_0 = \{\mathbf{x} \in \partial\Omega : r(\mathbf{x}) > r_0\}$. Then for δ sufficiently small

$$\int_{\partial\Omega_0} \frac{\delta e^{-\frac{r^2}{4\delta^2}}}{r^2} dS(\mathbf{x}) < \delta^3 \int_{\partial\Omega_0} dS(\mathbf{x}) = O\left(\delta^3\right) \tag{6.12}$$

We note that $R_{\mu\nu} \geq \pi^2$ for any μ and ν other than $\mu = \nu = 0$. This, together with (6.12) proves the proposition. □

In deriving other correction terms, we make similar assumptions about neglecting the other terms in the μ, ν summation and integrating over just one patch. These assumptions are made for an integrand like that in (6.11) but with a higher power of t in the denominator. In the proof for these cases, the integrals and estimates differ from those of Proposition 6.2.2, but the idea is the same, so these proofs will not be included here.

6.3 The Double Layer Potential

The double layer potential is:

$$\int_{\partial\Omega} \left[\mathbf{n}\left(\mathbf{x}\right) \cdot \nabla G\left(\mathbf{x}' - \mathbf{x}\right)\right] f\left(\mathbf{x}\right) dS\left(\mathbf{x}\right) \tag{6.13}$$

In the double layer potential, the singularity of the integrand is increased due to the gradient on the Green's function. The normal vector and this gradient, however, become orthogonal at $\mathbf{x}'$, and the dot product between them counters the increased singularity enough to allow the integral to converge. We will use the same approach with it that we take with the single layer potential. We will use our smoothed Green's function and will look for a correction term.

Proposition: 6.3.1. *With G, G_δ, and $\partial\Omega$ as defined, with $\mathbf{x}' \in \partial\Omega$, and with H the*

mean curvature of the surface $\partial\Omega$,

$$\int_{\partial\Omega}\left[\mathbf{n}\left(\mathbf{x}\right)\cdot\nabla G\left(\mathbf{x}'-\mathbf{x}\right)\right]f\left(\mathbf{x}\right)dS\left(\mathbf{x}\right)=\int_{\partial\Omega}\left[\mathbf{n}\left(\mathbf{x}\right)\cdot\nabla G_{\delta}\left(\mathbf{x}'-\mathbf{x}\right)\right]f\left(\mathbf{x}\right)dS\left(\mathbf{x}\right)$$
$$+\frac{f\left(\mathbf{x}'\right)H\left(\mathbf{x}'\right)}{\sqrt{\pi}}\delta+O\left(\delta^{3}\right)$$

Proof. This proof will follow the same steps as the proof to Proposition 6.2.1. We will only go into detail where the two proofs differ. We again take $\mathbf{x}'=0$. The error is:

$$\epsilon=\frac{1}{8\pi^{3/2}}\int_{\partial\Omega}\left(\sum_{\mu,\nu}\int_{0}^{\delta^{2}}\mathbf{n}\left(\mathbf{x}\right)\cdot\nabla\left(\frac{e^{k^{2}t-\frac{\left(x-2\pi\mu\right)^{2}+\left(y-2\pi\nu\right)^{2}+z^{2}}{4t}}}{t^{3/2}}\right)dt\right)f\left(\mathbf{x}\right)dS\left(\mathbf{x}\right)$$

As before, only the $\mu=\nu=0$ terms of the sum will contribute significant error, and we will be able to limit the $\partial\Omega$ integral to just one coordinate patch. Ignoring these negligible terms and extending the domain of integration to all of $\mathbb{R}^{2}$, we have

$$\epsilon=\frac{1}{8\pi^{3/2}}\int_{0}^{\delta^{2}}\frac{e^{k^{2}t}}{t^{3/2}}\left(\int_{\mathbb{R}^{2}}\mathbf{n}\left(\mathbf{x}\right)\cdot\nabla\left(e^{-\frac{r(\alpha)^{2}}{4t}}\right)f\left(\alpha\right)\left|\frac{\partial\mathbf{x}}{\partial\alpha_{1}}\times\frac{\partial\mathbf{x}}{\partial\alpha_{2}}\right|d\alpha\right)dt$$

$$=-\frac{1}{16\pi^{3/2}}\int_{0}^{\delta^{2}}\frac{e^{k^{2}t}}{t^{5/2}}\left(\int_{\mathbb{R}^{2}}\left[\mathbf{n}\left(\mathbf{x}\right)\cdot\mathbf{x}\left(\alpha\right)\right]e^{-\frac{r(\alpha)^{2}}{4t}}f\left(\alpha\right)\left|\frac{\partial\mathbf{x}}{\partial\alpha_{1}}\times\frac{\partial\mathbf{x}}{\partial\alpha_{2}}\right|d\alpha\right)dt$$

Here we see how the gradient of the Green's function increases the singularity of the integral. In the single layer potential, the t in the denominator was raised to a $\frac{3}{2}$ power, but here it is $\frac{5}{2}$.

We introduce the same normal coordinate system $(\mathbf{T_1},\mathbf{T_2},\mathbf{n_0})$ that we used in the proof of Proposition 6.2.1. We then have

$$\epsilon=-\frac{1}{16\pi^{3/2}}\int_{0}^{\delta^{2}}\frac{e^{k^{2}t}}{t^{5/2}}\left(\int_{\mathbb{R}^{2}}\left[\mathbf{n}\left(\mathbf{x}\right)\cdot\mathbf{x}\left(\alpha\right)\right]e^{-\frac{r(\alpha)^{2}}{4t}}f\left(\alpha\right)\left|\mathbf{T_1}\times\mathbf{T_2}\right|d\alpha\right)dt$$

The integrand here has the same exponential dependence as the integrand in the single layer potential. We therefore make the same change of variables $\alpha \to \xi$.

$$\epsilon = -\frac{1}{16\pi^{3/2}} \int_0^{\delta^2} \frac{e^{k^2 t}}{t^{5/2}} \left(\int_{\mathbb{R}^2} \left[\mathbf{n}\left(\mathbf{x}\right) \cdot \mathbf{x}\left(\xi\right) \right] e^{-\frac{|\xi|^2}{4t}} f\left(\xi\right) \det\left(\partial\alpha/\partial\xi\right) \left| \mathbf{T_1} \times \mathbf{T_2} \right| d\xi \right) dt$$

We expand $\mathbf{x}$ as in (6.7), and we also expand the normal vector $\mathbf{n}\left(\mathbf{x}\right)$ as in [2] and [8]:

$$\mathbf{x}\left(\alpha\right) = \mathbf{T_1}(0)\alpha_1 + \mathbf{T_2}(0)\alpha_2 + \frac{1}{2}\kappa_1 \mathbf{n_0} \alpha_1^2 + \frac{1}{2}\kappa_2 \mathbf{n_0} \alpha_2^2 + O\left(|\alpha|^3\right)$$

$$\mathbf{n}\left(\alpha\right) = \mathbf{n_0} - \kappa_1 \mathbf{T_1} \alpha_1 - \kappa_2 \mathbf{T_2} \alpha_2 + O\left(|\alpha|^2\right)$$

The dot product in the integrand above becomes

$$\begin{aligned} \mathbf{x} \cdot \mathbf{n}\left(\mathbf{x}\right) &= -\frac{1}{2}\kappa_1 \alpha_1^2 - \frac{1}{2}\kappa_2 \alpha_2^2 + O\left(|\alpha|^3\right) \\ &= -\frac{1}{2}\kappa_1 \xi_1^2 - \frac{1}{2}\kappa_2 \xi_2^2 + O\left(|\xi|^3\right) \end{aligned} \tag{6.14}$$

The dot product leaves no terms of order α or larger. We will see as we perform the integration how this cancellation counters the increased singularity from the gradient.

As before,

$$f\left(\xi\right) = f\left(0\right) + f_j\left(0\right)\xi_j + f_{ij}\left(0\right)\xi_i \xi_j + O\left(|\xi|^3\right)$$

and

$$\det\left(\partial\alpha/\partial\xi\right) = 1 + O\left(|\xi|^2\right)$$

$$\left|\mathbf{T_1} \times \mathbf{T_2}\right| = 1 + O\left(|\xi|^2\right)$$

The integrand of the $d\xi$ integral is thus

$$\begin{aligned}
e^{-\frac{|\xi|^2}{4t}} &\times \left(-\frac{1}{2}\kappa_1\xi_1^2 - \frac{1}{2}\kappa_2\xi_2^2 + O\left(|\xi|^3\right)\right) \\
&\times \left(f(0) + f_j(0)\,\xi_j + f_{ij}(0)\,\xi_i\xi_j + O\left(|\xi|^3\right)\right) \\
&\times \left(1 + O\left(|\xi|^2\right)\right) \times \left(1 + O\left(|\xi|^2\right)\right) \\
&= e^{-\frac{|\xi|^2}{4t}} \left(-\frac{1}{2}\kappa_1\xi_1^2 f(0) - \frac{1}{2}\kappa_2\xi_2^2 f(0) + O\left(|\xi|^3\right)\right) \\
&= e^{-\frac{|\xi|^2}{4t}} \left(-\frac{1}{2}\kappa_1\xi_1^2 f(0) - \frac{1}{2}\kappa_2\xi_2^2 f(0) + R(\xi)\right)
\end{aligned}$$

where (again, by the Taylor series remainder theorem) the remainder function $R(\xi)$ has the form

$$R(\xi) = C_1\xi_1^3 + C_2\xi_2^3 + C_3\xi_1^2\xi_2 + C_4\xi_1\xi_2^2$$

Each of these terms, however, is odd and will integrate to zero! The remainder function must really be $O\left(|\xi|^4\right)$

$$R(\xi) = C_1\xi_1^4 + C_2\xi_2^4 + C_3\xi_1^3\xi_2 + C_4\xi_1\xi_2^3 + C_5\xi_1^2\xi_2^2$$

The $C_3\xi_1^3\xi_2$ and $C_4\xi_1\xi_2^3$ terms are odd in ξ_i and will also integrate to zero, so we will drop them. We will make the change of variables $\xi = \delta\zeta$. We write the remainder function as $R(\xi) = \delta^4\left(C_1\zeta_1^4 + C_2\zeta_2^4 + C_5\zeta_1^2\zeta_2^2\right) = \delta^4\tilde{R}(\zeta)$. The error is now

$$\begin{aligned}
\epsilon &= \frac{\delta^4}{16\pi^{3/2}} \int_0^{\delta^2} \frac{e^{k^2 t}}{t^{5/2}} \left(\int_{\mathbb{R}^2} e^{-\frac{\delta^2|\zeta|^2}{4t}} \left(\frac{1}{2}\kappa_1\zeta_1^2 f(0) + \frac{1}{2}\kappa_2\zeta_2^2 f(0) + \delta^2\tilde{R}(\zeta)\right) d\zeta\right) dt \\
&= \frac{f(0)\,\delta^4}{32\pi^{3/2}} \int_0^{\delta^2} \frac{e^{k^2 t}}{t^{5/2}} \left(\int_{\mathbb{R}^2} \left(\kappa_1\zeta_1^2 + \kappa_2\zeta_2^2\right) e^{-\frac{\delta^2|\zeta|^2}{4t}} d\zeta\right) dt + I_{\tilde{R}}
\end{aligned}$$

We will change to polar coordinates. Let $|\zeta| = s$, $\zeta_1 = s\cos\theta$, and $\zeta_2 = s\sin\theta$. It is here as we use (6.2) to perform the ds integral that we see how the higher order terms

left by the normal dot product cancel the increased singularity in the dt integral:

$$\begin{aligned}
\epsilon &= \frac{f(0)\,\delta^4}{32\pi^{3/2}} \int_0^{\delta^2} \frac{e^{k^2 t}}{t^{5/2}} \left(\int_0^{\infty} \int_0^{2\pi} \left(\kappa_1 \cos^2\theta + \kappa_2 \sin^2\theta\right) s^3 e^{-\frac{\delta^2 s^2}{4t}} ds d\theta \right) dt + I_{\tilde{R}} \\
&= \frac{f(0)\,(\kappa_1+\kappa_2)\,\delta^4}{32\pi^{1/2}} \int_0^{\delta^2} \frac{e^{k^2 t}}{t^{5/2}} \left(\int_0^{\infty} s^3 e^{-\frac{\delta^2 s^2}{4t}} ds \right) dt + I_{\tilde{R}} \\
&= \frac{f(0)\,(\kappa_1+\kappa_2)}{4\pi^{1/2}} \int_0^{\delta^2} \frac{e^{k^2 t}}{t^{1/2}} dt + I_{\tilde{R}} \\
&= \frac{f(0)\,(\kappa_1+\kappa_2)}{2\pi^{1/2}} \delta + O\left(\delta^3\right) + I_{\tilde{R}} \\
&= \frac{f(0)\,H(0)}{\pi^{1/2}} \delta + O\left(\delta^3\right) + I_{\tilde{R}}
\end{aligned}$$

where $H = \frac{\kappa_1+\kappa_2}{2}$ is the mean curvature of the surface.

We will examine the $\tilde{R}$ integral, $I_{\tilde{R}}$.

$$\begin{aligned}
I_{\tilde{R}} &= -\frac{\delta^6}{16\pi^{3/2}} \int_0^{\delta^2} \frac{e^{k^2 t}}{t^{5/2}} \left(\int_{\mathbb{R}^2} \left(C_1 \zeta_1^4 + C_2 \zeta_2^4 + C_5 \zeta_1^2 \zeta_2^2\right) e^{-\frac{\delta^2 |\zeta|^2}{4t}} d\zeta \right) dt \\
&= C\delta^6 \int_0^{\delta^2} \frac{e^{k^2 t}}{t^{5/2}} \left(\int_0^{\infty} s^5 e^{-\frac{\delta^2 s^2}{4t}} ds \right) dt \\
&= C \int_0^{\delta^2} t^{1/2} e^{k^2 t} dt \\
&= C \int_0^{\delta^2} t^{1/2} + k^2 t^{3/2} + \ldots dt \\
&= O\left(\delta^3\right)
\end{aligned} \tag{6.15}$$

We now have the result

$$\epsilon = \frac{f(0)\,H(0)}{\pi^{1/2}} \delta + O\left(\delta^3\right)$$

□

We explain how to implement this correction term in Section 7.3.5.

6.4 The Singular Müller Integrals

Having become familiar with the analysis and geometry necessary to derive corrections to the smoothed single and double layer potentials, we can now look at the actual singular integrals of Müller's equations. There are two such singular integrals, which we will call $I1$ and $I2$.

6.4.1 The First Singular Integral

The first of our singular integrals from Müller's equations is

$$I1 = \int_{\partial\Omega} \left[\mathbf{n}\left(\mathbf{x}'\right) \times \mathbf{j}\left(\mathbf{x}\right)\right] \left(k_{ext}^2 G^{ext} - k_{int}^2 G^{int}\right) dS\left(\mathbf{x}\right) \tag{6.16}$$

The Green's functions above are evaluated at $(\mathbf{x}' - \mathbf{x})$. This is a vector valued integral related to a single layer potential. In fact, each of the three components is a single layer potential. The integrand here differs from the single layer potential (6.3) due to the difference in two Green's functions $(k_{ext}^2 G^{ext} - k_{int}^2 G^{int})$, but, of course, we can separate this integral into the difference of two single layer potentials. We can therefore, using Proposition 6.2.1, write

$$\begin{aligned} I1 &= \int_{\partial\Omega} \left[\mathbf{n}\left(\mathbf{x}'\right) \times \mathbf{j}\left(\mathbf{x}\right)\right] \left(k_{ext}^2 G^{ext} - k_{int}^2 G^{int}\right) dS\left(\mathbf{x}\right) \\ &= \int_{\partial\Omega} \left[\mathbf{n}\left(\mathbf{x}'\right) \times \mathbf{j}\left(\mathbf{x}\right)\right] \left(k_{ext}^2 G_\delta^{ext} - k_{int}^2 G_\delta^{int}\right) dS\left(\mathbf{x}\right) \\ &\quad + \frac{\mathbf{n}\left(\mathbf{x}'\right) \times \mathbf{j}\left(\mathbf{x}'\right)\left(k_{ext}^2 - k_{int}^2\right)}{\sqrt{\pi}} \delta + O\left(\delta^3\right) \end{aligned} \tag{6.17}$$

6.4.2 The Second Singular Integral

The other singular integral that we must deal with is:

$$I2 = \int_{\partial\Omega} \mathbf{n}(\mathbf{x}') \times \left[\mathbf{j}(\mathbf{x}) \times \nabla\left(\epsilon_{ext} G^{ext} - \epsilon_{int} G^{int}\right)\right] dS(\mathbf{x}) \tag{6.18}$$

We can proceed to find a correction term for this integral in the same way that we have done. The analysis is not much more difficult, but there is a new wrinkle. When we introduce the principal directions and normal coordinates, we must write the tangential surface vector $\mathbf{j}(\mathbf{x})$ as as linear combination of the principal directions

$$\mathbf{j}(\alpha) = j_1(\alpha)\,\mathbf{T_1}(\alpha) + j_2(\alpha)\,\mathbf{T_2}(\alpha)$$

for some j_1 and j_2. We can then expand $\mathbf{j}(\alpha)$ and compute the cross products in (6.18). In the end, we find the correction term to be

$$\frac{(\epsilon_{ext} - \epsilon_{int})(\kappa_1 - \kappa_2)}{2\sqrt{\pi}} \left(j_1(\mathbf{x}')\,\mathbf{T_1}(\mathbf{x}') - j_2(\mathbf{x}')\,\mathbf{T_2}(\mathbf{x}')\right)\delta$$

This is the correction term, and it therefore is an invariant quantity. Unfortunately, it is not a recognizable invariant quantity. We cannot use this term because it would require actually computing in the normal coordinates $(\mathbf{n_0}, \mathbf{T_1}, \mathbf{T_2})$. This would involve an impractical amount of computation. We need a different approach for $I2$.

We can split this integral up into two easier pieces using the vector identity

$$\mathbf{A} \times (\mathbf{B} \times \mathbf{C}) = (\mathbf{A} \cdot \mathbf{C})\,\mathbf{B} - (\mathbf{A} \cdot \mathbf{B})\,\mathbf{C}$$

This integral becomes the difference of two integrals $I2 = I2A - I2B$, with

$$I2A = \int_{\partial\Omega} \left[\mathbf{n}(\mathbf{x}') \cdot \nabla\left(\epsilon_{ext} G^{ext} - \epsilon_{int} G^{int}\right)\right] \mathbf{j}(\mathbf{x})\, dS(\mathbf{x})$$

and

$$I2B = \int_{\partial\Omega} \left[\mathbf{n}\left(\mathbf{x}'\right) \cdot \mathbf{j}\left(\mathbf{x}\right)\right] \nabla \left(\epsilon_{ext} G^{ext} - \epsilon_{int} G^{int}\right) dS\left(\mathbf{x}\right)$$

We will need correction terms for each of these integrals.

The Integral I2A

The integral $I2A$

$$I2A = \int_{\partial\Omega} \left[\mathbf{n}\left(\mathbf{x}'\right) \cdot \nabla \left(\epsilon_{ext} G^{ext} - \epsilon_{int} G^{int}\right)\right] \mathbf{j}\left(\mathbf{x}\right) dS\left(\mathbf{x}\right)$$

is very closely related to a double layer potential. It is not, strictly speaking, an actual double layer potential because the normal vector in the dot product is not a variable normal $\mathbf{n}\left(\mathbf{x}\right)$ but instead is a normal vector fixed at the singular point $\mathbf{n}\left(\mathbf{x}'\right)$. The analysis involved in smoothing and correction for this integral is identical to that of the true double layer potential in Proposition 6.3.1 with one exception. Here, the dot product of (6.14) has the opposite sign. The end result is that

$$\begin{aligned} I2A &= \int_{\partial\Omega} \left[\mathbf{n}\left(\mathbf{x}'\right) \cdot \nabla \left(\epsilon_{ext} G^{ext} - \epsilon_{int} G^{int}\right)\right] \mathbf{j}\left(\mathbf{x}\right) dS\left(\mathbf{x}\right) \\ &= \int_{\partial\Omega} \left[\mathbf{n}\left(\mathbf{x}'\right) \cdot \nabla \left(\epsilon_{ext} G_{\delta}^{ext} - \epsilon_{int} G_{\delta}^{int}\right)\right] \mathbf{j}\left(\mathbf{x}\right) dS\left(\mathbf{x}\right) \\ &\quad - \frac{\mathbf{j}\left(\mathbf{x}'\right) H\left(\mathbf{x}'\right) \left(\epsilon_{ext} - \epsilon_{int}\right)}{\sqrt{\pi}} \delta + O\left(\delta^3\right) \end{aligned} \tag{6.19}$$

The Integral I2B

The integral $I2B$

$$I2B = \int_{\partial\Omega} \left[\mathbf{n}\left(\mathbf{x}'\right) \cdot \mathbf{j}\left(\mathbf{x}\right)\right] \nabla \left(\epsilon_{ext} G^{ext} - \epsilon_{int} G^{int}\right) dS\left(\mathbf{x}\right)$$

is related to neither the single nor the double layer potential, but it can be analyzed in the same way that our other integrals have been analyzed. In the double layer potential, the dot product between the orthogonal vectors has the effect of reducing the singularity of the integrand by an order. Remembering that the vector $\mathbf{j}(\mathbf{x})$ is a surface current that is tangential to $\partial\Omega$, we see that there is a similar reduction in the order of the singularity from the dot product in $I2B$.

We can investigate smoothing and correction for integral $I2B$ as before. The only thing that is new is dealing with the tangential vector $\mathbf{j}(\mathbf{x})$. When we introduce the α parameterization of the surface, we write this vector as

$$\mathbf{j}(\alpha) = j_1(\alpha)\,\mathbf{T_1}(\alpha) + j_2(\alpha)\,\mathbf{T_2}(\alpha)$$

We can take derivatives and expansions of this term like the others. In the now-familiar normal coordinates $(\mathbf{n_0}, \mathbf{T_1}, \mathbf{T_2})$, the end result is a correction term

$$-\frac{(\epsilon_{ext} - \epsilon_{int})\left(\kappa_1(\mathbf{x}')\,j_1(\mathbf{x}')\,\mathbf{T_1}(\mathbf{x}') + \kappa_2(\mathbf{x}')\,j_2(\mathbf{x}')\,\mathbf{T_2}(\mathbf{x}')\right)}{\sqrt{\pi}}\delta \tag{6.20}$$

We state this correction term without proof. The proof follows the proofs of Propositions 6.2.1 and 6.3.1 and would be redundant at this point.

If we write $(\kappa_1(\mathbf{x}')\,j_1(\mathbf{x}')\,\mathbf{T_1}(\mathbf{x}') + \kappa_2(\mathbf{x}')\,j_2(\mathbf{x}')\,\mathbf{T_2}(\mathbf{x}'))$ as a 2-vector in the coordinates $(\mathbf{T_1}, \mathbf{T_2})$

$$\begin{bmatrix} \kappa_1(\mathbf{x}')\,j_1(\mathbf{x}') \\ \kappa_2(\mathbf{x}')\,j_2(\mathbf{x}') \end{bmatrix}$$

then the correction term (6.20) is recognizable as a matrix vector product

$$-\frac{(\epsilon_{ext} - \epsilon_{int})}{\sqrt{\pi}} \begin{bmatrix} \kappa_1(\mathbf{x}') & 0 \\ 0 & \kappa_2(\mathbf{x}') \end{bmatrix} \begin{bmatrix} j_1(\mathbf{x}') \\ j_2(\mathbf{x}') \end{bmatrix} \delta$$

The matrix in this product

$$\begin{bmatrix} \kappa_1(\mathbf{x}') & 0 \\ 0 & \kappa_2(\mathbf{x}') \end{bmatrix}$$

has the principal curvatures as its eigenvalues and the principal directions as its eigenvectors. It is recognizable as the differential of the Gauss map $DN_{\mathbf{x}'}$ (see [13]). Writing the action of $DN_{\mathbf{x}'}$ on a vector $\mathbf{j}(\mathbf{x}')$ as $DN_{\mathbf{x}'}\mathbf{j}(\mathbf{x}')$, we can therefore say of integral $I2B$

$$\begin{aligned} I2B &= \int_{\partial\Omega} \left[\mathbf{n}(\mathbf{x}') \cdot \mathbf{j}(\mathbf{x})\right] \nabla \left(\epsilon_{ext} G^{ext} - \epsilon_{int} G^{int}\right) dS(\mathbf{x}) \\ &= \int_{\partial\Omega} \left[\mathbf{n}(\mathbf{x}') \cdot \mathbf{j}(\mathbf{x})\right] \nabla \left(\epsilon_{ext} G^{ext}_{\delta} - \epsilon_{int} G^{int}_{\delta}\right) dS(\mathbf{x}) \\ &\quad - \frac{(\epsilon_{ext} - \epsilon_{int}) DN_{\mathbf{x}'}\mathbf{j}(\mathbf{x}')}{\sqrt{\pi}} \delta + O\left(\delta^3\right) \end{aligned} \tag{6.21}$$

We explain how to compute this correction term in Section 7.3.5.

6.5 Discretization Error

Implementation of the scattering problem requires many evaluations of Müller's integrals. We do this numerically with the trapezoid rule. The required discretization of the integrals introduces another error. In [7], it is shown that an analogous discretization error is small as long as δ is larger than the grid spacing $h = \frac{2\pi}{N}$ and the geometry is well represented by the grid. We therefore have reason to believe that the discretization error is small, a belief that is consistent with our implementation (see Chapter 8).

6.6 The Corrected Müller Integral Equations

We present in summary the correction results of this section as they appear in the integral equations (4.16):

$$
\begin{aligned}
\mathbf{j}_{inc}\left(\mathbf{x}'\right) = & \frac{\mu_{int}+\mu_{ext}}{2\mu_{ext}}\mathbf{j}_{int}\left(\mathbf{x}'\right) \\
& -\frac{1}{\mu_{ext}}\int_{\partial\Omega}\mathbf{n}\left(\mathbf{x}'\right)\times\left[\mathbf{j}_{int}\left(\mathbf{x}\right)\times\nabla\left(\mu_{ext}G^{ext}-\mu_{int}G^{int}\right)\right]dS\left(\mathbf{x}\right) \\
& \qquad +\frac{\left(\mu_{ext}-\mu_{int}\right)}{\mu_{ext}\sqrt{\pi}}\left(H\left(\mathbf{x}'\right)+DN_{\mathbf{x}'}\right)\mathbf{j}_{int}\left(\mathbf{x}'\right)\delta \\
& -\frac{i}{\mu_{ext}\omega}\int_{\partial\Omega}\left[\mathbf{n}\left(\mathbf{x}'\right)\times\mathbf{j}'_{int}\left(\mathbf{x}\right)\right]\left(k_{ext}^{2}G_{\delta}^{ext}-k_{int}^{2}G_{\delta}^{int}\right)dS\left(\mathbf{x}\right) \\
& \qquad -\frac{i\left(k_{ext}^{2}-k_{int}^{2}\right)}{\mu_{ext}\omega\sqrt{\pi}}\left(\mathbf{n}\left(\mathbf{x}'\right)\times\mathbf{j}'_{int}\left(\mathbf{x}'\right)\right)\delta \\
& -\frac{i}{\mu_{ext}\omega}\int_{\partial\Omega}\mathbf{n}\left(\mathbf{x}'\right)\times\left[\left(\mathbf{j}'_{int}\left(\mathbf{x}\right)\cdot\nabla\right)\nabla\left(G^{ext}-G^{int}\right)\right]dS\left(\mathbf{x}\right) \\
& +O\left(\delta^{3}\right) \\
\mathbf{j}'_{inc}\left(\mathbf{x}'\right) = & \frac{\epsilon_{int}+\epsilon_{ext}}{2\epsilon_{ext}}\mathbf{j}'_{int}\left(\mathbf{x}'\right) \\
& -\frac{1}{\epsilon_{ext}}\int_{\partial\Omega}\mathbf{n}\left(\mathbf{x}'\right)\times\left[\mathbf{j}'_{int}\left(\mathbf{x}\right)\times\nabla\left(\epsilon_{ext}G_{\delta}^{ext}-\epsilon_{int}G_{\delta}^{int}\right)\right]dS\left(\mathbf{x}\right) \\
& \qquad +\frac{\left(\epsilon_{ext}-\epsilon_{int}\right)}{\epsilon_{ext}\sqrt{\pi}}\left(H\left(\mathbf{x}'\right)+DN_{\mathbf{x}'}\right)\mathbf{j}'_{int}\left(\mathbf{x}'\right)\delta \\
& -\frac{i}{\epsilon_{ext}\omega}\int_{\partial\Omega}\left[\mathbf{n}\left(\mathbf{x}'\right)\times\mathbf{j}_{int}\left(\mathbf{x}\right)\right]\left(k_{ext}^{2}G_{\delta}^{ext}-k_{int}^{2}G_{\delta}^{int}\right)dS\left(\mathbf{x}\right) \\
& \qquad -\frac{i\left(k_{ext}^{2}-k_{int}^{2}\right)}{\epsilon_{ext}\omega\sqrt{\pi}}\left(\mathbf{n}\left(\mathbf{x}'\right)\times\mathbf{j}_{int}\left(\mathbf{x}'\right)\right)\delta \\
& -\frac{i}{\epsilon_{ext}\omega}\int_{\partial\Omega}\mathbf{n}\left(\mathbf{x}'\right)\times\left[\left(\mathbf{j}_{int}\left(\mathbf{x}\right)\cdot\nabla\right)\nabla\left(G^{ext}-G^{int}\right)\right]dS\left(\mathbf{x}\right) \\
& +O\left(\delta^{3}\right)
\end{aligned}
\tag{6.22}
$$

Chapter 7

Implementation

The goal of the scattering problem is to find the total electric and magnetic fields in the presence of the scatterer. We have shown in Chapter 4 how this problem reduces to finding the surface currents (the tangential components of the fields) on the surface of the scatterer. We find these by solving the Müller integral equations. Since these equations are well-posed, we can be sure that solutions exist. We are interested in numerically approximating solutions of the integral equations under various conditions. Here we outline the numerical implementation of our solution to the scattering problem.

7.1 Inputs and Outputs

We begin by listing the quantities of interest.

7.1.1 Inputs

We have freedom to vary many physical and numerical parameters of the problem.

Physical Parameters

1. *Geometry of the scatterer.* We specify two functions $z = F_1(x, y)$ and $z = F_2(x, y)$ that represent the front and the back of the scatterer. The functions must be 2π periodic in both x and y and cannot intersect. Under these restrictions, we are free to choose any C^3 geometry.

2. *Physical parameters of the scatterer and of free space.* We choose the permittivities ϵ_{ext} and ϵ_{int} and the permeabilities μ_{ext} and μ_{int}. Here, we have always chosen $\epsilon_{ext} = \mu_{ext} = \mu_{int} = 1$. The permittivity of the scatterer ϵ_{int} can be chosen to be a positive real number (a lossless material) or can have a positive imaginary part (a lossy material).

3. *Angles of incidence.* The angles of incidence θ and ϕ of the fields as defined in Section 2.5 must be specified. These lead to the parameters α and β as defined in Section 2.6. Thus far, we have chosen to implement scattering problems only for normally incident fields ($\theta = \phi = 0$).

4. *Frequency.* The frequency ω of the incident wave determines the wave numbers k_{ext} and k_{int}. The frequency cannot be chosen too large, and we have implemented problems with ω ranging from 0 to 2. There are certain frequencies which will result in the λ singularity of the Green's function (see Section 3.4). We avoid these exact frequencies, although we can come very close to them without adverse numerical effects (see Section 7.3.6).

Numerical Parameters

1. *Grid size.* An $N \times N$ grid is established on the 2π by 2π periodic block. Because we use fast Fourier transforms to compute some parts of our Green's functions (see Section 7.4.1), it is necessary that N be even.

2. *Smoothing parameter.* The smoothing parameter δ determines the extent to which we smooth the singular Green's functions before correction. This is explained in detail in Chapter 6. The results of that section rely on δ being small. We have found experimentally that δ's in the range of $\frac{1}{2}h \leq \delta \leq 2h$ for $h = \frac{2\pi}{N}$ are effective.

3. *Ewald parameter.* This positive constant is arbitrary, but choosing it carefully affects the convergence rates of the Green's functions. See Sections 5.3 and 7.4.1 as well as [11] for details. We have found experimentally that $E = \frac{1}{2}$ works well for our range of frequencies.

4. *GMRES tolerance.* We solve the linear system of equations using GMRES (see Section 7.4.5). We must set a tolerance for convergence as outlined in [24]. For all results in Chapter 8, we have this set to 10^{-4}.

5. *ℓ sum tolerance.* In the Ewald forms of the Green's function (see Chapter 5), we have summations over ℓ. We set a tolerance for convergence for these sums. The tems in these sums are stricly decreasing, so we approximate them by including terms until they are smaller in magnitude than our set tolerance. For all results in Chapter 8, we have this set to 10^{-6}.

6. *μ, ν sum tolerance.* In the Ewald form $G1$, we have a double infinite sum over μ and ν (5.7). Unless we implement the $G1$ storage strategy of Section 7.4.2, we must set a tolerance for convergence for these sums. In Section 7.3.3, we discuss how this tolerance is used to determine convergence. For the results reported here, we have this set to 10^{-6}.

7. *Fourier m, n sum tolerance* In the Fourier representation of the Green's function (3.10), we have a double infinite sum over m and n, and we must set a

tolerance for convergence for these sums. In Section 7.3.3, we discuss how this tolerance is used to determine convergence. For the results reported here, we have this set to 10^{-6}.

8. *Far field distance* To compute the transmission coefficient (see Section 2.7), we need to evaluate integrals at a large distance from the scatterer (so that the decaying modes have neglibile effect). We have set this distance to $z = 250.0$.

7.1.2 Outputs

The quantity that we would like as an output of our numerical process is the transmission coefficient (see Section 2.7). Of course, having a solution to the integral equations (4.16), we can also find the electric and magnetic fields at any point using (4.17).

In practice, we would like to solve more than one scattering problem at a time. Specifically, we would like to run through a range of frequencies ω for a given scatterer. We can then look at the transmission coefficient as a function of frequency. In this way, we are able to see resonances that occur at different frequencies or other frequency-dependent features of the problem.

7.2 Overview of the Method

Here we outline the steps taken to approximate solutions to a number of numerical scattering problems over a range of frequencies on a single scatterer. We establish the experiments by specifying the input parameters and creating a grid in x and y.

7.2.1 Preprocessing

To save computational time, we precompute and store various quantities. Some quantities are frequency independent and can be stored and used for many frequencies, while other quantities must be computed and stored anew for each frequency. All of the precomputed quantities will be discussed in Section 7.4.

7.2.2 The Main Computations

Most of the computation is in the setting up and solving of the Müller integral equations

$$\mathbf{J_{inc}} = A\mathbf{J_{int}}$$

We accomplish this in the following steps

1. The incident fields are converted to incident surface currents according to (4.6).
2. The matrix A in the linear system is filled. This step requires the computation of Green's functions including interactions of all points on the surface $\partial\Omega$.
3. The linear system is solved for the internal surface currents.

Building the linear system and solving it are the two most computationally expensive pieces of implementation. We must evaluate many expensive Green's functions. The preprocessing steps, however, can offset much of this expense, and we also take advantage of symmetry in the problem to accelerate computation (see Section 7.4.3).

Filling the matrix A in the linear system involves numerically approximating the integrals of Müller's equations (4.16) at every point on $\partial\Omega$. We approximate the integrals with the trapezoid method. It is here that we use the smoothed Green's functions and add the appropriate correction terms from Chapter 6.

The linear system is well-posed, and, in theory, we ought to be able to choose from many methods to approximate its solution. In practice, however, we must use an iterative method. As outlined in Section 7.3.7, the matrix A in the system has $144N^4$ complex entries, and it is dense. Noniterative methods require the full storage of all of these entries. With an iterative method, however, we can can get away with storing less. Instead of filling A completely, we merely store all of the Green's function interactions involved in A. These are about $25N^4$ complex numbers that do not change with each iteration. We can use these values to compute the action of A on a vector $\mathbf{J}$ at each iteration. This is more expensive computationally than storing all of A and computing $A\mathbf{J}$, but the memory savings is necessary.

7.2.3 Postprocessing

Once the linear system (4.19) has been solved for the interior surface currents, these are used to find the transmission coefficient according to Section 2.7. For these computations, the Green's functions are evaluated at large distances $|z|$, and we can therefore use the Fourier form of the Green's function (3.10).

7.3 Numerical Issues

7.3.1 Special Functions

Computing the Green's functions requires the evaluation of many exponential integrals. These can be evaluated according to the iterative relationships described in Appendix C. Thus, computation of the exponential integral of any order will require evaluation of the complex complementary error function erfc. Real-valued complementary error functions are commonly built in to C and FORTRAN libraries. For the complex-valued functions, however, we will need our own fast algorithm. We

have implemented the algorithm of [31] for this purpose.

7.3.2 The Green's Functions

Evaluating the Green's functions is a major numerical task of this problem. We need the Green's function with various derivatives. We also need various differences of external smoothed Green's functions and internal smoothed Green's functions with their derivatives.

Most of the Green's function evaluations are done in setting up the linear system (4.19) to solve the integral equations. The Green's functions used in the integral equations are the smoothed Green's functions. The functions needed are

$$k_{ext}^2 G_\delta^{ext} - k_{int}^2 G_\delta^{int}$$

$$\nabla \left(G_\delta^{ext} - G_\delta^{int} \right)$$

$$\nabla \left(\epsilon_{ext} G_\delta^{ext} - \epsilon_{int} G_\delta^{int} \right)$$

$$(\mathbf{j} \cdot \nabla) \nabla \left(G_\delta^{ext} - G_\delta^{int} \right)$$

This last quantity can be written

$$(\mathbf{j} \cdot \nabla) \nabla \left(G_\delta^{ext} - G_\delta^{int} \right) =$$

$$j_x \begin{bmatrix} \partial_{xx} \left(G_\delta^{ext} - G_\delta^{int} \right) \\ \partial_{xy} \left(G_\delta^{ext} - G_\delta^{int} \right) \\ \partial_{xz} \left(G_\delta^{ext} - G_\delta^{int} \right) \end{bmatrix} + j_y \begin{bmatrix} \partial_{xy} \left(G_\delta^{ext} - G_\delta^{int} \right) \\ \partial_{yy} \left(G_\delta^{ext} - G_\delta^{int} \right) \\ \partial_{yz} \left(G_\delta^{ext} - G_\delta^{int} \right) \end{bmatrix} + j_z \begin{bmatrix} \partial_{xz} \left(G_\delta^{ext} - G_\delta^{int} \right) \\ \partial_{yz} \left(G_\delta^{ext} - G_\delta^{int} \right) \\ \partial_{zz} \left(G_\delta^{ext} - G_\delta^{int} \right) \end{bmatrix}$$

We use the smoothed Green's function in all integrals, even those that are not singular. We have shown, using the techniques of Chapter 6, that no correction terms are necessary for the integrals that are not singular. Of course, we could choose to use the smoothed Green's function only in the singular integrals. The method is third order either way.

Outside of the set-up of the integral equations, we need only evaluate Green's functions in our postprocessing to find the fields at desired points or to find the

transmission coefficient. Every form of Green's function that is needed is included in a list in Appendix A.

When evaluating the Green's functions for the integral equations, it is possible to calculate all of the needed functions within one loop. This minimizes the number of expensive evaluations of exponential integrals.

7.3.3 Double Infinite Sums

In evaluating the Green's functions, we encounter various double-infinite sums of the type

$$A = \sum_{m,n} A_{mn} = \sum_{m=-\infty}^{\infty} \sum_{n=-\infty}^{\infty} A_{mn}$$

In each case, the terms of the sum are decreasing rapidly in m and n. We will need to evaluate such sums numerically. For a prescribed tolerance, we achieve this by summing around perimeters in m and n until a perimeter's contribution is small. The following steps explain this process:

1. Set $p = 0, S_p = 0$.
2. While $S_p > tolerance$
   (a) $S_p \rightarrow \sum A_{mn}$ where the sum is over all m, n such that $m + n = \pm p$ and $-p \leq m, n \leq p$
   (b) $A \rightarrow A + S_p$
   (c) $p \rightarrow p + 1$

Since our sums converge quickly and the terms decay so quickly in m and n, we can get away with this crude convergence criteria. We often will compute various of these sums within one loop. This is the case when we are evaluating the Green's functions

in the integral equations. The pseudocode above holds, but we must keep track of S_p for each quantity that we compute. We only exit the while loop when the largest of these S_p's is smaller than the tolerance.

7.3.4 Evaluating the Smoothed Green's Functions

The smoothed Green's function introduced in Chapter 6 must be written in a different form for fast numerical implementation. The smoothed Green's function is

$$G1_\delta(x,y,z) = \frac{1}{8\pi^{3/2}} \sum_{\mu,\nu} e^{-2\pi i(\alpha\mu+\beta\nu)} \int_{\delta^2}^{E^2} \frac{e^{k^2 t - \frac{R_{\mu\nu}^2}{4t}}}{t^{3/2}} dt$$

for $R_{\mu\nu}^2 = (x+2\pi\mu)^2 + (y+2\pi\nu)^2 + z^2$. If we write this in another way, we see that

$$G1_\delta(x,y,z) = \frac{1}{8\pi^{3/2}} \sum_{\mu,\nu} e^{-2\pi i(\alpha\mu+\beta\nu)} \int_{0}^{E^2} \frac{e^{k^2 t - \frac{R_{\mu\nu}^2}{4t}}}{t^{3/2}} dt$$

$$- \frac{1}{8\pi^{3/2}} \sum_{\mu,\nu} \int_{0}^{\delta^2} \frac{e^{k^2 t - \frac{R_{\mu\nu}^2}{4t}}}{t^{3/2}} dt$$

Now, we can follow the steps outlined in Chapter 5 to write G_δ in terms of exponential integral functions

$$G1_\delta(x,y,z) = \frac{1}{8\pi^{3/2}} \sum_{\mu,\nu} e^{-2\pi i(\alpha\mu+\beta\nu)} \sum_{\ell=0}^{\infty} \frac{k^{2\ell} E^{2\ell-1}}{\ell!} \mathrm{ExpInt}_{\ell+1/2}\left(\frac{R_{\mu\nu}^2}{4E^2}\right)$$

$$- \frac{1}{8\pi^{3/2}} \sum_{\mu,\nu} e^{-2\pi i(\alpha\mu+\beta\nu)} \sum_{\ell=0}^{\infty} \frac{k^{2\ell} \delta^{2\ell-1}}{\ell!} \mathrm{ExpInt}_{\ell+1/2}\left(\frac{R_{\mu\nu}^2}{4\delta^2}\right)$$

These sums can be written together as

$$G1_\delta(x,y,z) = \frac{1}{8\pi^{3/2}} \sum_{\mu,\nu} e^{-2\pi i(\alpha\mu+\beta\nu)} \times \sum_{\ell=0}^{\infty} \frac{k^{2\ell}}{\ell!} \left(E^{2\ell-1} \operatorname{ExpInt}_{\ell+1/2}\left(\frac{R_{\mu\nu}^2}{4E^2}\right) - \delta^{2\ell-1} \operatorname{ExpInt}_{\ell+1/2}\left(\frac{R_{\mu\nu}^2}{4\delta^2}\right)\right) \tag{7.1}$$

We can thus easily compute G_δ, and this result extends to all of the needed derivatives of the Green's function. However, we can now see the main drawback to our smoothing and correction method. We are required to make two calls to ExpInt functions for every call to G_δ. These exponential integral functions are computed via iterations and are somewhat expensive (See Appendix C). We have reduced this computational cost by interpolating the exponential integrals (see Section 7.4.4).

We need to be able to evaluate G_δ at the singular point $\mathbf{x} = \mathbf{0}$. This is, of course, straightforward for the smooth $G2$ part of the Green's function. The $G1_\delta$, however, requires a bit of work. We cannot evaluate (7.1) at $\mathbf{x} = \mathbf{0}$ since $\operatorname{ExpInt}_{\frac{1}{2}}(0)$ is not defined. We must return to our older form of $G1_\delta$:

$$G1_\delta(\mathbf{0}) = \frac{1}{8\pi^{3/2}} \int_{\delta^2}^{E^2} \frac{e^{k^2 t}}{t^{3/2}} dt + \frac{1}{8\pi^{3/2}} \sum e^{-2\pi i(\alpha\mu+\beta\nu)} \int_{\delta^2}^{E^2} \frac{e^{k^2 t - \frac{(2\pi\mu)^2+(2\pi\nu)^2}{4t}}}{t^{3/2}} dt$$

where the summation is taken over all μ and ν except for $\mu = \nu = 0$. We can integrate the first integral above through the substitution $u = t^{1/2}$ and then through integration by parts:

$$\int_{\delta^2}^{E^2} \frac{e^{k^2 t}}{t^{3/2}} dt = 2\left(\frac{e^{k^2\delta^2}}{\delta} - \frac{e^{k^2 E^2}}{E}\right) + 2\sqrt{\pi} k i \left[\operatorname{erfc}(iEk) - \operatorname{erfc}(i\delta k)\right]$$

The remaining integrals (those for μ and ν other than $\mu = \nu = 0$) can be computed as in (7.1). For most of our needed derivatives of G_δ, the $\mu = \nu = 0$ term in the summation will be 0 when evaluated at $\mathbf{x} = \mathbf{0}$. However, in the second derivatives $G_{\delta_{xx}}$, $G_{\delta_{yy}}$, and $G_{\delta_{zz}}$, there is a nonzero contribution. We will illustrate with $G_{\delta_{xx}}$.

$$G_{\delta_{xx}}(x,y,z) = -\frac{1}{16\pi^{3/2}} \sum_{\mu,\nu} e^{-2\pi i(\alpha\mu+\beta\nu)} \int_{\delta^2}^{E^2} \frac{e^{k^2 t - \frac{R_{\mu\nu}^2}{4t}}}{t^{5/2}} dt$$

$$+ \frac{1}{32\pi^{3/2}} \sum_{\mu,\nu} e^{-2\pi i(\alpha\mu+\beta\nu)} (x+2\pi\mu)^2 \int_{\delta^2}^{E^2} \frac{e^{k^2 t - \frac{R_{\mu\nu}^2}{4t}}}{t^{7/2}} dt$$

Thus

$$G_{\delta_{xx}}(\mathbf{0}) = -\frac{1}{16\pi^{3/2}} \int_{\delta^2}^{E^2} \frac{e^{k^2 t}}{t^{5/2}} dt$$

$$- \frac{1}{16\pi^{3/2}} \sum e^{-2\pi i(\alpha\mu+\beta\nu)} \int_{\delta^2}^{E^2} \frac{e^{k^2 t - \frac{R_{\mu\nu}^2}{4t}}}{t^{5/2}} dt$$

$$+ \frac{1}{32\pi^{3/2}} \sum_{\mu,\nu} e^{-2\pi i(\alpha\mu+\beta\nu)} (x+2\pi\mu)^2 \int_{\delta^2}^{E^2} \frac{e^{k^2 t - \frac{R_{\mu\nu}^2}{4t}}}{t^{7/2}} dt$$

where the summation without indexes is taken over all μ and ν except for $\mu = \nu = 0$. Again, we can integrate the first integral above through a substitution and integration by parts:

$$\int_{\delta^2}^{E^2} \frac{e^{k^2 t}}{t^{5/2}} dt = \frac{2}{3} \left(\frac{(1+2k^2\delta^2)\, e^{k^2\delta^2}}{\delta^3} - \frac{(1+2k^2E^2)\, e^{k^2E^2}}{E^3} \right)$$

$$+ \frac{4}{3}\sqrt{\pi} k^3 i \left[\operatorname{erfc}(iEk) - \operatorname{erfc}(i\delta k) \right]$$

This integral also appears in $G_{\delta_{yy}}$ and $G_{\delta_{zz}}$. The other integrals in these second derivatives can be computed easily through exponential integral functions as in (7.1).

7.3.5 The Correction Terms

The correction terms for our smoothed integrals involve such geometric constants as the mean curvature and the principal curvatures. To implement these corrections, we will need to write these in terms of known quantities. For surface described by $z = f(x, y)$ as ours, the mean curvature is [13]

$$H = \frac{(1 + f_y)^2 f_{xx} + 2 f_x f_y f_{xy} + (1 + f_x)^2 f_{yy}}{2\left(1 + f_x^2 + f_y^2\right)^{3/2}}$$

The other correction term that needs to be rewritten is the action of the differential of the Gauss map on a vector $DN_{\mathbf{x}'}\mathbf{j}(\mathbf{x}')$. This is a matrix vector product that takes — in the normal coordinate basis $(\mathbf{T_1}, \mathbf{T_2})$ — the form

$$\begin{bmatrix} \kappa_1(\mathbf{x}') & 0 \\ 0 & \kappa_2(\mathbf{x}') \end{bmatrix} \begin{bmatrix} j_1(\mathbf{x}') \\ j_2(\mathbf{x}') \end{bmatrix}$$

We follow [13] to write this in the (x, y) basis. The matrix vector product becomes

$$\begin{bmatrix} a_{11} & a_{12} \\ a_{21} & a_{22} \end{bmatrix} \begin{bmatrix} j_x(\mathbf{x}') \\ j_y(\mathbf{x}') \end{bmatrix} \tag{7.2}$$

where the a_{ij}'s can be written as in terms of the coefficients of the first and second fundamental forms (E, F, G and e, f, g respectively):

$$\begin{aligned} a_{11} &= \frac{fF - eG}{EG - F} \\ a_{12} &= \frac{gF - fG}{EG - F} \\ a_{21} &= \frac{eF - fE}{EG - F} \\ a_{22} &= \frac{fF - gE}{EG - F} \end{aligned} \tag{7.3}$$

The coefficients can be written in our (x, y) basis. With the point $\mathbf{x}$

$$\mathbf{x} = \begin{bmatrix} x \\ y \\ f(x, y) \end{bmatrix} \tag{7.4}$$

the outward normal unit vector

$$\mathbf{n} = \frac{1}{\sqrt{1 + f_x^2 + f_y^2}} \begin{bmatrix} f_x \\ f_y \\ -1 \end{bmatrix} \tag{7.5}$$

and with the tangent vectors

$$\frac{\partial \mathbf{x}}{\partial x} = \begin{bmatrix} 1 \\ 0 \\ f_x \end{bmatrix} \quad \text{and} \quad \frac{\partial \mathbf{x}}{\partial y} = \begin{bmatrix} 0 \\ 1 \\ f_y \end{bmatrix}$$

we can write

$$e = \mathbf{n} \cdot \mathbf{x}_{xx}$$

$$f = \mathbf{n} \cdot \mathbf{x}_{xy}$$

$$g = \mathbf{n} \cdot \mathbf{x}_{yy}$$

and

$$E = \mathbf{x}_x \cdot \mathbf{x}_x$$

$$F = \mathbf{x}_x \cdot \mathbf{x}_y$$

$$G = \mathbf{x}_y \cdot \mathbf{x}_y$$

Then, from (7.3), (7.4), and (7.5), the matrix elements a_{ij} are

$$a_{11} = \frac{f_{xy}f_xf_y - f_{xx}\left(1+f_y^2\right)}{1+f_x^2+f_y^2}$$

$$a_{12} = \frac{f_{yy}f_xf_y - f_{xy}\left(1+f_y^2\right)}{1+f_x^2+f_y^2}$$

$$a_{21} = \frac{f_{xx}f_xf_y - f_{xy}\left(1+f_x^2\right)}{1+f_x^2+f_y^2}$$

$$a_{22} = \frac{f_{xy}f_xf_y - f_{yy}\left(1+f_x^2\right)}{1+f_x^2+f_y^2}$$

and the product of (7.2) is

$$\frac{1}{\left(1+f_x^2+f_y^2\right)^{3/2}}\begin{bmatrix}\left(f_{xy}f_xf_y - f_{xx}\left(1+f_y^2\right)\right)j_x + \left(f_{yy}f_xf_y - f_{xy}\left(1+f_y^2\right)\right)j_y \\ \left(f_{xx}f_xf_y - f_{xy}\left(1+f_x^2\right)\right)j_x + \left(f_{xy}f_xf_y - f_{yy}\left(1+f_x^2\right)\right)j_y\end{bmatrix}$$

This vector is in the (x, y) basis, and we can write it

$$\left(f_{xy}f_xf_y - f_{xx}\left(1+f_y^2\right)\right)j_x + \left(f_{yy}f_xf_y - f_{xy}\left(1+f_y^2\right)\right)j_y\frac{\partial \mathbf{x}}{\partial x}$$

$$+\left(f_{xx}f_xf_y - f_{xy}\left(1+f_x^2\right)\right)j_x + \left(f_{xy}f_xf_y - f_{yy}\left(1+f_x^2\right)\right)j_y\frac{\partial \mathbf{x}}{\partial y}$$

Distributing and simplifying this expression, we see that the matrix vector product $DN_{\mathbf{x}'}\mathbf{j}\left(\mathbf{x}'\right)$ in the correction term can be written

$$\frac{1}{\left(1+f_x^2+f_y^2\right)^{3/2}}\begin{bmatrix}-j_x\left(f_y^2f_{xx} - f_xf_yf_{xy} + f_{xx}\right) - j_y\left(f_y^2f_{xy} - f_xf_yf_{yy} + f_{xy}\right) \\ j_x\left(f_x^2f_{xy} - f_xf_yf_{xx} + f_{xy}\right) + j_y\left(f_x^2f_{yy} - f_xf_yf_{xy} + f_{yy}\right) \\ -j_x\left(f_xf_{xx} + f_yf_{xy}\right) - j_y\left(f_yf_{yy} + f_xf_{xy}\right)\end{bmatrix}$$

7.3.6 The λ Singularity

For certain frequencies, there can be a mode in the Green's function for which λ_{mn} is close to zero. Physically, these frequencies can give rise to transmission resonances

known as Wood's anomalies (see Section 2.8). Mathematically, the analyticity of the Green's function breaks down at these λ singularities. We are careful to not choose frequencies for which $\lambda_{mn} = 0$, and we have worked with frequency ranges such that only λ_{mn}^{int} can be near 0. At such frequencies, we would like to be certain that the numerical effects of dividing by a small value are not a problem in our evaluation of the Green's functions.

Since we only approach λ singularities in the interior Green's functions, we can take advantage of the fact that our interior Green's functions do not need to decay in z. We can replace a singular mode in the interior Green's function

$$\frac{1}{8\pi^2}\frac{e^{-\sqrt{-\lambda_{mn}}|z|}}{\sqrt{-\lambda_{mn}}}P_{mn}$$

with a mode in which the singularity has been subtracted out:

$$\frac{1}{16\pi^2}\frac{\left(e^{-\sqrt{-\lambda_{mn}}|z|} - e^{\sqrt{-\lambda_{mn}}|z|}\right)}{\sqrt{-\lambda_{mn}}}P_{mn} \tag{7.6}$$

This is replaces our interior Green's function with a different, better-behaved Green's function. We can compute this mode using a Taylor series of (7.6), and we can thus avoid dividing by something small. This gives us assurance that behavior seen around the λ singularities is physical and not numerical.

Unfortunately, this change is not easy to track through the Ewald splitting process, and it is limited in its usefulness. It can, however, be used when λ is real and approaches 0 from the right. When this happens, we can compute the new mode (7.6) by recognizing that only $G2$ is changed. For the mode in question, we can eliminate the λ singularity by replacing

$$\mathrm{ExpInt}_{\frac{1}{2}}\left(-\lambda_{mn}E^2\right)$$

in the $G2$ summations with

$$\frac{\mathrm{ExpInt}_{\frac{1}{2}}\left(-\lambda_{mn}E^2\right) + \overline{\mathrm{ExpInt}_{\frac{1}{2}}\left(-\lambda_{mn}E^2\right)}}{2} = \mathrm{Re}\left(\mathrm{ExpInt}_{\frac{1}{2}}\left(-\lambda_{mn}E^2\right)\right)$$

This is still an acceptable interior Green's function, and for λ small we can avoid division by λ by replacing this quantity with a few terms of its Taylor series:

$$\mathrm{Re}\left(\mathrm{ExpInt}_{\frac{1}{2}}\left(-\lambda_{mn}E^2\right)\right) \approx -2 - \frac{2\lambda E^2}{3}$$

7.3.7 Size

Solving a scattering problem through integral equation methods has many advantages, but there are trade-offs. The greatest drawback of this method is that it leads to a large, dense linear system (4.19). Although the system is well-posed, it can become too large for practical computing purposes. The system in question is

$$\mathbf{J_{inc}} = A\mathbf{J_{int}}$$

With our scatterer described by an $N \times N$ grid in x and y, we have $2N^2$ surface points (N^2 points on the near surface defined by $F_1(x, y)$ and N^2 points on the far surface defined by $F_2(x, y)$). The vectors $\mathbf{J_{inc}}$ and $\mathbf{J_{int}}$ must include values for both $\mathbf{j} = -\mathbf{n} \times \mathbf{H}$ and $\mathbf{j}' = \mathbf{n} \times \mathbf{E}$ at every point on the discretized surface. For each of these, we have an x, y, and z component. The vectors $\mathbf{J_{inc}}$ and $\mathbf{J_{int}}$ thus have length $12N^2$, and the matrix A has $144N^4$ complex-valued entries.

The large numerical size is problematic in two ways. The first is that we are limited by memory restrictions in how much we can refine our grid. The second is in the time to run computations. We have found that the slowest parts of the numerical implementation are the computing of the Green's functions and the GMRES itera-

tions. We have devised some acceleration techniques that make this method more practical.

7.4 Acceleration Techniques

There are various ways in which we can improve the speed of our numerical approximations. Some of these have been fully implemented with success, and some are ideas still worth exploring.

7.4.1 Fast Fourier Transforms

Using fast Fourier transforms (FFTs) to compute the $G2$ sums of the Green's functions is the single largest time saver that we have implemented. This technique is possible only because of the restricted geometry where $z = f(x, y)$ and would not be an option for a more general scatterer. In actual implementation, we use this technique for various differences of exterior and interior Green's functions and their derivatives, but for simplicity we outline it only for the basic Green's function. The results are easily extended to every needed form of $G2$. From Chapter 5,

$$G2(x, y, z) = \frac{1}{8\pi^{5/2}} \sum_{m,n} P_{mn} \sum_{\ell=0}^{\infty} \frac{(-z)^{2\ell}}{4^{\ell}\ell! E^{2\ell-1}} \operatorname{ExpInt}_{\ell+1/2}\left(-\lambda_{mn} E^2\right)$$

with $P_{mn} = e^{ix(m+\alpha)+iy(n+\beta)}$. Rearranging terms, we have

$$G2(x, y, z) = \frac{e^{ix\alpha+iy\beta}}{8\pi^{5/2}} \sum_{\ell=0}^{\infty} \frac{(-z)^{2\ell}}{4^{\ell}\ell! E^{2\ell-1}} \sum_{m,n} e^{imx+iny} \operatorname{ExpInt}_{\ell+1/2}\left(-\lambda_{mn} E^2\right)$$

We can compute the double infinite sums

$$\sum_{m,n} e^{imx+iny} \operatorname{ExpInt}_{\ell+1/2}\left(-\lambda_{mn} E^2\right)$$

through FFTs as follows. Our discretized grid has points at

$$x_j = \frac{2\pi}{N} j \quad \text{and} \quad y_k = \frac{2\pi}{N} k$$

for $j, k = 0 \ldots N-1$. We define S^ℓ_{jk} as

$$S^\ell_{jk} = \sum_{m,n} e^{imx_j + iny_k} \operatorname{ExpInt}_{\ell+1/2}\left(-\lambda_{mn} E^2\right)$$

Then S^ℓ_{jk} can be approximated

$$\begin{aligned} S^\ell_{jk} &\approx \sum_{m=-\frac{N}{2}}^{\frac{N}{2}-1} \sum_{n=-\frac{N}{2}}^{\frac{N}{2}-1} e^{imx_j + iny_k} \operatorname{ExpInt}_{\ell+1/2}\left(-\lambda_{mn} E^2\right) \\ &= \sum_{m=-\frac{N}{2}}^{\frac{N}{2}-1} \sum_{n=-\frac{N}{2}}^{\frac{N}{2}-1} e^{\frac{2\pi imj}{N} + \frac{2\pi ink}{N}} \operatorname{ExpInt}_{\ell+1/2}\left(-\lambda_{mn} E^2\right) \end{aligned} \tag{7.7}$$

We show below that this approximation does not inroduce large error. This expression is a 2D discrete Fourier transform, and it can be computed quickly through FFTs. For a given ℓ, we then have a vector of stored S^ℓ_{jk}'s for $j, k = 0 \ldots N-1$ for use as needed in computing $G2$. We store these vectors for integers ℓ up to $\ell = 50$. The Green's functions as we need them in the integral equations are evaluated not at $\mathbf{x}$ but rather at $\mathbf{x}' - \mathbf{x}$. This is not a problem, as we still have all of the needed sums stored in the S^ℓ_{jk}'s. Indeed, for $G2\left(\mathbf{x_{j'k'}} - \mathbf{x_{jk}}\right)$, the exponential integral sum is

$$\begin{aligned} &\sum_{m,n} e^{im\left(x_{j'} - x_j\right) + in\left(y_{k'} - y_k\right)} \operatorname{ExpInt}_{\ell+1/2}\left(-\lambda_{mn} E^2\right) \\ &\approx \sum_{m=-\frac{N}{2}}^{\frac{N}{2}-1} \sum_{n=-\frac{N}{2}}^{\frac{N}{2}-1} e^{\frac{2\pi im\left(j'-j\right)}{N} + \frac{2\pi in\left(k'-k\right)}{N}} \operatorname{ExpInt}_{\ell+1/2}\left(-\lambda_{mn} E^2\right) \\ &= S^\ell_{j'-j,k'-k} \end{aligned}$$

for $j, j'k, k' = 0 \ldots N-1$. If either $j'-j$ or $k'-k$ is negative, we use the facts that $S^{\ell}_{-j,k} = S^{\ell}_{-j+N,k}$ and $S^{\ell}_{j,-k} = S^{\ell}_{j,-k+N}$.

G2 Estimates

We compute most of the sums that appear in the Green's functions by adding terms until the terms are smaller than a prescribed tolerance. When we compute and store the m and n sums of $G2$ with FTTs, we cannot do this. We must be certain in advance to include enough terms in the S^{ℓ}_{jk} sums.

$$S^{\ell}_{jk} \approx \sum_{m=-\frac{N}{2}}^{\frac{N}{2}-1} \sum_{n=-\frac{N}{2}}^{\frac{N}{2}-1} e^{imx_j+iny_k} \operatorname{ExpInt}_{\ell+1/2}\left(-\lambda_{mn}E^2\right)$$

We need to show that $\operatorname{ExpInt}_{\ell+1/2}\left(-\lambda_{mn}E^2\right)$ is small for any m or n greater than or equal to $\frac{N}{2}$ in magnitude. Recall that $\lambda_{mn} = k^2 - (m+\alpha)^2 - (n+\beta)^2 = \omega^2\epsilon\mu - (m+\alpha)^2 - (n+\beta)^2$. From Appendix C, for $x > 1$ and $n > \frac{1}{2}$, we have

$$\operatorname{ExpInt}_n(x) \leq \frac{2e^{-x}}{x}$$

Thus

$$\operatorname{ExpInt}_{\ell+1/2}\left(-\lambda_{mn}E^2\right) < \frac{2e^{-E^2\left((m+\alpha)^2+(n+\beta)^2-\omega^2\epsilon\mu\right)}}{E^2\left((m+\alpha)^2+(n+\beta)^2-\omega^2\epsilon\mu\right)}$$

For $m = \frac{N}{2}$, this is largest if $n = \alpha = \beta = 0$. The largest term not included in the S^{ℓ}_{jk} approximation must then be smaller than:

$$\frac{2e^{-E^2\left(N^2/4-\omega^2\epsilon\mu\right)}}{E^2\left(N^2/4-\omega^2\epsilon\mu\right)}$$

Even for N as small as 16 and E as small as $\frac{1}{2}$, this term on the order of 10^{-8} for our range of ω and ϵ. We can therefore be confident that we are not losing accuracy by using the stored FFTs in our $G2$ computations.

The Ewald Parameter

By precomputing and the m, n sums in $G2$, we speed up the $G2$ computations considerably, but there is a second acceleration benefit as well. Recall from Section 5.3 that we need to pick the Ewald parameter E carefully to ensure quick convergence of both $G1$ and $G2$. Our fast method of computing $G2$ is not highly dependent on E. We can therefore choose E small to get better $G1$ convergence without slowing $G2$ convergence significantly.

Another advantage of this is that we can compute transmission coefficients for multiple frequencies without having to change E. This has not been possible in previous scattering work, and it greatly simplifies computations.

As mentioned, we have found experimentally that $E = \frac{1}{2}$ works well with our scattering parameters.

7.4.2 Green's Function Precomputing and Storage

Although memory is at a premium in our problem, there are certain quantities that are precomputed and stored to save computational time. Most of these come from the Green's functions.

G2 storage

We have already seen in Section 7.4.1 that we precompute and store the m, n sums from $G2$. We called these precomputed sums S_{jk}^{ℓ}. The $G2$ sums become

$$G2\left(x,y,z\right) = G2\left(x_j, y_k, z\right) = \frac{e^{ix_j\alpha + iy_k\beta}}{8\pi^{5/2}} \sum_{\ell=0}^{\infty} \frac{\left(-z\right)^{2\ell}}{4^{\ell}\ell! E^{2\ell-1}} S_{jk}^{\ell}$$

We can see that it will also be advantageous to precompute and store the factors

$$4^{\ell}\ell! E^{2\ell-1} \quad \text{and} \quad e^{ix_j\alpha + iy_k\beta}$$

as well as corresponding factors that appear in the needed derivatives of $G2$. Since we are able to use a fixed E for many frequencies, storing these coefficients can lead to meaningful computational savings.

G1 storage

$$G1\left(x,y,z\right) = \frac{1}{8\pi^{3/2}} \sum_{\mu,\nu} e^{-2\pi i(\alpha\mu + \beta\nu)} \sum_{\ell=0}^{\infty} \frac{k^{2\ell} E^{2\ell-1}}{\ell!} \operatorname{ExpInt}_{\ell+1/2}\left(\frac{R_{\mu\nu}^2}{4E^2}\right)$$

For $G1$ computations, we precompute the quantities

$$\frac{k^{2\ell} E^{2\ell-1}}{\ell!} \quad \text{and} \quad e^{-2\pi i(\alpha\mu + \beta\nu)}$$

Up to this point, none of our precomputed quantities require a significant amount of memory.

We now discuss another storage strategy for $G1$ that requires much more memory. We have only implemented it for small values of N (up to $N = 24$), as it requires

too much memory for larger N. We can rewrite $G1$ as

$$G1\left(x,y,z\right)=\frac{1}{8\pi^{3/2}}\sum_{\ell=0}^{\infty}\frac{k^{2\ell}E^{2\ell-1}}{\ell!}\sum_{\mu,\nu}e^{-2\pi i(\alpha\mu+\beta\nu)}\,\mathrm{ExpInt}_{\ell+1/2}\left(\frac{R_{\mu\nu}^{2}}{4E^{2}}\right)$$

$$=\frac{1}{8\pi^{3/2}}\sum_{\ell=0}^{\infty}\frac{k^{2\ell}E^{2\ell-1}}{\ell!}T^{\ell}\left(x,y,z\right)$$

with

$$T^{\ell}\left(x,y,z\right)=\sum_{\mu,\nu}e^{-2\pi i(\alpha\mu+\beta\nu)}\,\mathrm{ExpInt}_{\ell+1/2}\left(\frac{R_{\mu\nu}^{2}}{4E^{2}}\right)$$

Quantities similar to $T^{\ell}\left(x,y,z\right)$ can be stored for all of the necessary Green's functions. The great savings in this storage comes from the fact that $T^{\ell}\left(x,y,z\right)$ is frequency independent (since, thanks to the FFTs, we can choose E independent of ω). We can thus compute these quantities just once and use them for scattering problems of many different frequencies. This can lead to tremendous savings in computing $G1$. The cost is expensive, however, as we need to store a $T^{\ell}\left(x,y,z\right)$ for every possible (x,y,z) combination, for many integers ℓ, and for all of the possible derivatives and forms of $G1$. This is on the order of $25N^{4}$ complex numbers. Depending on the memory available, this may be an overly prohibitive cost.

7.4.3 Symmetry

There is a natural symmetry in the Green's functions that can be exploited. This will reduce the amount of computational time spent in evaluating Green's functions as well as the amount of memory required to store the functions. We make use of the fact that $G\left(\mathbf{x}-\mathbf{x}'\right)=G\left(\mathbf{x}'-\mathbf{x}\right)$. This fact is most easily recognized in the Fourier form of the Green's function (3.10), and it allows us to reduce computation and storage nearly in half. The derivatives of G all exhibit this same symmetry or a

corresponding antisymmetry.

7.4.4 Interpolation

Much of the computational expense of the Green's functions is in the evaluation of exponential integral functions (see Appendix C). These $\mathrm{ExpInt}_n(x)$ functions are single-variable functions. Whenever x is positive, $\mathrm{ExpInt}_n(x)$ is real-valued. These functions are smooth away from the singularity at $x = 0$ that appears for $n \leq 1$, and they decay quickly to zero. In short, the exponential integral functions $\mathrm{ExpInt}_n(x)$ are good candidates for accurate interpolation.

We have employed cubic-spline interpolation to approximate values of the exponential integral functions $\mathrm{ExpInt}_n(x)$. We can use accurate clamped cubic splines, since the derivatives of $\mathrm{ExpInt}_n(x)$ are easy to compute. We interpolate for all needed orders n and for x up to some x_{max} (we have used $x_{max} = 25$, where $\mathrm{ExpInt}_n(x)$ is on the order of 10^{-13}). For larger x, we can safely set $\mathrm{ExpInt}_n(x)$ to zero. This interpolation requires little storage, and it leads to a less expensive evaluation of $\mathrm{ExpInt}_n(x)$. We have found it to be worthwhile. To ensure good approximation close to $x = 0$, we take a sample of points for our splines that increase exponentially in density towards $x = 0$.

We are currently investigating the possibility of using interpolation to evaluate entire Green's functions. These are more difficult, since they are functions from $\mathbb{R}^3$. We have implemented 5-point Lagrange interpolation in the z direction for $G1$. It can be made accurate and saves computational time, but we must store values for each possible (x, y) and for each possible derivative and combination of Green's function. Still, this method shows promise. It could be extended from $G1$ to all of G, but we would then be sacrificing the FFT savings of $G2$ (see Section 7.4.1).

7.4.5 GMRES

As mentioned in Section 7.2.2, we must use iterative methods to approximate the solution of the linear system of equations that arises from the discretized integral equations. The size of the system precludes our using direct methods. However, iterative methods seem to converge quickly and are probably preferable regardless of problem size.

We have implemented the generalized minimal residual method (GMRES) of [32] as outlined in [24]. The GMRES method is a Krylov subspace method where each succeeding approximation is taken from a growing vector space. It has been proved that GMRES converges to the exact solution of an $N \times N$ linear system in at most N iterations. In practice, the hope is that an approximate solution can be obtained much more quickly.

A great advantage of GMRES for the linear system of our $12N^2 \times 12N^2$ scattering problem

$$\mathbf{J_{inc}} = A\mathbf{J_{int}}$$

is that it does not require storage of the $144N^4$ entry matrix A. It merely requires that we be able to apply A to a vector $\mathbf{J}$. Thus, instead of storing the huge matrix A, we can merely store all of the Green's functions needed to find $A\mathbf{J}$. This is a great savings in memory, and it is a significantly more simple thing to do. There is, of course, the trade-off of a higher computational cost to our GMRES iterations.

In practice, the GMRES iterations are one of the two time consuming processes in our numerical scattering experiments (the other, of course, being the Green's function evaluations). We have found that the number of iterations required is influenced by both the geometry of the scatterer and the presence or absence of resonances in the scatterer (see Chapter 8 for details). Still, in worst cases, seldom are more than 100

iterations needed for convergence within our tolerance of 10^{-4} using the convergence criteria of [24].

We have implemented a restarted GMRES with no success. The restarts tended to slow convergence dramatically. We have investigated various other acceleration techniques for our GMRES method but as of yet have not implemented any. Standard preconditioning matrices are known to be unsuccessful in electromagnetic scattering problems in general, and preconditioning is considered an open problem in this field [28]. Most preconditioning strategies that have been implemented are to be used in conjunction with fast summation methods [10]. It may also be possible to achieve some time savings through the use of Ayachour transformations [4], which do not require the computation of Given's rotations.

Following [3], we know that the linear system is well-conditioned except possibly near frequencies that are eigenvalues. From [34] and [33], we have reason to believe that the eigenvalues of the system have small imaginary parts. The resonances that we observe and discuss in Chapter 8 are believed to occur for real frequencies near these complex eigenvalues. We would therefore expect the linear system to have higher condition numbers near the resonances. This is precisely what has been observed (see Figure 8.9), as the system requires more GMRES iterations at frequencies near resonances.

As a check to our GMRES, we have also implemented the Bi-CGSTAB method of [41].

Chapter 8

Results

We have implemented the numerical scattering problem as described in Chapter 7 with various geometries and under various conditions. Here we outline the results of our experiments. We include a test case for which the exact solutions are known as well as many cases without known solutions. In all cases, we have observed convergence that appears to be third order in the grid size $h = \frac{2\pi}{N}$.

8.1 Richardson Extrapolation

Except in a very restricted geometry, we will not know the exact solutions which we are approximating numerically. In these cases, we would like to have some kind of check as to the order of convergence of the method. We use the ideas of Richardson extrapolation to achieve this. Suppose for a step size $h = \frac{2\pi}{N}$, a numerical method produces an approximation $A(h)$ to an exact quantity A with the following property

$$A - A(h) = Ch^3$$

for some constant C. We can then write

$$\begin{aligned}\frac{A(4h)-A(2h)}{A(2h)-A(h)} &= \frac{(A-A(2h))-(A-A(4h))}{(A-A(h))-(A-A(2h))} \\ &= \frac{C(4h)^3-C(2h)^3}{C(2h)^3-C(h)^3} \\ &= \frac{64Ch^3-8Ch^3}{8Ch^3-Ch^3} \\ &= 8\end{aligned}$$

We thus will often look for the ratio

$$R = \frac{A(4h)-A(2h)}{A(2h)-A(h)} = 8 \tag{8.1}$$

in our numerical methods. We will call such quotients Richardson ratios. Such a relationship provides evidence that our method is indeed converging with third order accuracy. Whenever analytical solutions are known, we will compare results with them. Otherwise, any claims of results consistent with third-order convergence will be referring to this process. Due to size limitations, we often compute numerical results for $N = 16$, $N = 24$, and $N = 32$. In this case, a ratio of 4 would indicate third-order convergence, although this is an imperfect test with such a coarse grid as is creates with $N = 16$.

8.2 A Green's Function Test

The Green's functions in our problem are complicated numerically, and it is helpful to have a way of testing the evaluation of these functions. A good, if incomplete, test can be found in integrating the Green's functions on a flat slab. This is the surface $\partial\Omega$ where the front and back of the scatterer are given respectively by $F_1(x,y) = 0$ and $F_2(x,y) = L$ for a constant L (see Figure 8.1). Unless stated otherwise, we

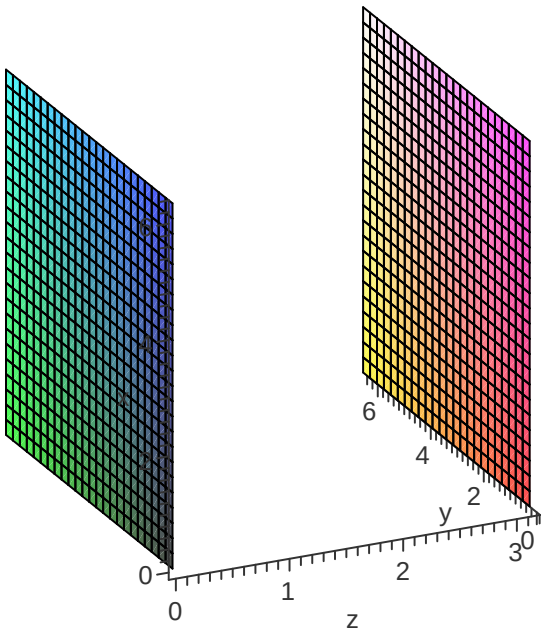

Figure 8.1: One periodic block of the flat slab scatterer

have set $L = \pi$ for all results in this chapter. This test will only work for normally incident waves (so $\alpha = \beta = 0$).

We integrate the Fourier form of the Green's function over the flat slab

$$\int_{\partial\Omega} G(\mathbf{x} - \mathbf{x}')\, dS(\mathbf{x}) = \frac{1}{8\pi^2} \int_{z=0} \sum_{m,n} \frac{e^{-\sqrt{-\lambda_{mn}}|z-z'|}}{\sqrt{-\lambda_{mn}}} P_{mn} dS(\mathbf{x})$$

$$+ \frac{1}{8\pi^2} \int_{z=L} \sum_{m,n} \frac{e^{-\sqrt{-\lambda_{mn}}|z-z'|}}{\sqrt{-\lambda_{mn}}} P_{mn} dS(\mathbf{x})$$

$$= \frac{1}{8\pi^2} \int_0^{2\pi} \int_0^{2\pi} \sum_{m,n} \frac{e^{-\sqrt{-\lambda_{mn}}|-z'|}}{\sqrt{-\lambda_{mn}}} e^{im(x-x')+in(y-y')} dxdy$$

$$+ \frac{1}{8\pi^2} \int_0^{2\pi} \int_0^{2\pi} \sum_{m,n} \frac{e^{-\sqrt{-\lambda_{mn}}|L-z'|}}{\sqrt{-\lambda_{mn}}} e^{im(x-x')+in(y-y')} dxdy$$

Now, the integrals $\int_0^{2\pi} \int_0^{2\pi} e^{im(x-x')+in(y-y')} dxdy$ are all equal to 0 except for the

$m = n = 0$ mode. Thus, remembering the sign conventions of Section 3.4,

$$\begin{aligned}\int_{\partial\Omega} G(\mathbf{x}-\mathbf{x}')\,dS(\mathbf{x}) &= \frac{1}{8\pi^2}\int_0^{2\pi}\int_0^{2\pi}\frac{e^{-\sqrt{-k^2}|-z'|}}{\sqrt{-k^2}}dxdy \\ &\quad + \frac{1}{8\pi^2}\int_0^{2\pi}\int_0^{2\pi}\frac{e^{-\sqrt{-k^2}|L-z'|}}{\sqrt{-k^2}}dxdy \\ &= \frac{i\left(e^{ik|z'|}+e^{ik|L-z'|}\right)}{2k}\end{aligned}$$

Similar reasoning tells us that the integrals of G_x, G_y, G_{xx}, G_{xy}, G_{yy}, G_{xz}, and G_{yz} are all zero. The remaining integrals of interest can also be found without difficulty:

$$\int_{\partial\Omega} G_z(\mathbf{x}-\mathbf{x}')\,dS(\mathbf{x}) = \frac{\operatorname{sgn}(z')\,e^{ik|z'|} - \operatorname{sgn}(L-z')\,e^{ik|L-z'|}}{2}$$

and

$$\int_{\partial\Omega} G_{zz}(\mathbf{x}-\mathbf{x}')\,dS(\mathbf{x}) = -\left(\frac{ik}{2}+\delta(z')\right)e^{ik|z'|} - \left(\frac{ik}{2}+\delta(L-z')\right)e^{ik|L-z'|}$$

We have found these flat slab integrals useful as a test for the evaluation of the Green's functions. These results on the flat slab can also be used to check the evaluation of the Green's functions that are needed in building the integral equation:

$$k_{ext}^2 G_{\delta_{ext}} - k_{int}^2 G_{\delta_{int}}$$

$$\nabla\left(G_{\delta_{ext}} - G_{\delta_{int}}\right)$$

$$\nabla\left(\epsilon_{ext} G_{\delta_{ext}} - \epsilon_{int} G_{\delta_{int}}\right)$$

$$(\mathbf{j}\cdot\nabla)\nabla\left(G_{\delta_{ext}} - G_{\delta_{int}}\right)$$

We can use these exact integrals to test our smoothed and corrected single layer potential (6.3) and the integral $I1$ (6.16). We do see third-order accuracy in these integrals. The double layer potential (6.13) and the singular integral $I2$ (6.18),

however, require a correction terms based on the curvature of the surface. On the flat slab, the curvature is zero, and we have third order convergence without correction.

8.3 Integrals on Curved Surfaces

A large part of this thesis is the method of smoothing and correcting singular integrals. The method is developed in Chapter 6. We would like to be able to test our method independent of the integral equation and the scattering problem. We have evaluated all of Müller's integrals on the surface defined by

$$F_1(x,y) = C\cos^2\left(\frac{x}{2}\right)\sin^2\left(\frac{y}{2}\right) \quad \text{and} \quad F_2(x,y) = L - C\cos^2\left(\frac{x}{2}\right)\sin^2\left(\frac{y}{2}\right) \tag{8.2}$$

The results presented here are for $L = 2$ and $C = \frac{1}{5}$. We call this surface the smoothed, dimpled scatterer (see Figure 8.2).

The single layer potential (see Section (6.3)) is the integral

$$slp(\mathbf{x}') = \int_{\partial\Omega} G(\mathbf{x}' - \mathbf{x})\,\phi(\mathbf{x})\,dS(\mathbf{x})$$

and the double layer potential (See Section (6.13)) is

$$dlp(\mathbf{x}') = \int_{\partial\Omega} \left[\mathbf{n}(\mathbf{x}) \cdot \nabla G(\mathbf{x}' - \mathbf{x})\right]\phi(\mathbf{x})\,dS(\mathbf{x})$$

We have developed the smoothing and correction method for each of these two types of integrals. We use the function $\phi(\mathbf{x}) = \cos(x)\cos(y)$. We have evaluated each at various points $\mathbf{x}'$ over the surface (8.2). The smoothed Green's functions were integrated, and the correction terms (6.17) were added to the sums. The integrals were evaluated with $N = 64$, $N = 128$, and $N = 256$, and a sampling of the ratios (8.1) are reported here in Table 8.1. The results in the table are a small sample of

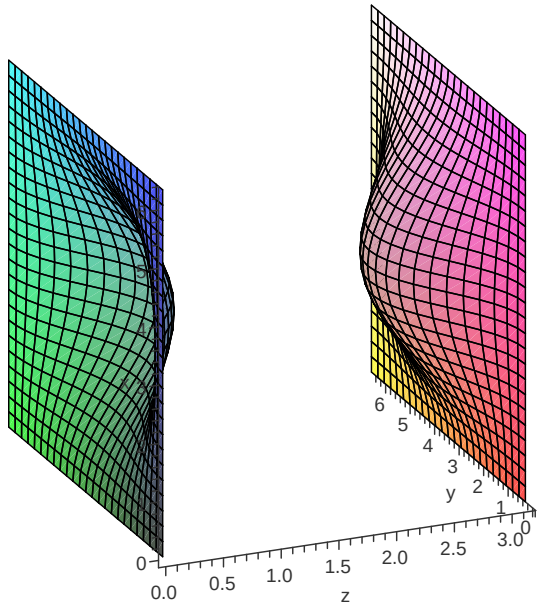

Figure 8.2: One periodic block of the smooth, dimpled scatterer

typical results for wave numbers k in the range $k = 0.8$ to $k = 1.8$ and smoothing parameters δ in the range $\delta = h$ to $\delta = 3h$. Recall that a ratio close to 8 would be consistent with third-order convergence.

We have found similar convergence results for all of the integrals needed in Müller's integral equations. Without correction terms, the ratios R for the singular integrals are very close to 2, indicating first order convergence. We have found similar convergence results for the other curved scatterers described below.

8.4 A Flat Slab Scattering Problem

We are, of course, most interested in the entire scattering problem. The flat slab geometry already detailed is a scatterer with an exact analytical solution. It therefore makes for a good test case.

point (x', y')	*slp* **ratio R**	*dlp* **ratio R**
$(0, 0)$	8.05	7.63
(π, π)	7.99	7.89
$\left(\frac{\pi}{2}, \frac{\pi}{2}\right)$	7.94	7.60
$\left(\frac{\pi}{8}, \frac{\pi}{4}\right)$	8.22	7.40
$\left(\frac{5\pi}{8}, \frac{7\pi}{4}\right)$	7.97	7.82
$\left(\frac{\pi}{2}, \frac{3\pi}{4}\right)$	7.79	7.90

Table 8.1: Table of Results for Single and Double Layer Potentials on a Smooth Dimpled Surface

8.4.1 Derivation of the Flat Slab Test Case

We can find an exact solution for the flat slab scatterer with normally incident fields (see Section 2.5 for a discussion of the incident fields). We need to solve the Helmholtz equation in all of space, and our space is broken into the three regions shown and labeled in Figure 8.3. In regions I (incident to the scatterer) and II (within the scatterer), we have fields propagating both to the left and to the right. In region III (transmitted past the scatterer), we can only have a transmitted field propagating to the right. The media constants of the all regions are set to 1 except for the permittivity of the scatterer ϵ_{int}. In region I, we thus have

$$\mathbf{E}(z) = \begin{bmatrix} E_0 e^{ik_{ext}z} + C_1 E_0 e^{-ik_{ext}z} \\ 0 \\ 0 \end{bmatrix}, \mathbf{H}(z) = \begin{bmatrix} 0 \\ E_0 e^{ik_{ext}z} - C_1 E_0 e^{-ik_{ext}z} \\ 0 \end{bmatrix}$$

In region II, we have

$$\mathbf{E}(z) = \begin{bmatrix} C_2 E_0 e^{ik_{int}z} + C_3 E_0 e^{-ik_{int}z} \\ 0 \\ 0 \end{bmatrix}, \mathbf{H}(z) = \begin{bmatrix} 0 \\ \sqrt{\epsilon_{int}} \left(C_2 E_0 e^{ik_{int}z} - C_3 E_0 e^{-ik_{int}z} \right) \\ 0 \end{bmatrix}$$

And in region III, the fields are

$$\mathbf{E}(z) = \begin{bmatrix} C_4 E_0 e^{ik_{ext}z} \\ 0 \\ 0 \end{bmatrix}, \mathbf{H}(z) = \begin{bmatrix} 0 \\ C_4 E_0 e^{ik_{ext}z} \\ 0 \end{bmatrix}$$

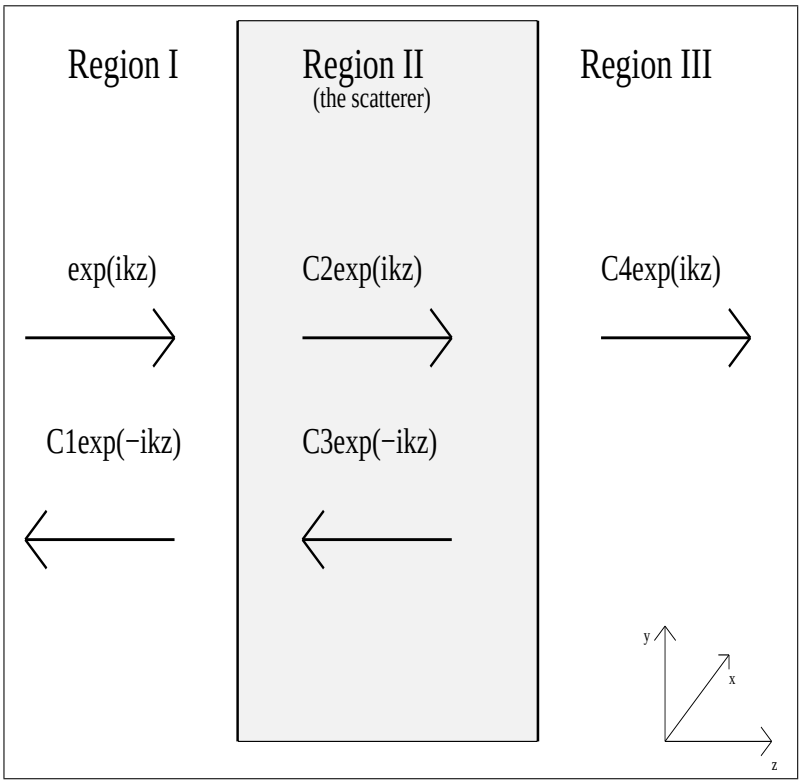

Figure 8.3: The flat slab scattering problem

For all three regions, we have used Maxwell's equations (2.2) to find **H** given **E**. We see that we have four unknowns - the coefficients C_1, C_2, C_3, and C_4 - which we think of as functions of the frequency ω. On the surface of the scatterer, we enforce the boundary conditions of tangential continuity:

$$\mathbf{n} \times \mathbf{E}_{\mathbf{ext}} = \mathbf{n} \times \mathbf{E}_{\mathbf{int}} \quad \text{and} \quad \mathbf{n} \times \mathbf{H}_{\mathbf{ext}} = \mathbf{n} \times \mathbf{H}_{\mathbf{int}}$$

These conditions give us four equations (two at $z = 0$ and two at $z = L$), and we

can solve for all four coefficients. The result is that **E** and **H** are as above with

$$C_1(\omega) = \frac{\theta - 1}{\theta + 1} + \frac{4\theta(1-\theta)e^{\frac{2i\omega L}{\theta}}}{(1+\theta)^3 - (1+\theta)(1-\theta)^2 e^{\frac{2i\omega L}{\theta}}}$$

$$C_2(\omega) = \frac{2\theta(1+\theta)}{(1+\theta)^2 - (1-\theta)^2 e^{\frac{2i\omega L}{\theta}}}$$

$$C_3(\omega) = \frac{2\theta(1-\theta)e^{\frac{2i\omega L}{\theta}}}{(1+\theta)^2 - (1-\theta)^2 e^{\frac{2i\omega L}{\theta}}}$$

$$C_4(\omega) = \frac{4\theta e^{i\left(\frac{\omega}{\theta}-\omega\right)L}}{(1+\theta)^2 - (1-\theta)^2 e^{\frac{2i\omega L}{\theta}}}$$

where we have substituted $\theta = \sqrt{\frac{1}{\epsilon_{int}}}$ to make the coefficients more presentable.

We now have exact expressions for the electric and magnetic fields. We can use these to find an exact expression for the transmission coefficient as a function of the frequency ω. This is outlined in detail in Section 2.7. For this simple case, however, the transmission coefficient reduces to the simple expression

$$T(\omega) = |C_4(\omega)|$$

Having solved for $C_4(\omega)$, we can find T

$$T(\omega) = \left(\frac{16\theta^2}{(1+\theta)^4 + (1-\theta)^4 - (1+\theta)^2(1-\theta)^2\left(e^{\frac{2i\omega L}{\theta}} + e^{\frac{-2i\omega L}{\theta}}\right)}\right)^{1/2}$$

$$= \left(\frac{16\theta^2}{(1+\theta)^4 + (1-\theta)^4 - 2(1-\theta^2)^2\cos\left(\frac{2\omega L}{\theta}\right)}\right)^{1/2}$$

$$= 4\theta\sqrt{\frac{1}{(1+\theta)^4 + (1-\theta)^4 - 2(1-\theta^2)^2\cos\left(\frac{2\omega L}{\theta}\right)}}$$

We see that the transmission coefficient is periodic has a maximum value of $T = 1$

wherever $\cos\left(2\omega\sqrt{\epsilon_{int}}L\right) = 1$ and a minimum value of $T = \sqrt{\frac{4\epsilon_{int}}{\epsilon_{int}^2+2\epsilon_{int}+1}}$ wherever $\cos\left(2\omega\sqrt{\epsilon_{int}}L\right) = -1$.

8.4.2 Results in the Flat Slab Test Case

We have implemented the numerical scattering experiment for the flat slab scatterer with various physical and numerical parameters. In all cases, the agreement is excellent. We present the results for $\epsilon_{int} = 5$ and $N = 32$ in Figure 8.4, where we see extremely good agreement. Figure 8.4 also includes results for the scattering experiment when the correction terms in the integral equations are omitted. The difference is striking and illustrates the benefit of third order convergence. Figure 8.5 gives results under the same physical conditions but with $N = 16$, and we can see very good agreement for such a coarse grid. We can see better in this figure how the approximations become worse as the frequency increases. In previous work with first order methods [5], it was necessary to refine the grid many times within this same frequency range in order to approximate the solution well.

Figure 8.6 gives results for $\epsilon_{int} = 15$. This is a more difficult case, since the frequency is higher and convergence of the Green's functions is therefore slower. The results are still very good.

We have also approximated transmission coefficients for lossy scatterers - scatterers where ϵ_{int} has an imaginary part. The results for $\epsilon_{int} = 15 + 0.5i$ are in Figure 8.7.

8.5 Smooth Dimpled Scatterer

Results for the smooth, dimpled scatterer (8.2) of Figure 8.2 with $L = \pi$ are in Figure 8.8. We notice interesting behavior at some frequencies, most notably a

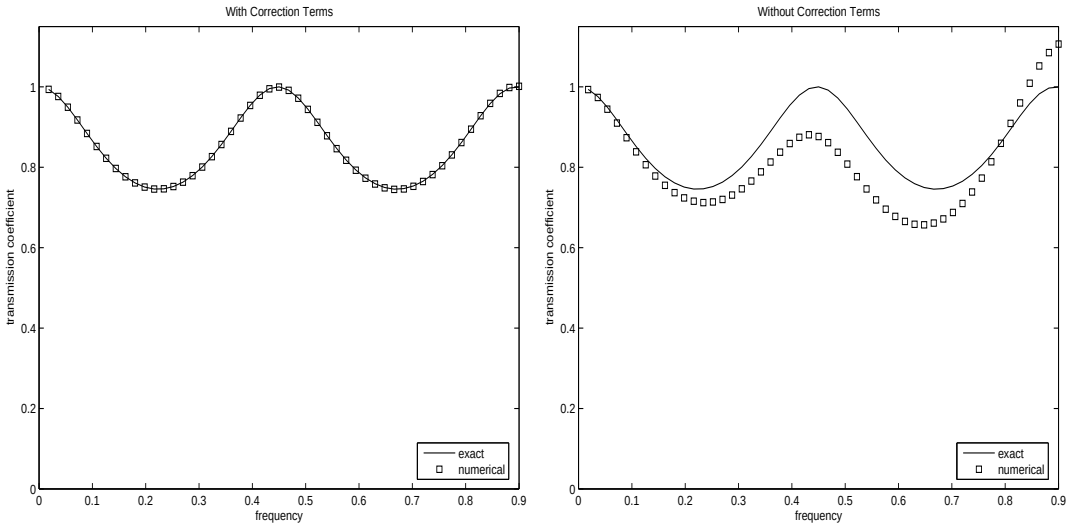

Figure 8.4: The flat slab test case. On the left are the numerical approximations with corrections. On the right, the corrections have been omitted. N=32. $\epsilon = 5$. $\delta = h$.

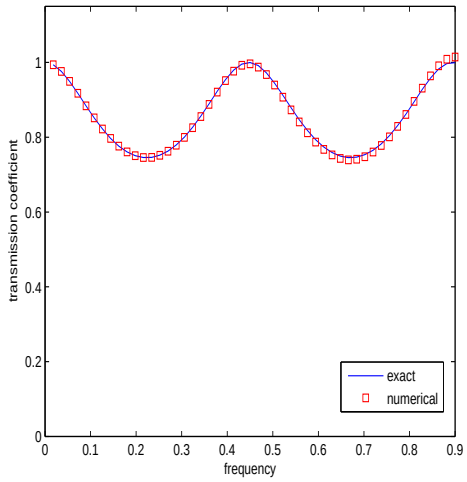

Figure 8.5: The flat slab test case for N=16. $\epsilon = 5$. $\delta = h$.

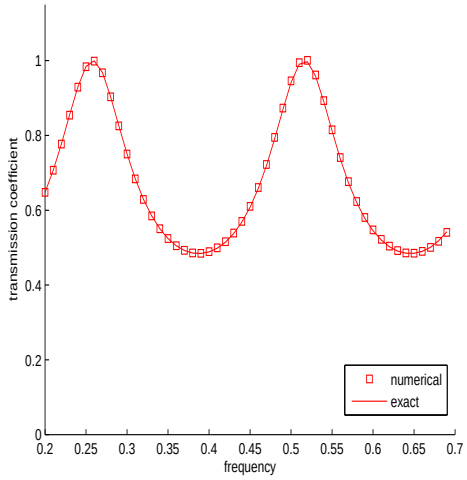

Figure 8.6: The flat slab test case with $\epsilon = 15$. $N = 32$. $\delta = h$.

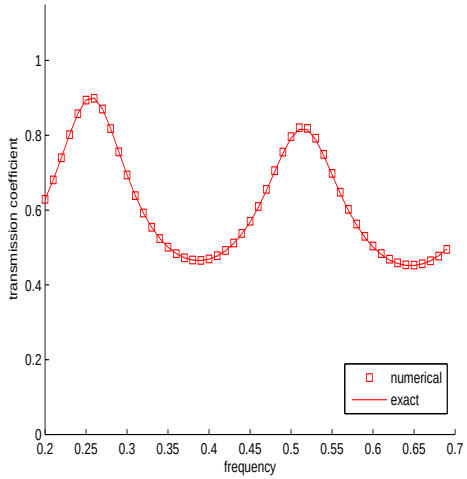

Figure 8.7: The flat slab test case with $\epsilon = 15 + 0.5i$. $N = 32$. $\delta = h$.

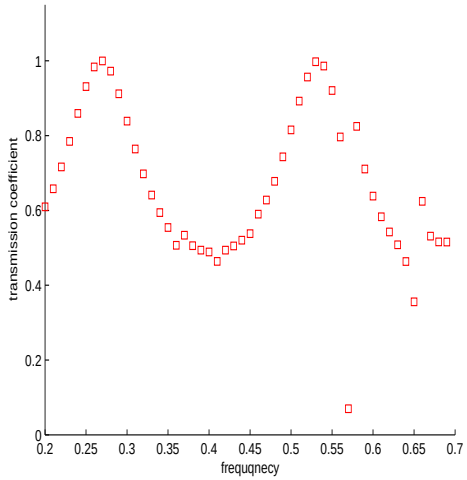

Figure 8.8: Transmission coefficients for the smooth dimpled scatterer. $\epsilon = 15$. $N = 32$. $\delta = h$.

sharp dip in transmission around $\omega = 0.57$. In general for out results, any interesting features in transmission occur at frequencies for which a λ_{mn} mode of the Green's function is close to zero. This behavior is not unexpected and is related to the Wood's anomaly (see Sections 2.8 and 8.7). Figure 8.9 shows the number of GMRES iterations required to solve the linear system at each frequency. It is clear that iterations increase with frequency, and it would appear that more iterations are required for frequencies near resonances as expected (see Section 7.4.5). We observe Richardson ratios (8.1) near 4, implying third order convergence.

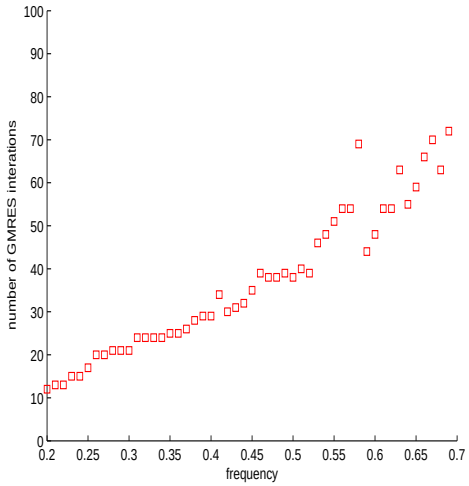

Figure 8.9: Numbers of GMRES iterations for the smooth dimpled scatterer. $\epsilon = 15$. $N = 32$. $\delta = h$.

8.6 Non-Smooth Dimpled Scatterer

We call the surface

$$F_1(x,y) = \begin{cases} C\left[1+\cos\left(\pi\sqrt{(x-\pi)^2+(y-\pi)^2}\right)\right] & \text{, for } (x-\pi)^2+(y-\pi)^2 < 1 \\ 0 & \text{, otherwise} \end{cases}$$

$$F_2(x,y) = L - F_1(x,y) \tag{8.3}$$

the non-smooth, dimpled scatterer (see Figure 8.10). This is the dimpled scatterer of [5]. This surface is not in C^2; there is a discontinuity in the second derivative. We test this surface by enforcing a grid where discontinuities in $\partial\Omega$ do not lie on grid points. Richardson ratios near 4 show that we can do this and still get good convergence. Figure 8.11 shows the results, which are for $C = \frac{1}{4}$ and $L = \pi$. Again, there are small dips and spikes at frequencies where a λ_{mn} is close to zero.

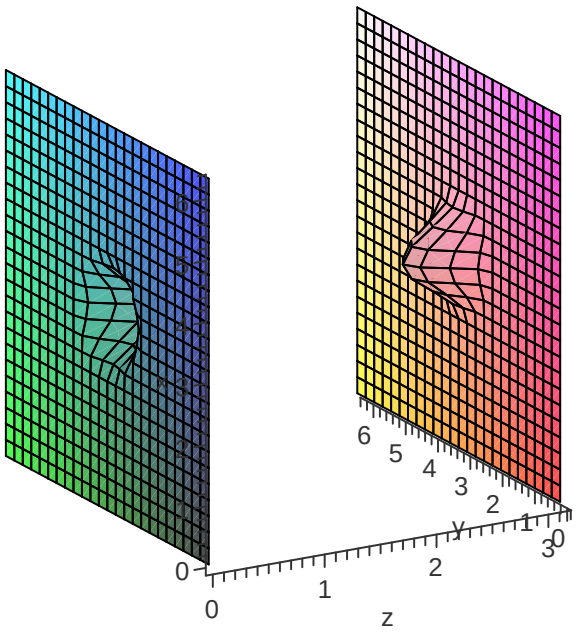

Figure 8.10: One periodic block of the non-smooth dimpled scatterer

8.7 Corrugated Roof Surface

The most interesting surface that we have experimented with thus far is the corrugated roof surface:

$$F_1(x,y) = C\sin^2\left(\frac{x}{2}\right) \quad \text{and} \quad F_2(x,y) = L - C\sin^2\left(\frac{x}{2}\right) \tag{8.4}$$

This is basically a 2D dimple, as the surface has no y dependence. It is seen in Figure 8.12. The results for $C = \frac{1}{5}$ and $L = \pi$ are seen in Figure 8.13, where we see the interesting behavior of the corrugated roof scatterer. There are two clear resonances in our evaluated frequency range. One is centered near $\omega = 0.37$ and the other near $\omega = 0.58$. Once again, these are frequencies for which there is a constant λ_{mn} in the Green's functions that is close to 0 (see Sections 3.4 and 7.3.6). These resonances are examples of Wood's anomaly (see Section 2.8). Wood's anomalies

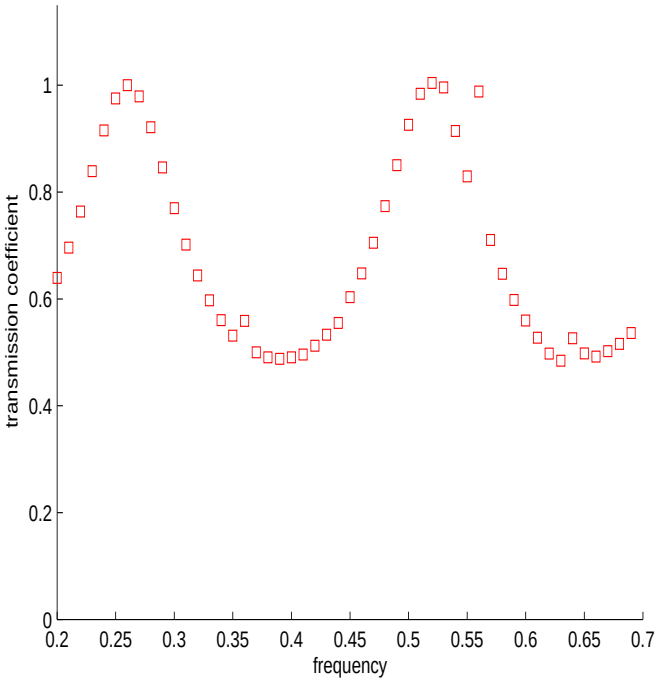

Figure 8.11: Transmission coefficients for the non-smooth dimpled scatterer. $\epsilon = 15$. $N = 32$. $\delta = h$.

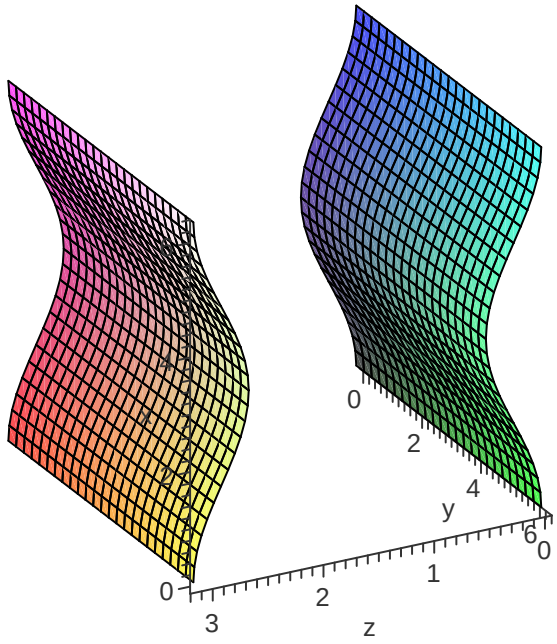

Figure 8.12: One periodic block of the corrugated roof scatterer

have been observed in scattering experiments where λ_{mn}^{ext} is near 0 [47] [19]. Here, we observe it for frequencies where λ_{mn}^{int} is near 0. Such an internal Wood's anomaly has previously been unknown. The resonance centered at $\omega = 0.37$ is particularly interesting, since there is a transmission spike up to full transmission. Figure 8.14 shows this resonance in more detail. As expected for Wood's anomaly, as we decrease the surface amplitude C, we see that the resonance shifts to the left and decreases in amplitude. We can see this in Figure 8.15

Figure 8.16 shows the ratios (8.1) of coefficients for $N = 16$, $N = 24$, and $N = 32$. For these grid sizes, a ratio of 4 indicates third-order convergence. We can see that the results are for the most part converging to third order, although the convergence is somewhat worse at higher frequencies. We suspect that the extremely coarse $N = 16$ grid is not refined enough to give good results here.

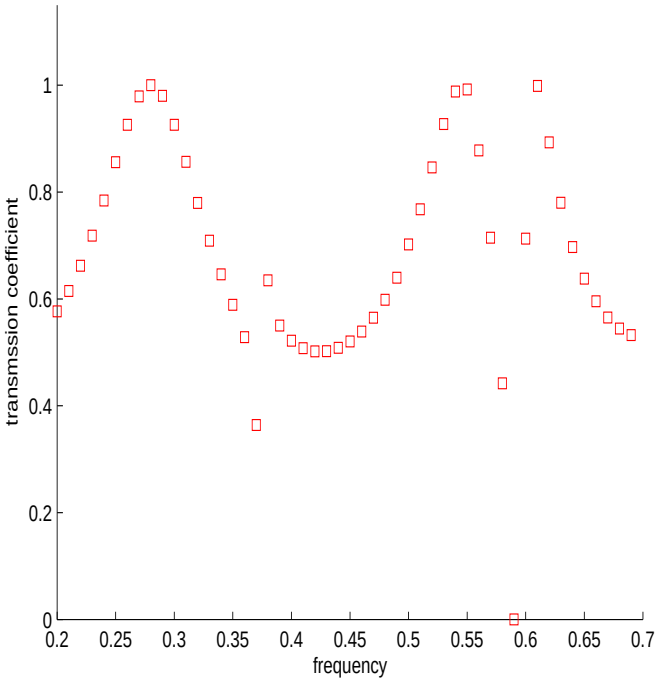

Figure 8.13: Transmission coefficients for the corrugated roof scatterer. $\epsilon = 15$. $N = 32$. $\delta = h$.

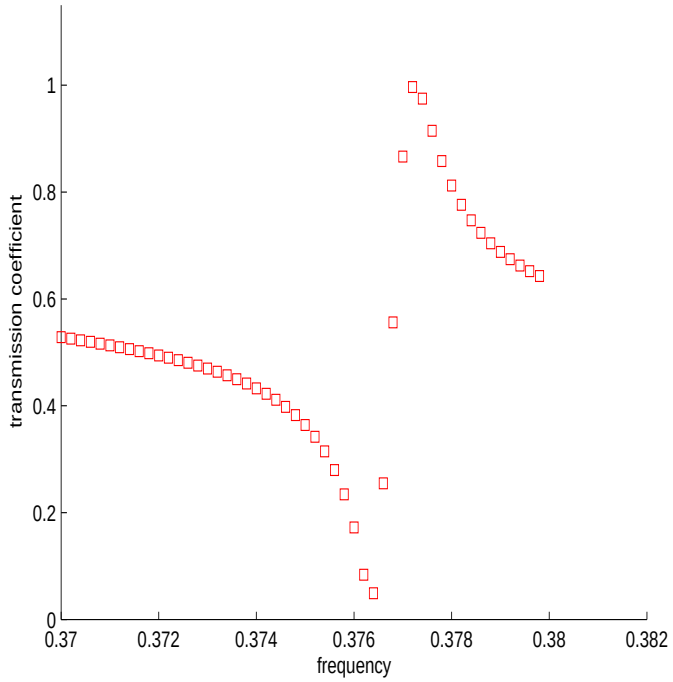

Figure 8.14: Closer look at the $\omega = 0.37$ resonance for the corrugated roof scatterer. $N = 32$. $\epsilon = 15$. $C = 0.25.\delta = h$

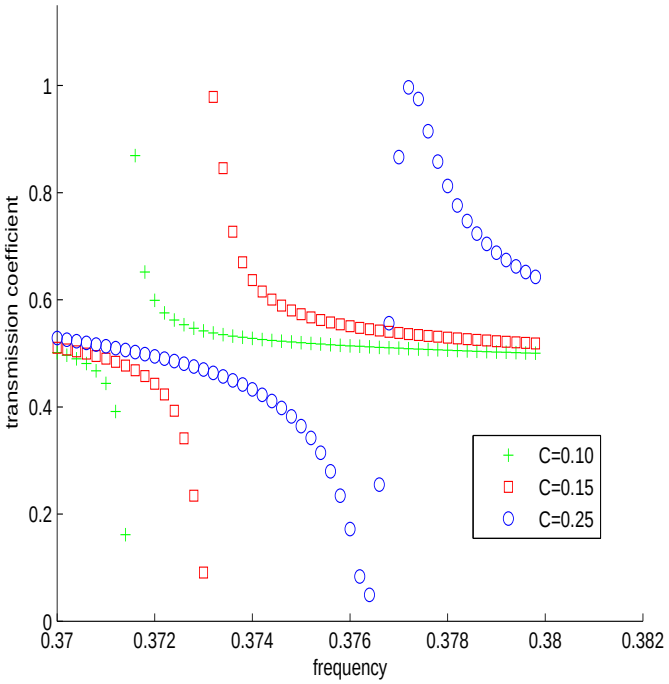

Figure 8.15: The $\omega = 0.37$ resonance for three values of the coefficient C on the corrugated roof scatterer. $N = 32$. $\epsilon = 15$. $\delta = h$

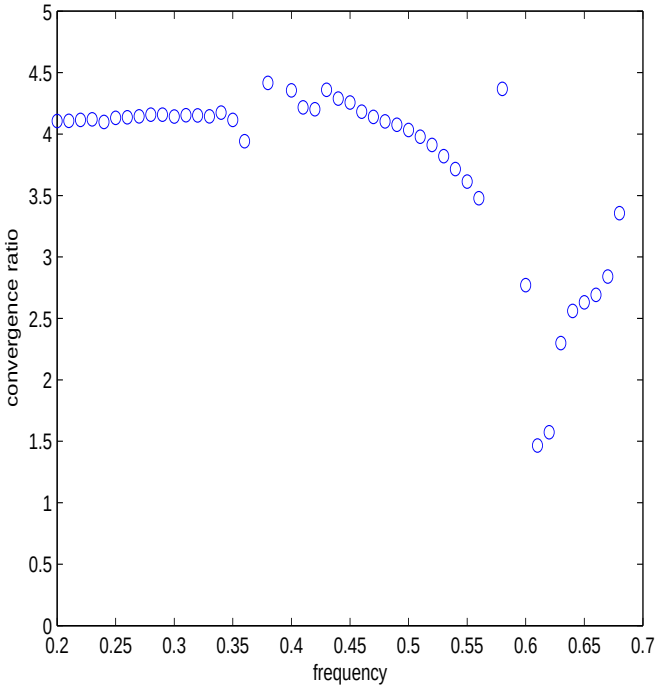

Figure 8.16: Richardson ratios (8.1) for the transmission coefficients on the corrugated roof scatterer for $N = 16$, $N = 24$, and $N = 32$. $\epsilon_{int} = 15$. $\delta = h$.

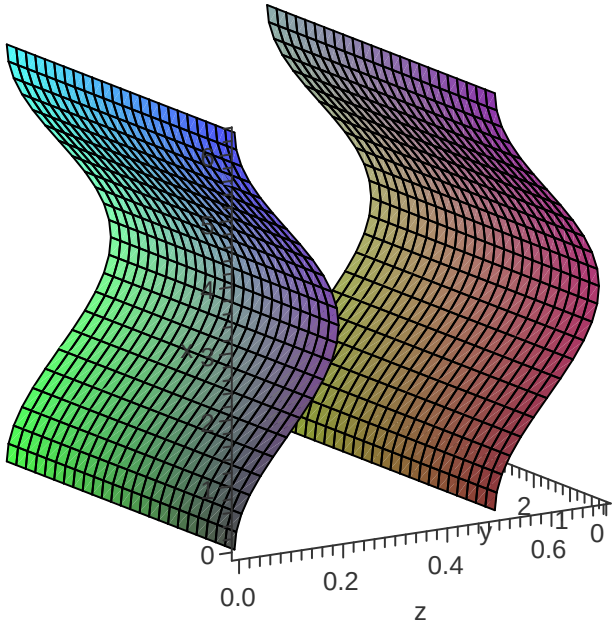

Figure 8.17: One periodic block of the wavy roof scatterer

To further investigate the nature of the resonances of this scatterer, we shift the corrugated roof surface slightly, so that the grooves are in sync. We will call this the wavy roof surface, and we define it

$$F_1(x,y) = C\sin^2\left(\frac{x}{2}\right) \quad \text{and} \quad F_2(x,y) = C\sin^2\left(\frac{x}{2}\right) + L \tag{8.5}$$

We can see this surface in Figure 8.17. This surface also leads to Wood's anomaly resonances. We would not, however, expect to see such resonances for small L. This is indeed what we find, as is seen in Figure 8.18

8.8 Discussion of Results

The results are promising. We see very good agreement with an exact test case, and we see third order convergence for most frequencies on curved surfaces. We have

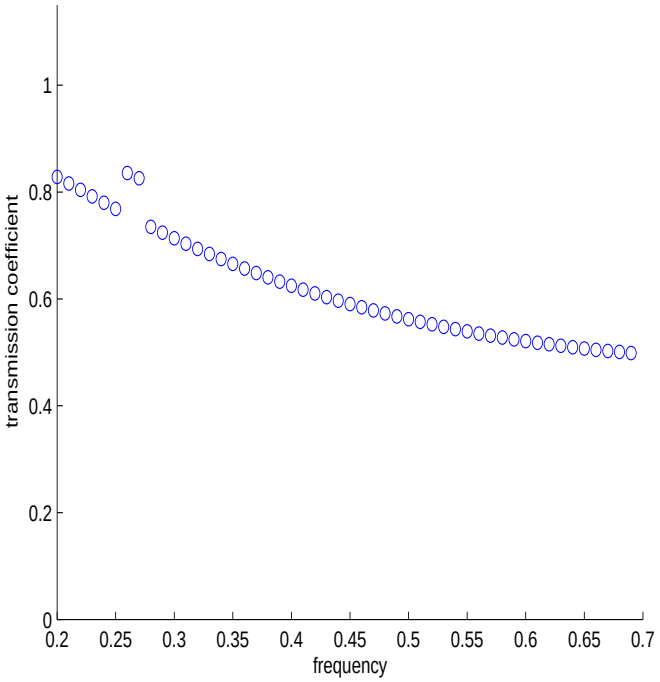

Figure 8.18: Transmission coefficients for the wavy roof scatterer with $L = \pi$. $N = 32$. $\epsilon = 15$. $C = 0.25.\delta = h$

seen also that the method is capable of resolving such interesting physical phenomena as transmission resonances. Comparing with results from a first order method [5], we can see the advantage of being able to approximate to $O(h^3)$ accuracy. In the coarse of testing the method, we have discovered Wood's anomaly resonances for the interior Green's function, a physical behavior which was previously unknown.

Chapter 9

Conclusion

We have successfully developed and implemented a third order accurate method for periodic electromagnetic scattering problems. We have adapted the Müller integral equations to a periodic geometry. Ewald splitting enabled us to quickly compute Green's functions and provided us with a clear way of regularizing the singular integrals of the integral equation. We were able to derive correction terms to compensate for the smoothing and have proved that the resulting error is small. We have devised various numerical acceleration techniques to make numerical implementation practical. The results for an exact test case are excellent, and results for all other scatterers show good convergence. Unlike other methods, we do not need to refine the grid significantly as we increase the frequency, and even coarse grids are capable of capturing qualitatively good information. The method has been shown to be capable of resolving resonances in transmission, and we have found an example of an interior Wood's anomaly.

There are various other geometries that we would like to implement. Scatterers with breaks in symmetry, such as off-set dimples or a cross-hatched corrugated roof, are the next logical thing to look at. We have implemented scattering problems with normally incident fields. From the 2D calculations of Venakides and Shipman [42]

[21] [34] [33], it would seem that there are many interesting features of these scatterers that will be found through implementing the problem for non-normal incident fields. Finally, the correction terms that we have derived are valid for any sufficiently smooth surface, but we have only implemented them here on surfaces that can be written $z = f(x, y)$. Following [7], we would like to implement our method for a more general surface. We will then have full freedom in the design of the scattering experiments.

Computational time and memory have emerged as serious limiting factors in these problems. Eventually, to increase the efficiency of the calculations, we would like to combine our method with a fast summation method. Such methods have been implemented for non-periodic electromagnetic scattering problems [26] [16]. The time savings would obviously be significant were this to be successfully adapted to the periodic scattering problem. We would also gain an extra benefit of being able to apply already developed preconditioning matrices to our GMRES algorithm [10].

Appendix A

Derivatives of the Green's Functions

Here we list all of the Green's functions and derivatives needed. Throughout, we use the notation

$$P_{mn} = e^{i(m+\alpha)(x'-x)+i(n+\beta)(x'-x)}$$

$$\lambda_{mn} = k^2 - (m+\alpha)^2 - (n+\beta)^2$$

A.1 Fourier Form

$$\begin{aligned}
G &= \frac{1}{8\pi^2}\sum_{m,n}\frac{e^{-\sqrt{-\lambda_{mn}}|z'-z|}}{\sqrt{-\lambda_{mn}}}P_{mn} \\
G_x &= -\frac{1}{8\pi^2}\sum_{m,n} i\,(m+\alpha)\,\frac{e^{-\sqrt{-\lambda_{mn}}|z'-z|}}{\sqrt{-\lambda_{mn}}}P_{mn} \\
G_y &= -\frac{1}{8\pi^2}\sum_{m,n} i\,(n+\beta)\,\frac{e^{-\sqrt{-\lambda_{mn}}|z'-z|}}{\sqrt{-\lambda_{mn}}}P_{mn} \\
G_z &= \frac{\operatorname{sgn}(z'-z)}{8\pi^2}\sum_{m,n} e^{-\sqrt{-\lambda_{mn}}|z'-z|}P_{mn}
\end{aligned} \tag{A.1}$$

$$
\begin{aligned}
G_{xx} &= -\frac{1}{8\pi^2}\sum_{m,n}(m+\alpha)^2\,\frac{e^{-\sqrt{-\lambda_{mn}}|z'-z|}}{\sqrt{-\lambda_{mn}}}P_{mn} \\
G_{yy} &= -\frac{1}{8\pi^2}\sum_{m,n}(n+\beta)^2\,\frac{e^{-\sqrt{-\lambda_{mn}}|z'-z|}}{\sqrt{-\lambda_{mn}}}P_{mn} \\
G_{xy} &= -\frac{1}{8\pi^2}\sum_{m,n}(m+\alpha)(n+\beta)\,\frac{e^{-\sqrt{-\lambda_{mn}}|z'-z|}}{\sqrt{-\lambda_{mn}}}P_{mn} \\
G_{xz} &= -\frac{\operatorname{sgn}(z'-z)}{8\pi^2}\sum_{m,n} i\,(m+\alpha)\,e^{-\sqrt{-\lambda_{mn}}|z'-z|}P_{mn} \\
G_{yz} &= -\frac{\operatorname{sgn}(z'-z)}{8\pi^2}\sum_{m,n} i\,(n+\beta)\,e^{-\sqrt{-\lambda_{mn}}|z'-z|}P_{mn} \\
G_{zz} &= -\frac{1}{4\pi^2}\sum_{m,n}\delta(z'-z)\,e^{-\sqrt{-\lambda_{mn}}|z'-z|}P_{mn} \\
&\quad + \frac{1}{8\pi^2}\sum_{m,n}\sqrt{-\lambda_{mn}}e^{-\sqrt{-\lambda_{mn}}|z'-z|}P_{mn}
\end{aligned}
\tag{A.2}
$$

A.2 Ewald Form G1

We use the Ewald Greens functions $G1$ and $G2$ only in the following expressions:

$$k_{ext}^2 G^{ext} - k_{int}^2 G^{int}$$

$$\nabla\left(G^{ext} - G^{int}\right)$$

$$\nabla\left(\epsilon_{ext}G^{ext} - \epsilon_{int}G^{int}\right)$$

$$(\mathbf{j}\cdot\nabla)\,\nabla\left(G^{ext} - G^{int}\right)$$

We actually need the smoothed versions G_δ of some of these. See Section 7.3.4 for information on how to adapt these formulas to compute smoothed Green's functions.

In addition to previously defined terms, we will now use the following notation:

$$e_{\mu\nu} = e^{-2\pi i(\alpha\mu+\beta\nu)}$$

$$R_{\mu\nu}^2 = (x+2\pi\mu)^2 + (y+2\pi\nu)^2 + z^2$$

$$\mathbf{R}_{\mu\nu} = \begin{bmatrix} x'-x+2\pi\mu \\ y'-y+2\pi\nu \\ z'-z \end{bmatrix}$$

The $G1$ sums that we need are:

$$k_{ext}^2 G1^{ext} - k_{int}^2 G1^{int} =$$

$$\frac{1}{8\pi^{3/2}} \sum_{\mu,\nu} e_{\mu\nu} \sum_{\ell=0}^{\infty} \frac{\left(k_{ext}^{2\ell} - k_{int}^{2\ell}\right) E^{2\ell-1}}{\ell!} \mathrm{ExpInt}_{\ell+\frac{1}{2}}\left(\frac{R_{\mu\nu}^2}{4E^2}\right)$$

$$\nabla\left(G1^{ext} - G1^{int}\right) =$$

$$\frac{1}{16\pi^{3/2}} \sum_{\mu,\nu} e_{\mu\nu}\mathbf{R}_{\mu\nu} \sum_{\ell=0}^{\infty} \frac{\left(k_{ext}^{2\ell+2} - k_{int}^{2\ell+2}\right) E^{2\ell-1}}{(\ell+1)!} \mathrm{ExpInt}_{\ell+\frac{1}{2}}\left(\frac{R_{\mu\nu}^2}{4E^2}\right)$$

$$\nabla\left(\epsilon_{ext} G1^{ext} - \epsilon_{int} G1^{int}\right) =$$

$$\frac{1}{16\pi^{3/2}} \sum_{\mu,\nu} e_{\mu\nu}\mathbf{R}_{\mu\nu} \sum_{\ell=-1}^{\infty} \frac{\left(\epsilon_{ext} k_{ext}^{2\ell+2} - \epsilon_{int} k_{int}^{2\ell+2}\right) E^{2\ell-1}}{(\ell+1)!} \mathrm{ExpInt}_{\ell+\frac{1}{2}}\left(\frac{R_{\mu\nu}^2}{4E^2}\right)$$

$$(\mathbf{j}\cdot\nabla)\nabla\left(G1^{ext} - G1^{int}\right) =$$

$$-\frac{\mathbf{j}}{16\pi^{3/2}} \sum_{\mu,\nu} e_{\mu\nu} \sum_{\ell=0}^{\infty} \frac{\left(k_{ext}^{2\ell+2} - k_{int}^{2\ell+2}\right) E^{2\ell-1}}{(\ell+1)!} \mathrm{ExpInt}_{\ell+\frac{1}{2}}\left(\frac{R_{\mu\nu}^2}{4E^2}\right)$$

$$+\frac{1}{32\pi^{3/2}} \sum_{\mu,\nu} e_{\mu\nu} \left(\mathbf{R}_{\mu\nu}\mathbf{R}_{\mu\nu}^{\mathbf{T}}\right)\mathbf{j} \sum_{\ell=-1}^{\infty} \frac{\left(\epsilon_{ext} k_{ext}^{2\ell+4} - \epsilon_{int} k_{int}^{2\ell+4}\right) E^{2\ell-1}}{(\ell+2)!} \mathrm{ExpInt}_{\ell+\frac{1}{2}}\left(\frac{R_{\mu\nu}^2}{4E^2}\right) \tag{A.3}$$

A.3 Ewald Form G2

In addition to previously defined terms, we will now use the following notation:

$$\lambda_{mn}^{ext} = k_{ext}^2 - (m+\alpha)^2 - (n+\beta)^2$$

$$\lambda_{mn}^{int} = k_{int}^2 - (m+\alpha)^2 - (n+\beta)^2$$

$$Q_{mn}^{\ell} = \left(\mathrm{ExpInt}_{\ell+\frac{1}{2}}\left(-\lambda_{mn}^{ext}E^2\right) - \mathrm{ExpInt}_{\ell+\frac{1}{2}}\left(-\lambda_{mn}^{int}E^2\right)\right)$$

$$kQ_{mn}^{\ell} = \left(k_{ext}^2\,\mathrm{ExpInt}_{\ell+\frac{1}{2}}\left(-\lambda_{mn}^{ext}E^2\right) - k_{int}^2\,\mathrm{ExpInt}_{\ell+\frac{1}{2}}\left(-\lambda_{mn}^{int}E^2\right)\right)$$

$$\epsilon Q_{mn}^{\ell} = \left(\epsilon_{ext}\,\mathrm{ExpInt}_{\ell+\frac{1}{2}}\left(-\lambda_{mn}^{ext}E^2\right) - \epsilon_{int}\,\mathrm{ExpInt}_{\ell+\frac{1}{2}}\left(-\lambda_{mn}^{int}E^2\right)\right)$$

The $G2$ sums that we need are:

$$k_{ext}^2 G2^{ext} - k_{int}^2 G2^{int} = \frac{1}{8\pi^{5/2}}\sum_{m,n} P_{mn}\sum_{\ell=0}^{\infty}\frac{(-1)^{\ell}(z'-z)^{2\ell}}{\ell!4^{\ell}E^{2\ell-1}}kQ_{mn}^{\ell}$$

$$D_x\left(G2^{ext} - G2^{int}\right) = -\frac{1}{8\pi^{5/2}}\sum_{m,n} i\,(m+\alpha)\,P_{mn}\sum_{\ell=0}^{\infty}\frac{(-1)^{\ell}(z'-z)^{2\ell}}{\ell!4^{\ell}E^{2\ell-1}}Q_{mn}^{\ell}$$

$$D_y\left(G2^{ext} - G2^{int}\right) = -\frac{1}{8\pi^{5/2}}\sum_{m,n} i\,(n+\beta)\,P_{mn}\sum_{\ell=0}^{\infty}\frac{(-1)^{\ell}(z'-z)^{2\ell}}{\ell!4^{\ell}E^{2\ell-1}}Q_{mn}^{\ell}$$

$$D_z\left(G2^{ext} - G2^{int}\right) = -\frac{1}{4\pi^{5/2}}\sum_{m,n} P_{mn}\sum_{\ell=1}^{\infty}\frac{(-1)^{\ell}(z'-z)^{2\ell-1}}{(\ell-1)!4^{\ell}E^{2\ell-1}}Q_{mn}^{\ell}$$

$$D_x\left(\epsilon_{ext}G2^{ext} - \epsilon_{int}G2^{int}\right) = -\frac{1}{8\pi^{5/2}}\sum_{m,n} i\,(m+\alpha)\,P_{mn}\sum_{\ell=0}^{\infty}\frac{(-1)^{\ell}(z'-z)^{2\ell}}{\ell!4^{\ell}E^{2\ell-1}}\epsilon Q_{mn}^{\ell}$$

$$D_y\left(\epsilon_{ext}G2^{ext} - \epsilon_{int}G2^{int}\right) = -\frac{1}{8\pi^{5/2}}\sum_{m,n} i\,(n+\beta)\,P_{mn}\sum_{\ell=0}^{\infty}\frac{(-1)^{\ell}(z'-z)^{2\ell}}{\ell!4^{\ell}E^{2\ell-1}}\epsilon Q_{mn}^{\ell}$$

$$D_z\left(\epsilon_{ext}G2^{ext} - \epsilon_{int}G2^{int}\right) = -\frac{1}{4\pi^{5/2}}\sum_{m,n} P_{mn}\sum_{\ell=1}^{\infty}\frac{(-1)^{\ell}(z'-z)^{2\ell-1}}{(\ell-1)!4^{\ell}E^{2\ell-1}}\epsilon Q_{mn}^{\ell} \tag{A.4}$$

We rewrite the last quantity that we need for $G2$:

$$(\mathbf{j}\cdot\nabla)\nabla\left(G^{ext}-G^{int}\right)=$$

$$j_x\begin{bmatrix}\partial_{xx}\left(G^{ext}-G^{int}\right)\\ \partial_{xy}\left(G^{ext}-G^{int}\right)\\ \partial_{xz}\left(G^{ext}-G^{int}\right)\end{bmatrix}+j_y\begin{bmatrix}\partial_{xy}\left(G^{ext}-G^{int}\right)\\ \partial_{yy}\left(G^{ext}-G^{int}\right)\\ \partial_{yz}\left(G^{ext}-G^{int}\right)\end{bmatrix}+j_z\begin{bmatrix}\partial_{xz}\left(G^{ext}-G^{int}\right)\\ \partial_{yz}\left(G^{ext}-G^{int}\right)\\ \partial_{zz}\left(G^{ext}-G^{int}\right)\end{bmatrix}$$

We thus need the second derivatives

$$\begin{aligned}
D_{xx}\left(G2^{ext}-G2^{int}\right)&=-\frac{1}{8\pi^{5/2}}\sum_{m,n}\left(m+\alpha\right)^2P_{mn}\sum_{\ell=0}^{\infty}\frac{\left(-1\right)^{\ell}\left(z'-z\right)^{2\ell}}{\ell!4^{\ell}E^{2\ell-1}}Q_{mn}^{\ell}\\
D_{xy}\left(G2^{ext}-G2^{int}\right)&=-\frac{1}{8\pi^{5/2}}\sum_{m,n}\left(m+\alpha\right)\left(n+\beta\right)P_{mn}\sum_{\ell=0}^{\infty}\frac{\left(-1\right)^{\ell}\left(z'-z\right)^{2\ell}}{\ell!4^{\ell}E^{2\ell-1}}Q_{mn}^{\ell}\\
D_{xz}\left(G2^{ext}-G2^{int}\right)&=\frac{1}{4\pi^{5/2}}\sum_{m,n}i\left(m+\alpha\right)P_{mn}\sum_{\ell=1}^{\infty}\frac{\left(-1\right)^{\ell}\left(z'-z\right)^{2\ell-1}}{(\ell-1)!4^{\ell}E^{2\ell-1}}Q_{mn}^{\ell}\\
D_{yy}\left(G2^{ext}-G2^{int}\right)&=-\frac{1}{8\pi^{5/2}}\sum_{m,n}\left(n+\beta\right)^2P_{mn}\sum_{\ell=0}^{\infty}\frac{\left(-1\right)^{\ell}\left(z'-z\right)^{2\ell}}{\ell!4^{\ell}E^{2\ell-1}}Q_{mn}^{\ell}\\
D_{yz}\left(G2^{ext}-G2^{int}\right)&=\frac{1}{4\pi^{5/2}}\sum_{m,n}i\left(n+\beta\right)P_{mn}\sum_{\ell=1}^{\infty}\frac{\left(-1\right)^{\ell}\left(z'-z\right)^{2\ell-1}}{(\ell-1)!4^{\ell}E^{2\ell-1}}Q_{mn}^{\ell}\\
D_{zz}\left(G2^{ext}-G2^{int}\right)&=\frac{1}{4\pi^{5/2}}\sum_{m,n}P_{mn}\sum_{\ell=1}^{\infty}\frac{\left(-1\right)^{\ell}\left(2\ell-1\right)\left(z'-z\right)^{2\ell-2}}{(\ell-1)!4^{\ell}E^{2\ell-1}}Q_{mn}^{\ell}
\end{aligned}\tag{A.5}$$

Appendix B

The Poisson Summation Formula

The Poisson summation formula is used in Chapters 3 and 5 in derivations of the Fourier and Ewald forms of the Green's function, respectively. Here we state the formula, prove it, and apply it to state the identities used.

Proposition: B.0.1 (Poisson summation formula)**.** *If f is in the Schwartz class of quickly decaying functions $\mathbb{S}(\mathbb{R})$, then*

$$\sum_{\mu=-\infty}^{\infty} f(x+T\mu) = \frac{1}{T} \sum_{m=-\infty}^{\infty} \hat{f}(m)\, e^{\frac{2\pi i m x}{T}}$$

Proof. Let

$$g(x) = \sum_{\mu=-\infty}^{\infty} f(x+T\mu)$$

Then $g(x)$ is a periodic function and can be written as a Fourier series

$$g(x) = \sum_{m=-\infty}^{\infty} \tilde{g}_m e^{\frac{2\pi i m x}{T}} \tag{B.1}$$

where the coefficients $\tilde{g}_m$ are

$$\begin{aligned}
\tilde{g}_m &= \frac{1}{T}\int_0^T g(x)\, e^{-\frac{2\pi i m x}{T}}\, dx \\
&= \frac{1}{T}\int_0^T \sum_{\mu=-\infty}^{\infty} f(x+T\mu)\, e^{-\frac{2\pi i m x}{T}}\, dx \\
&= \frac{1}{T}\sum_{\mu=-\infty}^{\infty}\int_0^T f(x+T\mu)\, e^{-\frac{2\pi i m x}{T}}\, dx
\end{aligned}$$

If we make a $w = x + T\mu$ substitution in the integral above, we see that

$$\begin{aligned}
\tilde{g}_m &= \frac{1}{T}\sum_{\mu=-\infty}^{\infty}\int_{T\mu}^{T(\mu+1)} f(w)\, e^{-\frac{2\pi i m (w-T\mu)}{T}}\, dw \\
&= \frac{1}{T}\sum_{\mu=-\infty}^{\infty}\int_{T\mu}^{T(\mu+1)} f(w)\, e^{-\frac{2\pi i m w}{T}}\, dw \\
&= \frac{1}{T}\int_{-\infty}^{\infty} f(w)\, e^{-\frac{2\pi i m w}{T}}\, dw \\
&= \frac{1}{T}\hat{f}(m)
\end{aligned}$$

We plug this expression for the coefficients $\tilde{g}_m$ back into the Fourier series (B.1), and we are done:

$$g(x) = \frac{1}{T}\sum_{m=-\infty}^{\infty}\hat{f}(m)\, e^{\frac{2\pi i m x}{T}}$$

□

We apply this identity twice in deriving various forms of our Green's function. Each time, the period $T = 2\pi$, so the summation formula that we use is actually

$$\sum_{\mu=-\infty}^{\infty} f(x+2\pi\mu) = \frac{1}{2\pi}\sum_{m=-\infty}^{\infty}\hat{f}(m)\, e^{imx}$$

In Chapter 3, we need to use this identity in the derivation of the Fourier form of the Green's function. We will state the exact result used as a corollary.

Corollary: B.0.2.

$$\sum_{\mu,\nu} \delta\left(x + 2\pi\mu\right) \delta\left(y + 2\pi\nu\right) = \frac{1}{4\pi^2} \sum_{m,n} e^{i(mx+ny)}$$

Proof. We simply apply the Poisson summation formula twice and use the fact that the Fourier transform of the Dirac delta function is 1.

$$\sum_{\mu,\nu} \delta\left(x + 2\pi\mu\right) \delta\left(y + 2\pi\nu\right)$$

$$= \sum_{\mu=-\infty}^{\infty} \delta\left(x + 2\pi\mu\right) \sum_{\nu=-\infty}^{\infty} \delta\left(y + 2\pi\nu\right)$$

$$= \frac{1}{2\pi} \sum_{\mu=-\infty}^{\infty} \delta\left(x + 2\pi\mu\right) \sum_{n=-\infty}^{\infty} \hat{\delta}\left(n\right) e^{iny}$$

$$= \frac{1}{2\pi} \sum_{n=-\infty}^{\infty} \hat{\delta}\left(n\right) e^{iny} \sum_{\mu=-\infty}^{\infty} \delta\left(x + 2\pi\mu\right)$$

$$= \frac{1}{4\pi^2} \sum_{n=-\infty}^{\infty} \hat{\delta}\left(n\right) e^{iny} \sum_{m=-\infty}^{\infty} \hat{\delta}\left(m\right) e^{imx}$$

$$= \frac{1}{4\pi^2} \sum_{m=-\infty}^{\infty} \sum_{n=-\infty}^{\infty} e^{imx} e^{iny}$$

$$= \frac{1}{4\pi^2} \sum_{m,n} e^{i(mx+ny)}$$

□

In Chapter 5, we use the Poisson summation formula to write $G1$ in summations over the periodic reflections instead of summations over Fourier modes. Before stating the exact identity needed, we will state a corollary which leads to it.

Corollary: B.0.3.

$$\sum_{m=-\infty}^{\infty} e^{-(m+\alpha)^2 t} e^{imx} = \sqrt{\frac{\pi}{t}} \sum_{\mu=-\infty}^{\infty} e^{-i(x+2\pi\mu)\alpha - \frac{(x+2\pi\mu)^2}{4t}}$$

Proof. This identity is also a direct consequence of the Poisson summation formula with $\hat{f}(m) = e^{-(m+\alpha)^2 t}$, so we will need the inverse Fourier transform $f(x)$

$$f(x) = \frac{1}{2\pi} \int_{-\infty}^{\infty} e^{-(m+\alpha)^2 t} e^{imx} dm$$

By completing the square, we have

$$f(x) = \frac{1}{2\pi} e^{-ix\alpha - \frac{x^2}{4t}} \int_{-\infty}^{\infty} e^{-\left(m+\alpha+\frac{ix}{2t}\right)^2 t} dm$$

By comparing this integral to the normal probability density function with standard deviation $1/\sqrt{2t}$, we get

$$f(x) = \frac{1}{2\pi} \sqrt{\frac{\pi}{t}} e^{-ix\alpha - \frac{x^2}{4t}}$$

Now the Poisson summation formula gives us the result. □

Now we will state and prove the identity used in Chapter 5.

Corollary: B.0.4.

$$e^{i(\alpha x+\beta y)} \sum_{m,n} e^{imx+iny-(x+\alpha)^2 t-(y+\beta)^2 t} = \frac{\pi}{t} \sum_{\mu,\nu} e^{-2\pi i(\alpha\mu+\beta\nu)} e^{-\frac{(x+2\pi\mu)^2+(y+2\pi\nu)^2}{4t}}$$

Proof. We simply apply Corollary B.0.3 to the left hand side twice - once for the m summation and once for the n summation - as in the proof of Corollary B.0.2. $\square$

Appendix C

The Exponential Integral Function

The exponential integral of order n is defined as

$$\mathrm{ExpInt}_n(x) = \int_1^\infty \frac{e^{-xt}}{t^n} dt \tag{C.1}$$

for $\Re(x) > 0$. The sums $G1$ and $G2$ in the Ewald form of the Green's function include exponential integral functions (see Chapter 5), so we need to be familiar with some of their properties. The functions that appear in our Green's functions are all of half integer orders of at least $-\frac{1}{2}$. The following facts allow us to compute all needed exponential integral functions:

$$\begin{aligned}
\mathrm{ExpInt}_{\frac{1}{2}}(x) &= \sqrt{\frac{\pi}{x}}\,\mathrm{erfc}\left(\sqrt{x}\right) \\
\mathrm{ExpInt}_{n+1}(x) &= \frac{1}{n}\left[e^{-x} - x\,\mathrm{ExpInt}_n(x)\right] \\
\mathrm{ExpInt}_{-\frac{1}{2}}(x) &= \frac{1}{x}\left[\mathrm{ExpInt}_{\frac{1}{2}}(x) + e^{-x}\right] \\
\frac{d}{dz}\left[\mathrm{ExpInt}_n(x)\right] &= -\,\mathrm{ExpInt}_{n-1}(x)
\end{aligned} \tag{C.2}$$

These statements show how all of the exponential integral functions we will need can be related to the complementary error function erfc and to square root functions. This is nice for two reasons. First, fast algorithms exist for computing the complementary error function [31]. Second, the complementary error function can be extended to include arguments in the whole complex plane. This fact is essential in ensuring that our Green's function be analytic in λ away from $\lambda = 0$.

C.1 Singularities

For order $n \leq 1$, exponential integral functions are singular as $x \to 0$ (recall that we use the traditional branch cut along the negative real axis, which we always approach from above). For $n > 1$, $\mathrm{ExpInt}_n(x)$ is finite at $x = 0$. By looking at (C.2), we can see the exact nature of the singularities that we will encounter. We start with

$$\begin{aligned}
\mathrm{ExpInt}_{\frac{1}{2}}(x) &= \sqrt{\frac{\pi}{x}}\,\mathrm{erfc}\left(\sqrt{x}\right) \\
&= \sqrt{\frac{\pi}{x}}\left(1 - \mathrm{erf}\,\sqrt{x}\right) \\
&= \sqrt{\frac{\pi}{x}}\left(1 - \frac{2}{\sqrt{\pi}}\left(x^{1/2} - \frac{1}{3}x^{3/2} + \frac{1}{10}x^{5/2} - \ldots\right)\right) \\
&\to \sqrt{\frac{\pi}{x}} \quad \text{as} \quad x \to 0
\end{aligned} \tag{C.3}$$

We will also need

$$\begin{aligned}
\mathrm{ExpInt}_{-\frac{1}{2}}(x) &= \frac{1}{x}\left[\mathrm{ExpInt}_{\frac{1}{2}}(x) + e^{-x}\right] \\
&\to \frac{\sqrt{\pi}}{x^{3/2}} \quad \text{as} \quad x \to 0
\end{aligned} \tag{C.4}$$

C.2 Decay

The exponential integral function of any order decays quickly as x increases on the positive real axis. This decay ensures quick convergence of the Green's function terms after Ewald splitting (see Chapter 5). Proposition C.2.1 will provide a bound on the decay of these functions (tighter bounds are possible but unnecessary for our purposes):

Proposition: C.2.1. *For any $x > 1$ and for any half integer $n \geq -\frac{1}{2}$,*

$$\mathrm{ExpInt}_n(x) \leq \frac{2e^{-x}}{x} \tag{C.5}$$

Proof. It is clear from the definition (C.1) that $\mathrm{ExpInt}_n(x) > \mathrm{ExpInt}_m(x)$ for $n < m$, so it is enough to prove our bound on $\mathrm{ExpInt}_{-\frac{1}{2}}(x)$. Recall that here we only consider $x > 1$:

$$\begin{aligned} \mathrm{ExpInt}_{-\frac{1}{2}}(x) &= \frac{1}{x}\left[\mathrm{ExpInt}_{\frac{1}{2}}(x) + e^{-x}\right] \\ &= \frac{1}{x}\left[\sqrt{\frac{\pi}{x}}\,\mathrm{erfc}\left(\sqrt{x}\right) + e^{-x}\right] \end{aligned} \tag{C.6}$$

From [1], we have the following inequality for $x > 0$,

$$\mathrm{erfc}\, x \leq \frac{2}{\sqrt{\pi}} \frac{e^{-x^2}}{x + \sqrt{x^2 + \frac{4}{\pi}}}$$

Inserting this inequality into (C.6),

$$\begin{aligned}
\mathrm{ExpInt}_{-\frac{1}{2}}(x) &\leq \frac{1}{x}\left[\sqrt{\frac{\pi}{x}}\left(\frac{2}{\sqrt{\pi}}\frac{e^{-x}}{\sqrt{x}+\sqrt{x+\frac{4}{\pi}}}\right)+e^{-x}\right] \\
&= \frac{2e^{-x}}{x^2+x\sqrt{x^2+\frac{4x}{\pi}}}+\frac{e^{-x}}{x} \\
&\leq \frac{2e^{-x}}{x}
\end{aligned}$$

□

Appendix D

An Alternate Derivation for a Correction Term

The correction terms of Chapter 6 can be derived without using the simplifying concepts from differential geometry. We will present one such derivation as an example of how this can be done.

Proposition: D.0.2. *With G, G_δ, and $\partial\Omega$ as defined in Chapter 6, with $\mathbf{x}' \in \partial\Omega$, and with $\mathbf{v}(\mathbf{x})$ a vector tangential to $\partial\Omega$,*

$$\int_{\partial\Omega} [\mathbf{n}(\mathbf{x}') \cdot \mathbf{v}(\mathbf{x})] \nabla G(\mathbf{x}-\mathbf{x}')\, dS(\mathbf{x}) = \int_{\partial\Omega} [\mathbf{n}(\mathbf{x}') \cdot \mathbf{v}(\mathbf{x})] \nabla G_\delta(\mathbf{x}-\mathbf{x}')\, dS(\mathbf{x})$$

$$+ \frac{1}{\sqrt{\pi}\left(1+f_1^2+f_2^2\right)^{3/2}} \begin{bmatrix} v_x\left(f_2^2 f_{11} - f_1 f_2 f_{12} + f_{11}\right) + v_y\left(f_2^2 f_{12} - f_1 f_2 f_{22} + f_{12}\right) \\ -v_x\left(f_1^2 f_{12} - f_1 f_2 f_{11} + f_{12}\right) - v_y\left(f_1^2 f_{22} - f_1 f_2 f_{12} + f_{22}\right) \\ v_x\left(f_1 f_{11} + f_2 f_{12}\right) + v_y\left(f_2 f_{22} + f_1 f_{12}\right) \end{bmatrix} \delta$$

$$+ O\left(\delta^3\right)$$

where v_x and v_y are the x and y components of $\mathbf{v}(\mathbf{x})$ and where all functions in the correction term are evaluated at the point $\mathbf{x}'$.

Proof. We begin in the now customary way with $\mathbf{x}' = \mathbf{0}$ and with the error

$$\epsilon = \frac{1}{8\pi^{3/2}} \int_{\partial\Omega} \left(\sum_{\mu,\nu} \int_0^{\delta^2} \mathbf{n_0} \cdot \mathbf{v}(\mathbf{x}) \nabla \left(\frac{e^{k^2 t - \frac{(x+2\pi\mu)^2 + (y+2\pi\nu)^2 + z^2}{4t}}}{t^{3/2}} \right) dt \right) dS(\mathbf{x})$$

and once again limit ourselves to the $\mu = \nu = 0$ term on just one coordinate patch, extending the patch to all of $\mathbb{R}^2$. We will use (α_1, α_2) as coordinates in the patch, where α_1 and α_2 are aligned with x and y, respectively. Within the patch, we can represent a point on the surface as

$$\mathbf{x}(\alpha) = \begin{bmatrix} \alpha_1 \\ \alpha_2 \\ f(\alpha) \end{bmatrix}$$

for some function f. The error becomes

$$\begin{aligned} \epsilon &= \frac{1}{8\pi^{3/2}} \int_0^{\delta^2} \frac{e^{k^2 t}}{t^{3/2}} \left(\int_{\mathbb{R}^2} \mathbf{n_0} \cdot \mathbf{v}(\alpha) \nabla \left(e^{-\frac{r(\alpha)^2}{4t}} \right) \left| \frac{\partial \mathbf{x}}{\partial \alpha_1} \times \frac{\partial \mathbf{x}}{\partial \alpha_2} \right| d\alpha \right) dt \\ &= -\frac{1}{16\pi^{3/2}} \int_0^{\delta^2} \frac{e^{k^2 t}}{t^{5/2}} \left(\int_{\mathbb{R}^2} [\mathbf{n_0} \cdot \mathbf{v}(\alpha)] \mathbf{x}(\alpha) e^{-\frac{r(\alpha)^2}{4t}} \left| \frac{\partial \mathbf{x}}{\partial \alpha_1} \times \frac{\partial \mathbf{x}}{\partial \alpha_2} \right| d\alpha \right) dt \end{aligned} \tag{D.1}$$

Again, we see increased singularity in the dt integral as we take the gradient of the Green's function. We will adopt a notation of omitting a function's argument if that argument is 0, so, for example, $f = f(0)$.

The outward unit normal vector is

$$\mathbf{n_0} = \frac{1}{\sqrt{1 + f_1^2 + f_2^2}} \begin{bmatrix} f_1 \\ f_2 \\ -1 \end{bmatrix}$$

The two tangent coordinate vectors are

$$\mathbf{T_1}(\alpha) = \frac{\partial \mathbf{x}}{\partial \alpha_1} = \begin{bmatrix} 1 \\ 0 \\ f_1(\alpha) \end{bmatrix} \quad \text{and} \quad \mathbf{T_2}(\alpha) = \frac{\partial \mathbf{x}}{\partial \alpha_2} = \begin{bmatrix} 0 \\ 1 \\ f_2(\alpha) \end{bmatrix}$$

Since $\mathbf{v}(\alpha)$ is a tangential vector, it is a linear combination of $\mathbf{T_1}(\alpha)$ and $\mathbf{T_2}(\alpha)$. With $v_x(\alpha)$ and $v_y(\alpha)$ the x and y components of $\mathbf{v}(\alpha)$, respectively,

$$\mathbf{v}(\alpha) = v_x(\alpha)\,\mathbf{T_1}(\alpha) + u_y(\alpha)\,\mathbf{T_2}(\alpha) = \begin{bmatrix} v_x(\alpha) \\ v_y(\alpha) \\ v_x(\alpha)\,f_1(\alpha) + v_y(\alpha)\,f_2(\alpha) \end{bmatrix}$$

We also have

$$\begin{aligned} \left| \frac{\partial \mathbf{x}}{\partial \alpha_1} \times \frac{\partial \mathbf{x}}{\partial \alpha_2} \right| &= |\mathbf{T_1}(\alpha) \times \mathbf{T_2}(\alpha)| \\ &= \sqrt{1 + f_1^2(\alpha) + f_2^2(\alpha)} \end{aligned}$$

We now expand $\mathbf{x}(\alpha)$, $\mathbf{T_1}(\alpha)$, and $\mathbf{T_2}(\alpha)$. Note that, because we are not in our special normal coordinates, we have $\alpha_1\alpha_2$ cross terms in our expansion for $\mathbf{x}(\alpha)$.

$$\mathbf{x}(\alpha) = \begin{bmatrix} \alpha_1 \\ \alpha_2 \\ f_1\alpha_1 + f_2\alpha_2 + \frac{1}{2}f_{11}\alpha_1^2 + f_{12}\alpha_1\alpha_2 + \frac{1}{2}f_{22}\alpha_2^2 + O\left(|\alpha|^3\right) \end{bmatrix}$$

$$\mathbf{T_1}(\alpha) = \begin{bmatrix} 1 \\ 0 \\ f_1 + f_{11}\alpha_1 + f_{12}\alpha_2 + +O\left(|\alpha|^2\right) \end{bmatrix}$$

$$\mathbf{T_2}(\alpha) = \begin{bmatrix} 0 \\ 1 \\ f_2 + f_{22}\alpha_2 + f_{12}\alpha_1 + O\left(|\alpha|^2\right) \end{bmatrix}$$

With these expansions, we can write

$$\mathbf{v}(\alpha) = \begin{bmatrix} v_x(\alpha) \\ v_y(\alpha) \\ v_x(\alpha)\,(f_1 + f_{11}\alpha_1 + f_{12}\alpha_2) + v_y(\alpha)\,(f_2 + f_{22}\alpha_2 + f_{12}\alpha_1) + O\left(|\alpha|^2\right) \end{bmatrix}$$

We can also expand

$$|\mathbf{T_1}(\alpha) \times \mathbf{T_2}(\alpha)| = \sqrt{1 + f_1^2 + f_2^2} + O(|\alpha|)$$

Now we can look at the dot product, and we see that there are no $O(1)$ terms. This first-order zero of the dot product cancels enough of the singularity to make the integral converge.

$$[\mathbf{n_0} \cdot \mathbf{v}(\alpha)]$$

$$= -\frac{v_x(\alpha) f_{11}\alpha_1 + v_x(\alpha) f_{12}\alpha_2 + v_y(\alpha) f_{22}\alpha_2 + v_y(\alpha) f_{12}\alpha_1}{\sqrt{1+f_1^2+f_2^2}} + O\left(|\alpha|^2\right)$$

We can see that upon expanding $v_x(\alpha)$ and $v_y(\alpha)$, we will be left with

$$[\mathbf{n_0} \cdot \mathbf{v}(\alpha)] = -\frac{v_x f_{11}\alpha_1 + v_x f_{12}\alpha_2 + v_y f_{22}\alpha_2 + v_y f_{12}\alpha_1}{\sqrt{1+f_1^2+f_2^2}} + O\left(|\alpha|^2\right)$$

From the integrand of our error integral (D.1) we now have

$$[\mathbf{n_0} \cdot \mathbf{v}(\alpha)]\, \mathbf{x}(\alpha)\, |\mathbf{T_1}(\alpha) \times \mathbf{T_2}(\alpha)| = \mathbf{X}(\alpha) + O\left(|\alpha|^3\right)$$

where

$$\begin{aligned}
X_x(\alpha) &= -\alpha_1 (v_x f_{11}\alpha_1 + v_x f_{12}\alpha_2 + v_y f_{22}\alpha_2 + v_y f_{12}\alpha_1) \\
X_y(\alpha) &= -\alpha_2 (v_x f_{11}\alpha_1 + v_x f_{12}\alpha_2 + v_y f_{22}\alpha_2 + v_y f_{12}\alpha_1) \\
X_z(\alpha) &= -v_x \left(f_{11}f_1\alpha_1^2 + f_{12}f_2\alpha_2^2 + f_{11}f_2\alpha_1\alpha_2 + f_{12}f_1\alpha_1\alpha_2\right) \\
&\quad - v_y \left(f_{22}f_2\alpha_2^2 + f_{12}f_1\alpha_1^2 + f_{22}f_1\alpha_1\alpha_2 + f_{12}f_2\alpha_1\alpha_2\right)
\end{aligned} \tag{D.2}$$

The exponential in our error (D.1) has some high order terms in it. We would like to eliminate the exponential dependence on these terms. We introduce a change of variables $\alpha \to \xi$ as a remedy. We let $|\xi|^2 = r^2$ with $\xi_j/|\xi| = \alpha_j/|\alpha|$. This simplifies the exponential in the desired way, and ξ still has the same direction as α.

After this substitution, we can write

$$\begin{aligned}
|\xi|^2 &= r^2 \\
&= \mathbf{x} \cdot \mathbf{x} \\
&= \alpha_1^2 + \alpha_2^2 + \left(f_1\alpha_1 + f_2\alpha_2 + O\left(|\alpha|^2\right)\right)^2 \\
&= \alpha_1^2 + \alpha_2^2 + f_1^2\alpha_1^2 + f_2^2\alpha_2^2 + 2f_1f_2\alpha_1\alpha_2 + O\left(|\alpha|^3\right)
\end{aligned}$$

Then

$$\begin{aligned}
|\xi| &= \sqrt{\alpha_1^2 + \alpha_2^2 + f_1^2\alpha_1^2 + f_2^2\alpha_2^2 + 2f_1f_2\alpha_1\alpha_2 + O\left(|\alpha|^3\right)} \\
&= \sqrt{\alpha_1^2 + \alpha_2^2 + f_1^2\alpha_1^2 + f_2^2\alpha_2^2 + 2f_1f_2\alpha_1\alpha_2 + O\left(|\alpha|^3\right)} \\
&= |\alpha|\sqrt{1 + f_1^2\frac{\alpha_1^2}{|\alpha|^2} + f_2^2\frac{\alpha_2^2}{|\alpha|^2} + 2f_1f_2\frac{\alpha_1\alpha_2}{|\alpha|^2} + O\left(|\alpha|\right)} \\
&= |\alpha|\sqrt{1 + f_1^2\frac{\alpha_1^2}{|\alpha|^2} + f_2^2\frac{\alpha_2^2}{|\alpha|^2} + 2f_1f_2\frac{\alpha_1\alpha_2}{|\alpha|^2}} + O\left(|\alpha|^2\right) \\
&= |\alpha|\sqrt{1 + f_1^2\frac{\xi_1^2}{|\xi|^2} + f_2^2\frac{\xi_2^2}{|\xi|^2} + 2f_1f_2\frac{\xi_1\xi_2}{|\xi|^2}} + O\left(|\alpha|^2\right)
\end{aligned}$$

Then, since $O\left(|\alpha|^2\right) = O\left(|\xi|^2\right)$,

$$|\alpha| = \frac{|\xi|}{\sqrt{1 + f_1^2\frac{\xi_1^2}{|\xi|^2} + f_2^2\frac{\xi_2^2}{|\xi|^2} + 2f_1f_2\frac{\xi_1\xi_2}{|\xi|^2}}} + O\left(|\xi|^2\right)$$

Since $\alpha_j = \frac{|\alpha|}{|\xi|}\xi_j$,

$$\alpha_j = \frac{\xi_j}{\sqrt{1 + f_1^2\frac{\xi_1^2}{|\xi|^2} + f_2^2\frac{\xi_2^2}{|\xi|^2} + 2f_1f_2\frac{\xi_1\xi_2}{|\xi|^2}}} + O\left(|\xi|^2\right) \tag{D.3}$$

We can write the error in terms of ξ

$$\epsilon = \frac{1}{16\pi^{3/2}} \int_0^{\delta^2} \frac{e^{k^2 t}}{t^{5/2}} \left(\int_{\mathbb{R}^2} \left[\mathbf{n_0} \cdot \mathbf{v}\left(\xi\right) \right] \mathbf{x}\left(\xi\right) e^{-\frac{|\xi|^2}{4t}} \det\left(\partial\alpha/\partial\xi\right) \left| \mathbf{T_1} \times \mathbf{T_2} \right| d\xi \right) dt$$

The part of the integrand in (D.2) can now be written in ξ (canceling some negatives along the way):

$$\left[\mathbf{n_0} \cdot \mathbf{v}\left(\xi\right) \right] \mathbf{x}\left(\xi\right) \left| \mathbf{T_1}\left(\xi\right) \times \mathbf{T_2}\left(\xi\right) \right| = \mathbf{X}\left(\xi\right) + O\left(\left|\xi\right|^3\right)$$

where

$$\begin{aligned}
X_x\left(\xi\right) &= \left|\xi\right|^2 \frac{\xi_1 \left(v_x f_{11} \xi_1 + v_x f_{12} \xi_2 + v_y f_{22} \xi_2 + v_y f_{12} \xi_1 \right)}{\left|\xi\right|^2 + f_1^2 \xi_1^2 + f_2^2 \xi_2^2 + 2 f_1 f_2 \xi_1 \xi_2} \\
X_y\left(\xi\right) &= \left|\xi\right|^2 \frac{\xi_2 \left(v_x f_{11} \xi_1 + v_x f_{12} \xi_2 + v_y f_{22} \xi_2 + v_y f_{12} \xi_1 \right)}{\left|\xi\right|^2 + f_1^2 \xi_1^2 + f_2^2 \xi_2^2 + 2 f_1 f_2 \xi_1 \xi_2} \\
X_z\left(\xi\right) &= \left|\xi\right|^2 \frac{v_x \left(f_{11} f_1 \xi_1^2 + f_{12} f_2 \xi_2^2 + f_{11} f_2 \xi_1 \xi_2 + f_{12} f_1 \xi_1 \xi_2 \right)}{\left|\xi\right|^2 + f_1^2 \xi_1^2 + f_2^2 \xi_2^2 + 2 f_1 f_2 \xi_1 \xi_2} \\
&\quad + \left|\xi\right|^2 \frac{v_y \left(f_{22} f_2 \xi_2^2 + f_{12} f_1 \xi_1^2 + f_{22} f_1 \xi_1 \xi_2 + f_{12} f_2 \xi_1 \xi_2 \right)}{\left|\xi\right|^2 + f_1^2 \xi_1^2 + f_2^2 \xi_2^2 + 2 f_1 f_2 \xi_1 \xi_2}
\end{aligned} \tag{D.4}$$

Now, in order to use this change of variables in the error integral, we will need to compute $\det\left(\partial\alpha/\partial\xi\right)$. We use (D.3) to take the necessary derivatives. Excluding the messy details, the determinant can then be found to be

$$\det\left(\partial\alpha/\partial\xi\right) = \frac{\left|\xi\right|^2}{\left|\xi\right|^2 + f_1^2 \xi_1^2 + f_2^2 \xi_2^2 + 2 f_1 f_2 \xi_1 \xi_2}$$

Our error can now be written

$$\epsilon = \frac{1}{16\pi^{3/2}} \int_0^{\delta^2} \frac{e^{k^2 t}}{t^{5/2}} \left(\int_{\mathbb{R}^2} \left(\mathbf{X}'\left(\xi\right) + \left|\xi\right|^2 R\left(\xi\right) \right) e^{-\frac{|\xi|^2}{4t}} d\xi \right) dt$$

where $R(\xi) = O(|\xi|)$ and

$$X'_x(\xi) = |\xi|^4 \frac{\xi_1 (v_x f_{11}\xi_1 + v_x f_{12}\xi_2 + v_y f_{22}\xi_2 + v_y f_{12}\xi_1)}{\left(|\xi|^2 + f_1^2\xi_1^2 + f_2^2\xi_2^2 + 2f_1 f_2 \xi_1\xi_2\right)^2}$$

$$X'_y(\xi) = |\xi|^4 \frac{\xi_2 (v_x f_{11}\xi_1 + v_x f_{12}\xi_2 + v_y f_{22}\xi_2 + v_y f_{12}\xi_1)}{\left(|\xi|^2 + f_1^2\xi_1^2 + f_2^2\xi_2^2 + 2f_1 f_2 \xi_1\xi_2\right)^2}$$

$$X'_z(\xi) = |\xi|^4 \frac{v_x (f_{11} f_1 \xi_1^2 + f_{12} f_2 \xi_2^2 + f_{11} f_2 \xi_1\xi_2 + f_{12} f_1 \xi_1\xi_2)}{\left(|\xi|^2 + f_1^2\xi_1^2 + f_2^2\xi_2^2 + 2f_1 f_2 \xi_1\xi_2\right)^2}$$

$$+ |\xi|^4 \frac{v_y (f_{22} f_2 \xi_2^2 + f_{12} f_1 \xi_1^2 + f_{22} f_1 \xi_1\xi_2 + f_{12} f_2 \xi_1\xi_2)}{\left(|\xi|^2 + f_1^2\xi_1^2 + f_2^2\xi_2^2 + 2f_1 f_2 \xi_1\xi_2\right)^2}$$

We will make the substitution $\xi \to \delta\zeta$. We can write $R(\xi) = \delta\tilde{R}(\zeta)$ for a bounded function $\tilde{R}(\zeta)$. We can now write the error as an integral in ζ

$$\epsilon = \frac{\delta^4}{16\pi^{3/2}} \int_0^{\delta^2} \frac{e^{k^2 t}}{t^{5/2}} \left(\int_{\mathbb{R}^2} \left(\mathbf{X}'(\zeta) + \delta |\zeta|^2 \tilde{R}(\zeta) \right) e^{-\frac{\delta^2 |\zeta|^2}{4t}} d\zeta \right) dt$$

$$= \frac{\delta^4}{16\pi^{3/2}} \int_0^{\delta^2} \frac{e^{k^2 t}}{t^{5/2}} \left(\int_{\mathbb{R}^2} \mathbf{X}'(\zeta) e^{-\frac{\delta^2 |\zeta|^2}{4t}} d\zeta \right) dt + I_{\tilde{R}}$$

with

$$X'_x(\zeta) = |\zeta|^4 \frac{\zeta_1 (v_x f_{11}\zeta_1 + v_x f_{12}\zeta_2 + v_y f_{22}\zeta_2 + v_y f_{12}\zeta_1)}{\left(|\zeta|^2 + f_1^2\zeta_1^2 + f_2^2\zeta_2^2 + 2f_1 f_2 \zeta_1\zeta_2\right)^2}$$

$$X'_y(\zeta) = |\zeta|^4 \frac{\zeta_2 (v_x f_{11}\zeta_1 + v_x f_{12}\zeta_2 + v_y f_{22}\zeta_2 + v_y f_{12}\zeta_1)}{\left(|\zeta|^2 + f_1^2\zeta_1^2 + f_2^2\zeta_2^2 + 2f_1 f_2 \zeta_1\zeta_2\right)^2}$$

$$X'_z(\zeta) = |\zeta|^4 \frac{v_x (f_{11} f_1 \zeta_1^2 + f_{12} f_2 \zeta_2^2 + f_{11} f_2 \zeta_1\zeta_2 + f_{12} f_1 \zeta_1\zeta_2)}{\left(|\zeta|^2 + f_1^2\zeta_1^2 + f_2^2\zeta_2^2 + 2f_1 f_2 \zeta_1\zeta_2\right)^2}$$

$$+ |\zeta|^4 \frac{v_y (f_{22} f_2 \zeta_2^2 + f_{12} f_1 \zeta_1^2 + f_{22} f_1 \zeta_1\zeta_2 + f_{12} f_2 \zeta_1\zeta_2)}{\left(|\zeta|^2 + f_1^2\zeta_1^2 + f_2^2\zeta_2^2 + 2f_1 f_2 \zeta_1\zeta_2\right)^2} \tag{D.5}$$

We will evaluate this integral by changing to polar coordinates. Let $|\zeta| = s$, $\zeta_1 =$

$s\cos\theta$, and $\zeta_2 = s\sin\theta$. The error becomes

$$\epsilon = \frac{\delta^4}{16\pi^{3/2}} \int_0^{\delta^2} \frac{e^{k^2 t}}{t^{5/2}} \left(\int_0^{\infty} \int_0^{2\pi} \mathbf{X}'(\theta)\, s^3 e^{-\frac{\delta^2 s^2}{4t}} d\theta ds \right) dt + I_{\tilde{R}}$$

with

$$X'_x(\theta) = \frac{v_x f_{11}\cos^2\theta + v_x f_{12}\cos\theta\sin\theta + v_y f_{22}\cos\theta\sin\theta + v_y f_{12}\cos^2\theta}{\left(1 + f_1^2\cos^2\theta + f_2^2\sin^2\theta + 2f_1 f_2\cos\theta\sin\theta\right)^2}$$

$$X'_y(\theta) = \frac{v_x f_{11}\cos\theta\sin\theta + v_x f_{12}\sin^2\theta + v_y f_{22}\sin^2\theta + v_y f_{12}\cos\theta\sin\theta}{\left(1 + f_1^2\cos^2\theta + f_2^2\sin^2\theta + 2f_1 f_2\cos\theta\sin\theta\right)^2}$$

$$X'_z(\theta) = \frac{v_x\left(f_{11}f_1\cos^2\theta + f_{12}f_2\sin^2\theta + f_{11}f_2\cos\theta\sin\theta + f_{12}f_1\cos\theta\sin\theta\right)}{\left(1 + f_1^2\cos^2\theta + f_2^2\sin^2\theta + 2f_1 f_2\cos\theta\sin\theta\right)^2}$$

$$+ \frac{v_y\left(f_{22}f_2\sin^2\theta + f_{12}f_1\cos^2\theta + f_{22}f_1\cos\theta\sin\theta + f_{12}f_2\cos\theta\sin\theta\right)}{\left(1 + f_1^2\cos^2\theta + f_2^2\sin^2\theta + 2f_1 f_2\cos\theta\sin\theta\right)^2}$$

Each of these three components is an elliptic integral that can be integrated in θ. The result is

$$\epsilon = \frac{\mathbf{C}\delta^4}{\left(1 + f_1^2 + f_2^2\right)^{3/2} 16\sqrt{\pi}} \int_0^{\delta^2} \frac{e^{k^2 t}}{t^{5/2}} \left(\int_0^{\infty} s^3 e^{-\frac{\delta^2 s^2}{4t}} d\theta ds \right) dt + I_{\tilde{R}}$$

with

$$C_x = v_x\left(f_2^2 f_{11} - f_1 f_2 f_{12} + f_{11}\right) + v_y\left(f_2^2 f_{12} - f_1 f_2 f_{22} + f_{12}\right)$$

$$C_y = -v_x\left(f_1^2 f_{12} - f_1 f_2 f_{11} + f_{12}\right) - v_y\left(f_1^2 f_{22} - f_1 f_2 f_{12} + f_{22}\right)$$

$$C_z = v_x\left(f_1 f_{11} + f_2 f_{12}\right) + v_y\left(f_2 f_{22} + f_1 f_{12}\right)$$

Now we can integrate in s and t as in Proposition 6.3.1. The result is

$$\epsilon = \frac{\mathbf{C}}{\left(1 + f_1^2 + f_2^2\right)^{3/2}\sqrt{\pi}}\delta + O\left(\delta^3\right) + I_{\tilde{R}}$$

with $\mathbf{C}$ as above.

We can proceed with the $I_{\tilde{R}}$ integral as in Proposition 6.3.1. By the same reasoning found there, this integral is $O(\delta^3)$, and we are done. $\square$

Bibliography

10pt9pt plus 3pt minus 5pt

[1] Milton Abramowitz and Irene A. Stegun, *Handbook of mathematical functions with formulas, graphs, and mathematical tables*, ninth dover printing, tenth GPO printing ed., Dover, New York, 1964.

[2] Rutherford Aris, *Vectors, tensors and the basic equations of fluid mechanics*, 2nd ed., Dover Publications, 1990.

[3] Kendall E. Atkinson, *The numerical solution of integral equations of the second kind*, Cambridge, 1997.

[4] E. H. Ayachour, *A fast implementation for GMRES method*, J. Comput. Appl. Math. **159** (2003), no. 2, 269–283.

[5] Andrew Barnes, *Electromagnetic scattering from three dimensional periodic structures*, Thesis, Duke Univeristy (2003).

[6] J. Thomas Beale, *A convergent boundary integral method for three-dimensional water waves*, Math. Comp. **70** (2001), no. 235, 977–1029.

[7] ———, *A grid-based boundary integral method for elliptic problems in three dimensions*, SIAM J. Numer. Anal. **42** (2004), no. 2, 599–620 (electronic).

[8] J. Thomas Beale and Ming-Chih Lai, *A method for computing nearly singular integrals*, SIAM J. Numer. Anal. **38** (2001), no. 6, 1902–1925 (electronic).

[9] Katarina Blagovic, Ivica Stevanovic, and Anja Skirvervik, *Convergence of infinite periodic Green's functions for the mixed potential integral function*, 17th International Conference on Applied Electromagnetics and Communications **1-3 October** (2003), no. Dubrovnik, Croatia, 423–426.

[10] Angelika Bunse-Gerstner and Ignacio Gutiérrez-Cañas, *A preconditioned GMRES for complex dense linear systems from electromagnetic wave scattering problems*, Linear Algebra Appl. **416** (2006), no. 1, 135–147.

[11] F. Capolino, D. R. Wilton, and W. A. Johnson, *Efficient computation of the 3d Green's function for the Helmholtz operator for a linear array of point sources using the Ewald method*, J. Comput. Phys. **223** (2007), no. 1.

[12] Filippo Capolino, Donald R. Wilton, and William A. Johnson, *Efficient computation of the 2-D Green's function for 1-D periodic structures using the Ewald method*, IEEE Trans. Antennas and Propagation **53** (2005), no. 9, 2977–2984.

[13] Manfredo P. do Carmo, *Differential geometry of curves and surfaces*, Prentice-Hall, 1976, 503 pages.

[14] Kokou Dossou, Michael A. Byrne, and Lindsay C. Botten, *Finite element computation of grating scattering matrices and application to photonic crystal band calculations*, J. Comput. Phys. **219** (2006), no. 1.

[15] T.W. Ebbessen, H.J. Lezec, H.F. Ghaemi, T. Thio, and P.A. Wolff, *Extraordinary optical transmission through sub-wavelength hole arrays*, Nature **391** (12 Feb, 1998), 667–669.

[16] F. Ecevit and F. Reitich, *A high-frequency integral equation method for electromagnetic and acoustic scattering simulations: rate of convergence of multiple-scattering iterations*, in Proceedings of Waves 2005 **Providence, RI** (2005).

[17] P.P. Ewald, *Die berechnung optischer und electrostatischer gitterpotentiale*, Ann. Phys. **64** (1921), 253–287.

[18] S. Fan and J. D. Joannopoulos, *Analysis of guided resonance in photonic crystal slabs*, Phys. Rev. B **65** (2002).

[19] Lan Gao and Junichi Nakayama, *Scattering of a TM plane wave from periodic random surfaces*, Waves Random Media **9** (1999), 53–67.

[20] David Griffiths, *Introduction to electrodynamics*, Prentice Hall, 1999.

[21] Mansoor A. Haider, Stephen P. Shipman, and Stephanos Venakides, *Boundary-integral calculations of two-dimensional electromagnetic scattering in infinite photonic crystal slabs: channel defects and resonances*, SIAM J. Appl. Math. **62** (2002), no. 6, 2129–2148 (electronic).

[22] Steven G Johnson, Shanhui Fan, Pierre R. Villeneuve, and J.D. Joannopoulos, *Guided modes in photonic crystal slabs*, Phys. Rev. B **60** (2002), no. 8, 5751–5758.

[23] Kirk E. Jordan, Gerard R. Richter, and Ping Sheng, *An efficient numerical evaluation of the Green's function for the Helmholtz operator on periodic structures*, J. Comput. Phys. **63** (1986), no. 1, 222–235.

[24] C.T. Kelley, *Iterative methods for linear and nonlinear equations*, SIAM, 1995.

[25] C. M. Linton, *The Green's function for the two-dimensional Helmholtz equation in periodic domains*, J. Engrg. Math. **33** (1998), no. 4, 377–402.

[26] E. McKay Hyde and Oscar P. Bruno, *A fast, higher-order solver for scattering by penetrable bodies in three dimensions*, J. Comput. Phys. **202** (2005), no. 1, 236–261.

[27] C. Müller, *Foundations of the mathematical theory of electromagnetic waves*, Springer, Berlin, 1969.

[28] David Nicholls, Nilima Nigam, and Fernando Reitich, *Advances in computational scattering*, Summary of Conference "Advances in Computational Scattering" at Banff International Research Station (Feb 18-23, 2006).

[29] Vassilis G. Papanicolaou, *Ewald's method revisited: rapidly convergent series representations of certain Green's functions*, J. Comput. Anal. Appl. **1** (1999), no. 1, 105–114.

[30] Giuseppe Pelosi, Alessandro Cocchi, and Stafano Selleri, *Electromagnetic scattering from infinite periodic structures with a localized impurity*, IEEE Transactions on Antennas and Propagation **49** (May, 2001), no. 5, 697–702.

[31] G. P. M. Poppe and C. M. J. Wijers, *Algorithm 680: evaluation of the complex error function*, ACM Trans. Math. Software **16** (1990), no. 1, 47.

[32] Youcef Saad and Martin H. Schultz, *GMRES: a generalized minimal residual algorithm for solving nonsymmetric linear systems*, SIAM J. Sci. Statist. Comput. **7** (1986), no. 3, 856–869.

[33] S. Shipman and S. Venakides, *Resonant transmission near nonrobust periodic slab modes*, Phys. Rev. E **71** (2005), 026611(1–10).

[34] Stephen P. Shipman and Stephanos Venakides, *Resonance and bound states in photonic crystal slabs*, SIAM J. Appl. Math. **64** (2003), no. 1, 322–342 (electronic).

[35] Stephen P. Shipman and Stephanos Venakides, *Resonant transmission near nonrobust periodic slab modes*, Physical Review E (Statistical, Nonlinear, and Soft Matter Physics) **71** (2005), no. 2, 026611.

[36] Surendra Singh, William F Richards, Joseph R Zinecker, and Donald R. Wilton, *Accelerating the convergence of series representing the free space periodic Green's function*, IEEE Transactions on Antennas and Propagation **38** (1990), no. 12, 1958–1962.

[37] V.G. Solov'ev, C.M. Torres, and S.G.Romanov, *Reflection, transmission, and scattering of light by photonic crystals based on opal films*, Russian Physics Journal **47** (2004), no. 3, 286–292.

[38] Elias M. Stein and Rami Shakarchi, *Fourier analysis: An introduction*, Princeton University Press, 2003.

[39] J. A. Stratton and L. J. Chu, *Diffraction theory of electromagnetic waves*, Phys. Rev. **56** (1939), no. 1, 99.

[40] M. Taylor, *Partial differential equations, vol. I – basic theory*, Springer-Verlag, 1996.

[41] H. A. van der Vorst, *Bi-CGSTAB: a fast and smoothly converging variant of Bi-CG for the solution of nonsymmetric linear systems*, SIAM J. Sci. Statist. Comput. **13** (1992), no. 2, 631–644.

[42] Stephanos Venakides, Mansoor A. Haider, and Vassilis Papanicolaou, *Boundary integral calculations of two-dimensional electromagnetic scattering by photonic crystal Fabry-Perot structures*, SIAM J. Appl. Math. **60** (2000), no. 5, 1686–1706 (electronic).

[43] John L. Volakis and Leo C. Kempel, *Electromagnetics: Computational methods and considerations*, IEEE Comput. Sci. Eng. **2** (1995), no. 1.

[44] R.W. Wood, *On the remarkable case of uneven distribution of a light in a diffractived grating spectrum*, Philo. Mag. **4** (1902), 396–402.

[45] K. Yasumoto and K. Yoshitomi, *Efficient calculation of lattice sums for free-space periodic Green's function*, IEEE Trans. Antennas Propag. **47** (1999), 1050–1055.

[46] Pasi Ylä-Oijala and Matti Taskinen, *Well-conditioned Müller formulation for electromagnetic scattering by dielectric objects*, IEEE Trans. Antennas and Propagation **53** (2005), no. 10, 3316–3323.

[47] V. V. Zalipaev and M. M. Popov, *Wood's anomalies in a problem of the diffraction of a planar wave by a smooth periodic boundary*, Zap. Nauchn. Sem. Leningrad. Otdel. Mat. Inst. Steklov. (LOMI) **186** (1990), no. Mat. Vopr. Teor. Rasprostr. Voln. 20, 87–100, 182.

Biography

Mike Nicholas is from Salt Lake City, Utah. He graduated with a BS in physics and a BA in mathematics from the University of Utah in 2001. In 2003, he completed an MA in mathematics at Duke University.